

**The Metabolomics of Acetaminophen Toxicity Observed in Human Biofluids and
Cultured Primary Human Hepatocytes**

Jason H. Winnike

A dissertation submitted to the faculty of the University of North Carolina at Chapel Hill in partial fulfillment of the requirements for the degree of Doctor of Philosophy in the Department of Biomedical Engineering

Chapel Hill
2010

Approved by

Advisor: Jeffrey M. Macdonald, Ph.D.

Reader: Oleg V. Favorov, Ph.D.

Reader: Thomas M. O'Connell, Ph.D.

Reader: Ivan I. Rusyn, M.D., Ph.D.

Reader: Paul B. Watkins, M.D.

©2010
Jason H. Winnike
ALL RIGHTS RESERVED

Abstract

Jason H. Winnike: The Metabolomics of Acetaminophen Toxicity Observed in Human Biofluids and Cultured Primary Human Hepatocytes
(Under the direction of Jeffrey M. Macdonald, Ph.D.)

The mechanisms of acetaminophen toxicity are well-established. However, the use of metabolomics to identify small molecule (< 1 kD) biomarkers of acetaminophen toxicity in human biofluids is novel. This research establishes the first pharmaco-metabolomic study of acetaminophen in a population of humans. This method makes use of multivariate statistical techniques to elucidate changes in the metabolome before clinical manifestation of acetaminophen toxicity. Furthermore, prior to this experimental analysis, another study was performed which demonstrated that the human metabolome normalized within 2 days of a standardized diet in an inpatient hospital setting.

The use of ^{13}C -labeled nutrient tracers to identify off-target enzyme (> 10 kD) inactivation in primary human hepatocyte cultures is original. By tracking the metabolism of ^{13}C tracers, a metabolomic surrogate of enzyme inactivation due to acetaminophen toxicity was discovered. The enzyme inactivation is likely via arylation by the cytochrome P450 bio-activated acetaminophen metabolic product N-acetyl-para-quinonimine. Furthermore, it was observed that the human hepatocytes appeared to be in a stressed metabolic state, due to the lack of glycolysis or glutaminolysis, even in the presence of high insulin and glucose concentrations. This metabolism was compared to that of primary rat hepatocyte cultures, which did not exhibit these features, likely due to absence of stress inducing hormones prior

to hepatocyte isolation. This has yet to be described in the literature, likely because this is the first report of the use of ^{13}C -labeled nutrients in primary human hepatocyte cultures.

Acknowledgements

It is a pleasure to thank the people who made this research possible. I would like to thank Dr. Jeffrey Macdonald for his invaluable guidance and advice during this work. Under his mentorship, I have learned how to become a more independent researcher. Much has been learned from the many discussions we have had regarding my research. I would also like to thank Dr. Thomas O’Connell for his advice and instruction during the time I worked under his mentorship. He opened up the world of nuclear magnetic resonance spectroscopy and multivariate statistical metabolomics to me. Additionally, my scientific documentation and organization skills were *greatly* enhanced. Dr. Paul Watkins was integral for insights into acetaminophen toxicity and for helping me make clinical relevance from scientific data. I thank Dr. Oleg Favorov for help in statistical interpretation of the data. Much was learned about how to make sense of multivariate data from courses taught by as well as personal conversations with him. Dr. Ivan Rusyn was quite helpful for me in taking a step back from my research and looking for the “big picture” relevance. This is of great importance for me to become a well rounded researcher.

I thank my lab mates for their help, discussions (scientific and nonscientific), and friendship.

I thank my family and friends for their support and encouragement over the years it took to conduct the research necessary to write this dissertation.

For their financial support I thank the General Clinical Research Center, the Center for Environmental Health and Susceptibility, and the Department of Biomedical Engineering of the University of North Carolina.

Table of Contents

| | | |
|-------|--|----|
| 1 | Introduction | 1 |
| 1.1 | Nuclear Magnetic Resonance (NMR) Spectroscopy | 2 |
| 1.1.1 | History..... | 2 |
| 1.1.2 | The NMR Phenomenon | 3 |
| 1.2 | The ^1H NMR Experiment..... | 4 |
| 1.2.1 | Spectral Processing..... | 7 |
| 1.3 | Metabolomics- Multivariate Statistics | 9 |
| 1.3.1 | Principal Component Analysis (PCA)..... | 9 |
| 1.3.2 | Orthogonal Partial Least Squares Discriminant Analysis (OPLS-DA) | 13 |
| 1.4 | Acetaminophen..... | 14 |
| 1.4.1 | History..... | 14 |
| 1.4.2 | Analgesia & Antipyresis..... | 14 |
| 1.4.3 | Pharmacokinetics | 16 |
| 1.4.4 | Cytochrome P450..... | 17 |
| 1.4.5 | Toxicity..... | 20 |
| 1.4.6 | Protein Targets of Acetaminophen | 23 |

| | | |
|-------|--|----|
| 1.5 | Metabolism..... | 26 |
| 1.5.1 | Glycolysis | 26 |
| 1.5.2 | Tricarboxylic Acid (TCA) Cycle..... | 29 |
| 1.5.3 | Regulation of Glucose Metabolism | 30 |
| 1.6 | Hepatocyte Cell Culture..... | 32 |
| 1.6.1 | History of Rat and Human Hepatocyte Culture..... | 33 |
| 1.6.2 | Dedifferentiation of Hepatocytes in 2D Culture and Media Formulations Concocted to Attenuate or Reverse this Dedifferentiation..... | 34 |
| 1.6.3 | Cryopreservation of Hepatocytes..... | 37 |
| 1.7 | Metabolomics- Stable Isotopes | 38 |
| 1.7.1 | Previous Isotope Tracking Experiments | 38 |
| 2 | The Effects of a Prolonged Standardized Diet on the Normalization of the Human Metabolome | 47 |
| 2.1 | Introduction | 47 |
| 2.2 | Methods..... | 49 |
| 2.2.1 | Study Design..... | 49 |
| 2.2.2 | Standardized Diet..... | 50 |
| 2.2.3 | Sample Collection..... | 50 |
| 2.2.4 | Sample Preparation | 50 |
| 2.2.5 | ¹ H NMR Spectroscopy..... | 51 |

| | | |
|-------|---|----|
| 2.2.6 | Spectral Processing | 51 |
| 2.2.7 | Multivariate Statistical Analysis | 52 |
| 2.3 | Results | 52 |
| 2.3.1 | Serum | 53 |
| 2.3.2 | Urine | 56 |
| 2.4 | Discussion | 58 |
| 3 | Early Prediction of Acetaminophen-Induced Hepatotoxicity with Pharmacometabolomics | 61 |
| 3.1 | Introduction | 61 |
| 3.2 | Methods | 63 |
| 3.2.1 | Clinical Trials..... | 63 |
| 3.2.2 | Sample Preparation | 63 |
| 3.2.3 | NMR Spectroscopy | 64 |
| 3.2.4 | Data Processing and Analysis..... | 64 |
| 3.2.5 | Multivariate Statistical Analysis | 65 |
| 3.3 | Results | 65 |
| 3.4 | Discussion | 72 |
| 4 | Stable Isotope Resolved Metabolomics of Acetaminophen Toxicity Reveals an Apparent Stressed Phenotype Exhibited in Primary Human Hepatocytes | 77 |
| 4.1 | Introduction | 77 |

| | | |
|-------|---|-----|
| 4.2 | Methods | 81 |
| 4.2.1 | Human Hepatocyte Isolation and Cultures | 81 |
| 4.2.2 | Rat Hepatocyte Isolation and Cultures | 81 |
| 4.2.3 | Hepatocyte Treatments | 82 |
| 4.2.4 | Metabolite Isolation | 84 |
| 4.2.5 | NMR Sample Preparation | 85 |
| 4.2.6 | NMR Spectroscopy | 86 |
| 4.2.7 | Data Processing and Analysis | 86 |
| 4.2.8 | Statistics | 87 |
| 4.3 | Results | 87 |
| 4.4 | Discussion | 97 |
| 4.4.1 | NMR Sensitivity and Calculation of ^{13}C Fractional Enrichment and Concentration between Samples from Humans and Rats..... | 98 |
| 4.4.2 | The Observed Metabolic State of the Rat Hepatocytes | 98 |
| 4.4.3 | The Observed Stressed Phenotype in the Human Hepatocytes Compared to Rat Hepatocytes | 99 |
| 4.4.4 | A Comparison of Acetaminophen Metabolite Distribution in Human Hepatocytes and <i>In Vivo</i> Human Biofluids | 101 |
| 4.4.5 | Fractional Enrichment of Acetaminophen-Glucuronide and Its Relationship with Glycolysis | 103 |

| | | |
|-------|--|-----|
| 4.4.6 | Fatty Acid Metabolism in Rat and Human Hepatocytes and the Effects of Acetaminophen | 105 |
| 4.4.7 | Enzyme Inhibition Due to Acetaminophen Toxicity | 106 |
| 4.5 | Conclusions | 108 |
| 5 | Conclusions and Perspectives, Pitfalls, and Future Directions | 109 |
| 5.1 | Conclusions and Perspectives | 109 |
| 5.2 | Pitfalls..... | 111 |
| 5.3 | Future Directions..... | 113 |
| | Appendix A- Creation of a Stable Isotope Metabolomic Model Applied to Rat Hepatocyte Cultures..... | 118 |
| | Appendix B- Temporal Effects on Cultured Rat Hepatocytes..... | 126 |
| | References..... | 128 |

List of Tables

| | |
|--|----|
| Table 1-1- List of protein targets of NAPQI..... | 24 |
| Table 3-1- Confusion matrix..... | 70 |

List of Figures

| | |
|--|----|
| Figure 1-1- The vector model of nuclei in an applied magnetic field | 3 |
| Figure 1-2- A nucleus in an applied magnetic field..... | 4 |
| Figure 1-3- The free induction decay of ethanol | 7 |
| Figure 1-4- Simulated principal components analysis..... | 10 |
| Figure 1-5- Simulated loadings plots..... | 12 |
| Figure 1-6- Arachidonic acid pathway | 15 |
| Figure 1-7- Metabolism and elimination of acetaminophen (APAP)..... | 16 |
| Figure 1-8- In vivo production of glutathione | 21 |
| Figure 1-9- The liver lobule..... | 22 |
| Figure 1-10- Metabolic scheme occurring in hepatocytes | 27 |
| Figure 1-11- Glycolysis | 28 |
| Figure 1-12- TCA Cycle | 30 |
| Figure 1-13- Regulation of glycolysis and gluconeogenesis in the hepatocyte..... | 32 |
| Figure 1-14- Creation of CO ₂ in the TCA cycle | 41 |
| Figure 1-15- Metabolism of propionate through the TCA cycle | 45 |
| Figure 2-1- Representative spectra from urine and serum..... | 53 |
| Figure 2-2- PCA scores plot of the serum samples..... | 55 |
| Figure 2-3- PCA scores plot of the urine samples | 57 |
| Figure 2-4- PCA scores plot of urine samples from days 1 - 3 for 65 subjects..... | 58 |
| Figure 3-1- ALT levels for the responders and non-responders | 66 |
| Figure 3-2- PCA scores plot for all responders and non-responders for days 5 - 10..... | 67 |
| Figure 3-3- OPLS-DA scores plots for days 9 - 10 and days 5 - 6..... | 69 |

| | |
|---|-----|
| Figure 3-4- SUS plot comparing models for days 9 – 10 and days 5 - 6..... | 72 |
| Figure 4-1- Representative spectra from human rat hepatocyte extracts..... | 88 |
| Figure 4-2- Rat hepatocytes given insulin or glucagon | 90 |
| Figure 4-3- Acetaminophen conjugates in fresh and cryopreserved human hepatocytes..... | 92 |
| Figure 4-4- Fractional enrichment of acetaminophen-glucuronide | 93 |
| Figure 4-5- Fractional enrichments of acetate and fumarate | 94 |
| Figure 4-6- Concentrations and fractional enrichments of alanine and lactate | 95 |
| Figure 5-1- The various ‘omics sciences | 116 |
| Figure A-1- Time course of lactate and ¹³ C enriched lactate in hepatocytes..... | 122 |
| Figure A-2- Labeling patterns of lactate and TCA cycle intermediates | 123 |
| Figure A-3- Chloroform extract fraction from representative cell extracts | 124 |
| Figure A-4- Spectra from rat hepatocytes exposed to 25, 12.5, and 2.5 mM glucose..... | 125 |
| Figure B-1- The change in metabolites 2 h, 24 h, and 48 h after plating | 127 |

List of Abbreviations and Symbols

| | |
|------------------|---|
| γ | gyromagnetic ratio |
| μ | magnetic moment |
| ρ | Pearson's correlation coefficient |
| Σ | sum |
| 1D | one dimensional |
| 180 _x | 180° NMR irradiation pulse |
| 2D | two dimensional |
| 90 _x | 90° NMR irradiation pulse |
| acetyl CoA | acetyl coenzyme A |
| ADP | adenosine diphosphate |
| ALT | alanine transferase |
| APAP | N-acetyl-para-aminophenol (acetaminophen) |
| AST | aspartate transferase |
| ATP | adenosine triphosphate |
| B ₀ | applied magnetic field |
| BUN | blood urea nitrogen |
| CBC | complete blood count |
| CNS | central nervous system |
| COX | cyclooxygenase enzyme |
| Cr | creatinine |
| cw | continuous wave |
| DNA | deoxyribonucleic acid |

| | |
|--------|-------------------------------------|
| FID | free induction decay |
| FT | Fourier transform |
| GSH | reduced glutathione |
| GST | glutathione-S-transferase |
| I | nuclear spin number |
| LB | line broadening |
| LDH | lactate dehydrogenase |
| M | molar |
| MHz | megahertz |
| NAC | N-acetyl cysteine |
| NAPQI | N-acetyl-para-benzoquinone imine |
| NMR | nuclear magnetic resonance |
| NSAID | nonsteroidal anti inflammatory drug |
| P | angular momentum |
| P1 | NMR irradiation pulse |
| P450 | cytochrome P450 enzymes |
| PC | principal component |
| PCA | principal component analysis |
| PNS | peripheral nervous system |
| ppm | parts per million |
| PT/PTT | partial thromboplastin time |
| RF | radiofrequency |
| RNA | ribonucleic acid |

| | |
|------|-------------------------------|
| S/N | signal to noise ratio |
| SULT | sulfotransferase |
| T | Tesla |
| TMAO | trimethylamine N-oxide |
| TSP | trimethylsilyl propionic acid |
| UDP | uridine diphosphate |
| UGT | UDP-glucuronosyl transferase |
| WBC | white blood cell |

1 Introduction

In order to suitably familiarize the reader with the material presented in this dissertation, the first chapter provides an appropriate introduction to the background for a few of the main subjects addressed. This dissertation is divided into three main parts. Chapter 1 is the introduction, providing background information relevant to the research presented in the following parts. The following section comprises three chapters, with the motivation of them originating from trying to better understand the effects, nontoxic and toxic, of acetaminophen in humans. Chapters 2 and 3 of the dissertation are on the subject of multivariate statistical metabolomics and Chapter 4 involves stable isotope metabolomics. Chapter 5 is a concluding chapter which discusses the pitfalls as well as future directions for the research. Finally, there are two appendices detailing work done creating stable isotope rat hepatocyte cultures which did not fit into any of the other chapters. The first multivariate statistical metabolomic experiment investigates the capacity for normalization of the human urinary and blood metabolome in a controlled clinical setting in order to determine the suitability of the study design for a metabolomic study. Next, the effects (hepatotoxic and otherwise) of acetaminophen on the human urinary metabolome were examined to create multivariate statistical models to predict and describe future manifestations of hepatotoxicity.

The work presented in the dissertation then shifts to take a stable isotope metabolomic-based approach for the study of acetaminophen toxicity in fresh and cryopreserved cultured primary human hepatocytes in an attempt to better understand the changes in metabolism caused by the acetaminophen. It involves tracking hepatocyte

metabolism by supplying them ^{13}C enriched media precursor metabolites substituted for their “normal” ^{12}C counterpart in media containing acetaminophen. Additionally, the peculiar metabolic phenotype of the human hepatocytes was compared to primary rat hepatocyte metabolism, again assayed via the tracking of metabolic products from ^{13}C -enriched metabolite precursors. Following this is a short section summarizing the totality of this dissertation with a description of potential future directions the results of this research have uncovered. Finally, information regarding the creation of a primary rat hepatocyte culture system which utilizes stable isotope enriched media formulations is presented in two appendices.

1.1 Nuclear Magnetic Resonance (NMR) Spectroscopy

1.1.1 History

The first publication of the observation of proton magnetic resonance occurred in 1946 by Felix Bloch and Edward Mills Purcell [1]. The first experiments were continuous wave (CW) NMR. In CW-NMR the frequency response of a system is probed by either modulating the strength of the magnetic field (which changes the resonant frequency of a given proton) or by modulating the frequency of the radiofrequency (RF) signals. These experiments suffered from poor signal-to-noise (S/N) ratios and took a long time. Fourier transform NMR (FT-NMR) solved these problems to an extent by irradiating the system with an RF signal containing all the frequencies of interest and recording the system response. FT-NMR also allowed for an increase in the S/N ratio by enabling one to repetitively acquire data opposed to the non-repetitive nature of CW-NMR. The frequency response of the system is obtained by a process known as Fourier transformation (FT).

1.1.2 The NMR Phenomenon

Atomic nuclei have a property called nuclear spin. This spin is quantized by a nuclear spin quantum number, I , which is greater than or equal to zero and is a multiple of $\frac{1}{2}$ [1]. It is this property of nuclear spin which makes nuclear magnetic resonance possible. When in the presence of a large external magnetic field, nuclei with a nonzero value line up parallel or antiparallel to the magnetic field. A small population excess of nuclei, approximately 1 nucleus per 1000000 at 1.5 T for example, align parallel to the field. The population difference increases with increasing magnetic field. The NMR spectroscopist relies on this excess to generate an NMR spectrum. The sensitivity of an NMR spectrometer is a measure of the minimum number of spins detectable. Thus, as the magnetic field increases (or temperature decreases), the population difference between the two energy states increases, increasing the sensitivity. However, NMR is not especially sensitive when compared to other methods such as mass spectrometry.

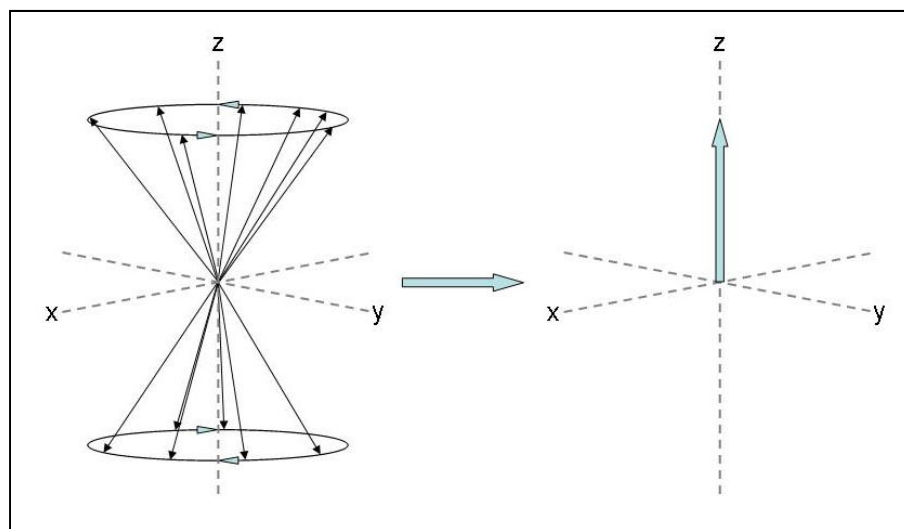


Figure 1-1- The many spins on the left can be simplified to the vector model on the right due to the slight excess of ($-1,000,001$ to $1,000,000$ at 1.5 T) that line up with the field rather than against the field.

The spinning nuclei can be modeled with classical mechanics and can be compared to a spinning toy top. The Earth's gravitational field would model the applied magnetic field. When one spins the top, it rotates as well as precesses; this behavior is similar to that of a nucleus in an external magnetic field. The spinning nucleus possesses angular momentum P as well as a gyromagnetic ratio γ , which is constant for any given isotope. The angular momentum and gyromagnetic ratio are used in the following equation to define the magnetic moment:

$$\mu = \gamma P$$

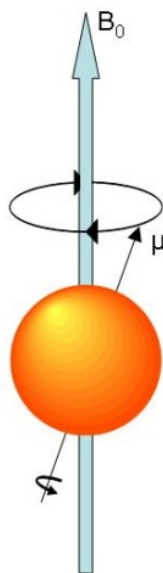


Figure 1-2- A nucleus with magnetic moment μ , lines up with and precesses about a static magnetic field B_0 .

1.2 The ^1H NMR Experiment

One of the simplest experiments one can do in NMR spectroscopy is to irradiate the sample for a few milliseconds with a radiofrequency (RF) pulse and observe the effects for a

few seconds after the irradiation. This would be repeated a number of times. There is a delay of usually a few seconds before repeat irradiation to allow the system to return to equilibrium. The irradiation pulse, also known as the acquisition or P1 (or 90° if applicable) pulse, irradiates the sample in the transverse plane (the x-y plane in Figure 1-1). According to the right-hand rule of electromagnetism, the vector model of the spins (the picture on the right side of Figure 1-1) will absorb energy from the applied RF pulse of a frequency specific to the chemical environment the nucleus is in, its resonant frequency, and will experience torque towards the transverse plane.

In a B_0 field of 9.4 T, protons precess, or resonate, about the B_0 field at a frequency of approximately 400 MHz. Thus a spectrometer with a 9.4 T magnet is frequently referred to as a 400, a 14.1 T magnet is frequently referred to as a 600, and a 16.4 T magnet is frequently referred to as a 700. If one were to visualize vector models of protons in the presence of a B_0 magnetic field from the perspective of a specific proton, that is the proton no longer spins but it is the outside world that is now spinning (known as the rotating frame of reference), one would get a picture similar to the picture in Figure 1-1. Since there are slightly more protons aligned with the magnetic field, all of the individual protons in equal chemical environments could be simplified to a single resultant vector, the picture on the right side of Figure 1-1. Now, still in the rotating frame of reference of a specific proton, if an RF pulse at a certain frequency were emitted along the +x axis for a specific amount of time, the resultant proton vector would be in the +y axis after irradiation (it would go farther around if the irradiation were longer and/or more powerful and less far if the irradiation were shorter and/or less powerful). The vector would then travel from the high energy state of being aligned with the +y axis back to the low energy state of being aligned with the +z axis in a few seconds,

releasing energy in the RF frequency range. This energy induces current flow in metal coils inside the NMR probe which are extremely close to the sample. The current is recorded and is called a free induction decay (FID). NMR spectroscopists are usually not interested in the FID, *per se*. What is most interesting is the frequency domain spectrum of the time domain FID. The FID is transformed into the frequency domain using the fast Fourier transform (FT). Because of this, NMR spectroscopy is often referred to as Fourier Transform- Nuclear Magnetic Resonance Spectroscopy (FT-NMR). The signal for ethanol is shown in both the time domain (FID) and in the frequency domain in Figure 1-3. It is apparent from the FID that the signal consists mainly of two different frequencies due to its periodic nature.

It can be seen by examining the spectrum of ethanol in D₂O in Figure 1-3 that the two signals, one from the CH₃ protons and the other from the CH₂ protons, are a quartet and a triplet. Protons bonded to atoms adjacent to another atom containing protons (that is protons 3 bonds away from other protons) split each other's peak according to the $n+1$ rule. That is, a signal which is split by n protons results in $n+1$ peaks. In addition, peak area is proportional to the number of protons generating the peak. In the case of ethanol, the CH₃ proton peak is split by the CH₂ protons resulting in a triplet of relative area 3. The CH₂ protons will be split by the CH₃ protons resulting in a quartet of relative area 2. The OH protons are not visible and do not cause splitting in this case because they disassociate from ethanol in the presence of D₂O. All of the above, in addition to the fact that NMR is nondestructive, makes NMR a powerful tool in substrate identification and quantification.

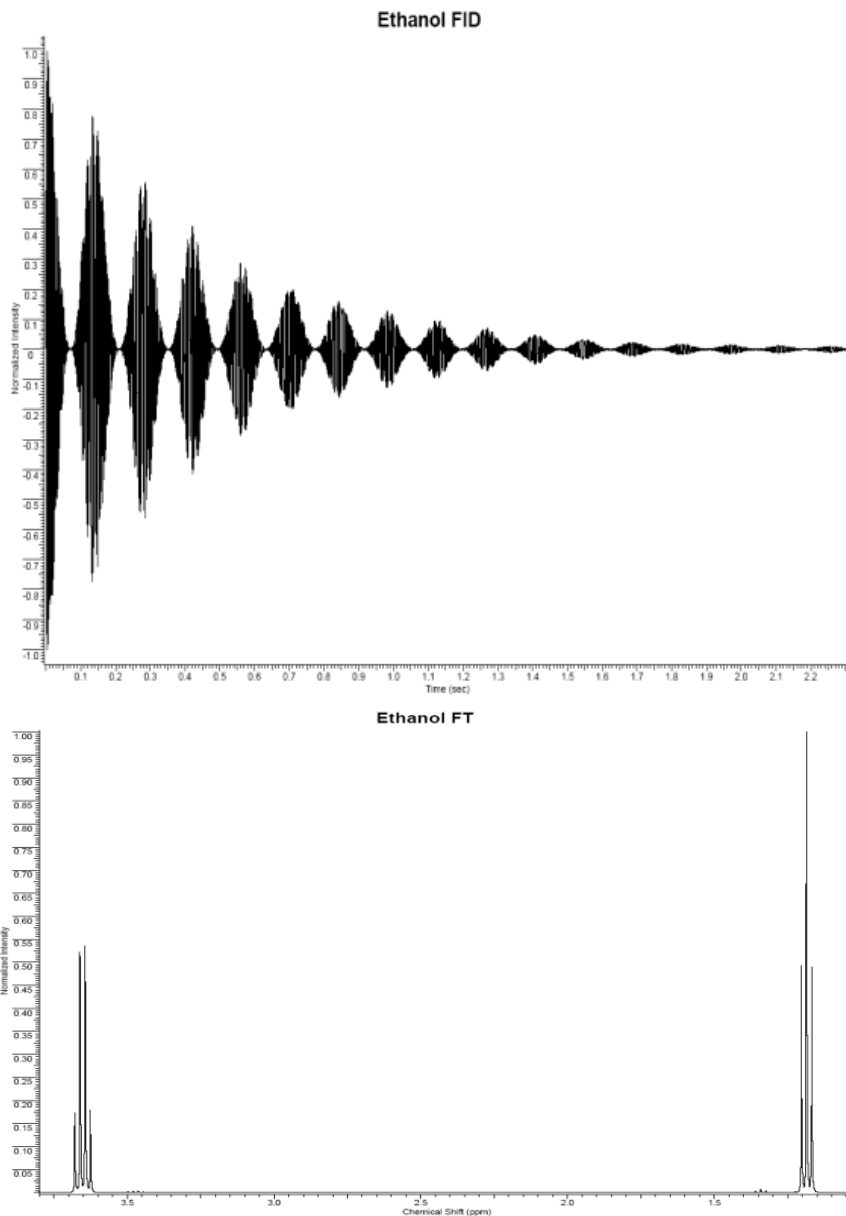


Figure 1-3- The free induction decay (FID) and corresponding Fourier transform (FT) of ethanol ($\text{CH}_3\text{CH}_2\text{OH}$) in deuterium oxide (D_2O).

1.2.1 Spectral Processing

After acquisition, there are a number of things that are done to the FID and the spectrum coming from the FID after Fourier transformation to enhance the quality of the data. One of the first things is to zero fill the FID. This appends a series of extra data points with a magnitude of 0 to the end of the FID. This enhances the digital resolution of the

resulting spectrum thus enhancing the lineshape of the signals in the spectra. The abrupt change in the magnitude in the FID at the spot where zero filling begins has adverse effects in the frequency domain resulting in sinc wiggles at the base of peaks. To counter this problem, an exponentially decaying window function is applied to the FID so that it decays more smoothly. Additionally, this window function serves to increase the S/N (at the expense of resolution) by attenuating the noise at the end of the FID.

FIDs are then Fourier transformed to observe them in the frequency domain. One of the first problems observable in the spectra are phase problems due to the fact that there are two orthogonal signal receivers. Some peaks may be in phase, 180° out of phase (characterized by an upside down peak), 90° out of phase (characterized by a peak shape of one side of the peak going up with the other side going down), or anywhere between 0° - 360° . Traditionally, phasing was done manually. Currently automatic phasing routines are regularly employed when analyzing numerous spectra. The spectra are then generally baseline corrected to flatten rolling baselines which makes peaks easier to identify and quantify.

The spectra must then be referenced. This is commonly done with trimethylsilyl propionic acid (TSP) or dimethyl-silapentane-sulfonic acid (DSS) in aqueous samples and tetramethylsilane (TMS) in organic samples. TSP is assigned the position in the spectra at 0 ppm. Since each spectrum consists of thousands of points, NMR spectra are frequently split along the x-axis if multivariate statistical analyses are being performed, to make the analysis and interpretation easier. The value of each bin is defined by the integral value of the spectrum occupying the bin area. Commonly, the area from 0 – 10 ppm, with the exception of the H_2O and urea peaks in urine, is binned with a bin size of 0.04 ppm. This results in

about 200 bins. Unbinned spectra are usually used to determine concentrations of identified compounds in the sample if multivariate statistical analyses are not being conducted.

Individual peaks are generally integrated or a peak fitting routine is employed for this type of measurement.

1.3 Metabolomics- Multivariate Statistics

1.3.1 Principal Component Analysis (PCA)

Principal component analysis, also known as the Karhunen-Loève transform, is a method in which multivariate, multidimensional data is simplified by choosing new orthogonal axes that maximize variance about the new axes. It is a method of data or dimension reduction. The axis describing principal component 1 (PC 1) is the dimension in the cluster of data which has the most variance. PC 2 is the next axis, orthogonal to PC 1, which encompasses the most remaining variance. The same goes for PC 3, PC 4, PC 5, etc. Figure 1-4 shows the result of PCA on trivial hypothetical data. Examining the figure, one can see that neither the x nor the y axes capture the spread of the data as well as the PC 1 axis.

To apply PCA on NMR data, the relatively continuous spectra must be made discrete by dividing spectra into pieces (bins) along the x-axis and integrating each piece. This changes spectra into histograms. One could take 100 NMR spectra consisting of 200 bins and express them all in 1 graph as single points in 200 dimensional space. This is purely a mathematical expression, as 200 dimensions cannot be visualized. Each of the 200 dimensions represents 1 bin and the distance along a given dimension represents the integral

value for that particular bin. PCA can be performed on data represented in this manner simplifying it making it possible to visualize most of the data.

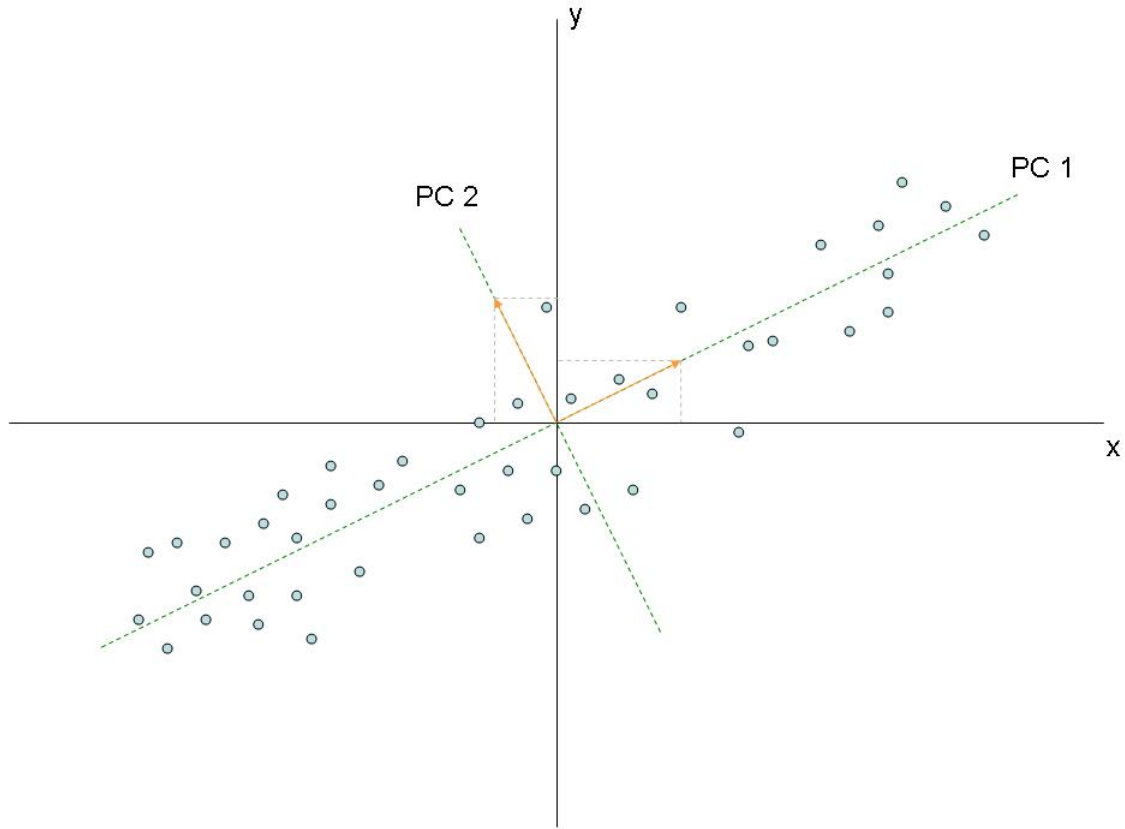


Figure 1-4- Simulated principal component analysis performed on two dimensional data recorded on x and y axes.

To perform PCA, the first step is to subtract the average value of a variable from each of the variables (for variable i in sample s):

$$V_{is} = V_{is} - \bar{V}_i \quad \text{for all } V_{is}$$

Next, the covariance matrix across all variables for all samples is calculated:

$$\text{Cov} = \begin{bmatrix} \text{cov } V_1 V_1 & \text{cov } V_1 V_2 & \text{cov } V_1 V_3 & \cdots & \text{cov } V_1 V_n \\ \text{cov } V_2 V_1 & \text{cov } V_2 V_2 & \text{cov } V_2 V_3 & \cdots & \text{cov } V_2 V_n \\ \text{cov } V_3 V_1 & \text{cov } V_3 V_2 & \text{cov } V_3 V_3 & \cdots & \text{cov } V_3 V_n \\ \vdots & \vdots & \vdots & \ddots & \vdots \\ \text{cov } V_n V_1 & \text{cov } V_n V_2 & \text{cov } V_n V_3 & \cdots & \text{cov } V_n V_n \end{bmatrix}$$

Where $\text{cov } V_1 V_2$ would be the covariance between variable 1 and variable 2 for all samples and would be calculated by the following formula:

$$\text{cov } V_1 V_2 = [(V_{11} - \bar{V}_1) \dots (V_{2n} - \bar{V}_2)]/n$$

Next, the eigenvalues and eigenvectors of the covariance matrix are calculated. The eigenvalues and their corresponding eigenvectors are sorted in decreasing order such that PC1 has the highest eigenvalue and thus contains the most variance of the data. Now the eigenvectors define the principal component and their associated eigenvalues represent how much variance the individual eigenvectors contain. To identify significant components, a scree test can be performed. This is a subjective test where the point of maximum inflection in the plot of eigenvalues versus PC number is identified. Principal components to the left of this point are then deemed significant and components to the right of this point are deemed insignificant.

One important piece of information obtained from PCA are the loadings plots of the principal components. The loadings plots from Figure 1-4 are shown in Figure 1-5. Loadings plots are generated by taking the unit vector representing a given PC and decomposing it to the component vectors. In the case of NMR spectra, this allows one to

determine how much each bin contributes to a given principal component. One can thus draw conclusions such as- bin X is the largest peak in the loadings plot for PC 1 and is therefore the largest contributor to the variance of the data set. The peak in bin X comes from metabolite Y and so this metabolite is a large contributor to the bin. Since this bin is one of the most significant contributors to PC1 then metabolite Y is one of the most significant metabolites describing this component. This is the method in which PCA can be used to identify potential biomarkers in biofluids.

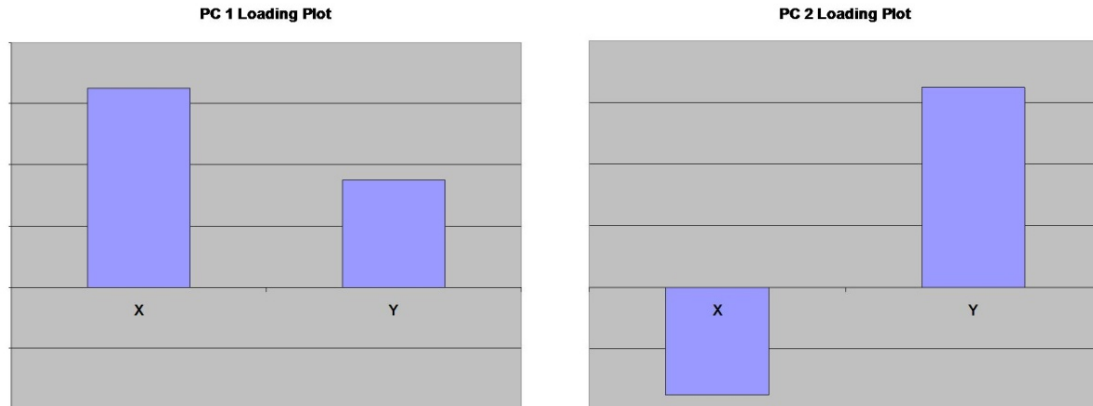


Figure 1-5- Loadings plots from Figure 1-4.

One use of PCA would be to perform the analysis on all of the samples from different time points of an experiment. An expectation of this would be that the points would track along a certain trajectory through time, possibly in response to some stimulus. Or, one could perform PCA on predose and postdose samples from an experiment. In these cases, loading plots for significant principal components could be used to determine biomarkers indicative of a temporal or dose dependant metabolic response, respectively. The metabolite(s) located in the bins with the largest peaks in the loadings plots could then be identified and graphed over time to determine metabolic response to the experimental stimulus. Another way to get

similar data to draw conclusions would be to perform biased analyses, such as orthogonal partial least squares discriminant analysis, described in the next section.

1.3.2 Orthogonal Partial Least Squares Discriminant Analysis (OPLS-DA)

To discuss OPLS-DA, one should first start with PLS-DA. PLS-DA is a multivariate statistical method which is somewhat similar to PCA. However, unlike PCA, which finds orthogonal dimensions in the data which capture maximal variance, PLS-DA finds orthogonal dimensions in the data which best describe class separation (or discrimination) using a partial least squares method. The results for PCA and PLS-DA are presented in similar ways, with scores plots and loadings plots. However, since this analysis is biased, care must be taken to not over fit the data. This is always a potential problem with using guided analyses consisting of data with more variables than samples, which is frequently the case with metabolomic analyses since NMR spectra from biofluids frequently contain hundreds of peaks. One method to check for over-fitting would be to perform cross validation, which is not something which is necessary with PCA since it is unbiased.

OPLS-DA is similar to PLS-DA. However, OPLS-DA defines dimensions in the data, orthogonal to the two dimensions defining class separation, which capture maximal remaining variance. Presumably, these dimensions contain data unrelated to class separation and can thus be removed. Generally, this also makes class separation in the scores plot look better and subsequent removal of more orthogonal dimensions causes the class separation in the scores plot to further improve. However, the data remains the same, so care must be taken to not over fit the data through removal of too many orthogonal dimensions and therefore, only 1 dimension is generally removed.

1.4 Acetaminophen

1.4.1 History

Acetaminophen (paracetamol, *N*-acetyl-para-aminophenol, APAP) is a common antipyretic and analgesic that is used worldwide and is known to be, for the most part, very safe. Acetaminophen was first synthesized in 1873; however, it was not medically used for another two decades [2]. At the time, acetanilide and phenacetin were popular antipyretic drugs. These two drugs were determined to have toxic side effects. Acetaminophen was discovered to be a metabolite of acetanilide and phenacetin, having the antipyretic and analgesic effects without the toxic side effects. In 1955, Acetaminophen first went on sale in the United States under the name Tylenol. The following year acetaminophen went on sale in the United Kingdom under the name Panadol.

1.4.2 Analgesia & Antipyresis

Arachidonic acid, a 20 carbon polyunsaturated fatty acid, is present in the cell membrane [3]. It is metabolized to prostanoids by cyclooxygenase (COX) enzymes. There are two known forms of the COX enzyme: COX-1 and COX-2. COX-1 is constitutively expressed in normal tissues. COX-1 expression plays a role in maintaining homeostatic pathways [4]. COX-2 is induced by cytokines in inflammatory cells at localized sites of injury [2]. When present in the cell, COX-2 catalyzes the formation of prostaglandins from arachidonic acid. Prostaglandins formed from COX-2 increase the sensitivity of nociceptors thus lowering the threshold for pain. Because acetaminophen does not have much of an effect outside of the CNS some think that there may be a third cyclooxygenase isoform,

COX-3, present only in the central nervous system (CNS), upon which acetaminophen acts [5]. Other pain relief drugs such as aspirin and ibuprofen are able to do this in the periphery and therefore, they have anti inflammatory properties. Aspirin, and to a lesser extent ibuprofen, also have gastrointestinal consequences due to COX-1 inhibition in the stomach. The appeal of acetaminophen is very much due to its lack of gastrointestinal toxicity due to its selective COX-2 inhibition.

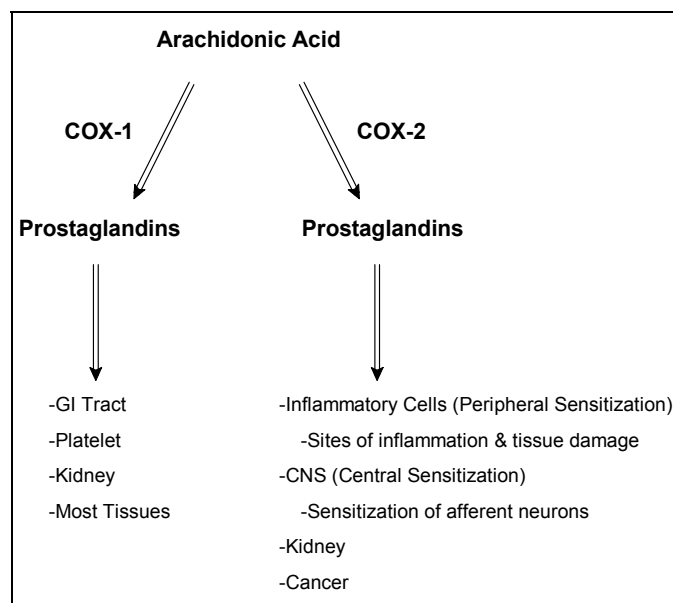


Figure 1-6- Arachidonic acid pathway.

Acetaminophen is often considered to be in a family of drugs known as non-steroidal anti-inflammatory drugs (NSAIDs) because of its analgesic and antipyretic properties. Acetaminophen does not however, have any anti inflammatory properties and is thus not an NSAID. While the mechanism of action is not entirely clear, it is believed that acetaminophen interferes with the synthesis of prostaglandins in the CNS possibly by inhibiting the action of COX thus increasing the threshold for pain.

Acetaminophen is also known to be an effective antipyretic. The hypothalamus is the part of the brain where body temperature is regulated. Inhibition of prostaglandin synthesis in the hypothalamus is likely the cause of the antipyretic effects of acetaminophen seen in the febrile patient.

1.4.3 Pharmacokinetics

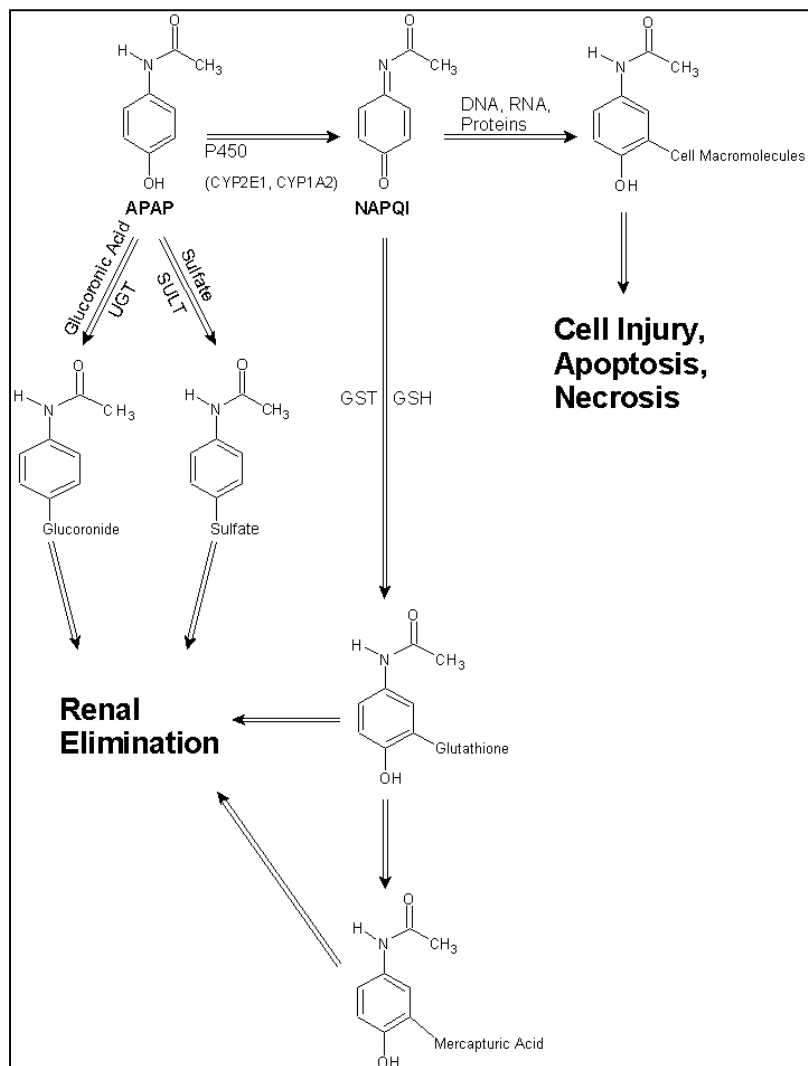


Figure 1-7- Metabolism and elimination of acetaminophen (APAP). UGT = UDP-glucuronosyltransferase, SULT = sulfotransferase, GSH = glutathione, GST = glutathione s-transferase.

Acetaminophen is rapidly and almost completely absorbed in the gastrointestinal tract [6]. Peak blood concentration is attained 30 - 60 minutes after ingestion and the half-life in blood is approximately 2 hours [6]. In the adult, approximately 90% of the acetaminophen is excreted in the urine within 24 hours as the glucuronide (50 - 60%), sulfate (30 - 40%) or cysteine (3 - 10%) metabolite [7, 8]. Small amounts of the drug (larger amounts for alcoholics or those taking super therapeutic doses) are metabolized by the cytochrome P450 system (P450).

1.4.4 Cytochrome P450

The liver is the primary detoxifying organ. A robust mechanism for detoxification is necessary due to the number of toxins and toxicants that the body has the potential to be exposed to. There are two phases of drug metabolism, phase I and phase II, with phase I metabolism frequently, but not always, preceding phase II metabolism. Phase I metabolism generally oxidizes, reduces, hydrolyzes, cyclizes, or decyclizes a xenobiotic to increase polarity of the molecule. One of the main mediators of oxidation is the cytochrome P450 set of enzymes. Intermediate metabolites of a drug can be created in this step. While generally, the purpose of phase I metabolism is to polarize a xenobiotic to facilitate excretion or phase II conjugation, sometimes xenobiotics are activated, inactivated, or metabolized to toxic compounds. Phase II metabolism is a conjugation reaction where the xenobiotic is usually bound to glucuronide, sulfonate, amino acids, methylated, or acetylated [9]. The phase II conjugated xenobiotic is generally, but not always, inactivated and more readily excreted in the urine than the parent drug.

Cytochromes P450 are located in the endoplasmic reticulum or inner membrane of the mitochondria of hepatocytes [10, 11]. About 60 different isoforms have been identified in man [12]. These isoforms are grouped into families according to genetic homology. Several P450 isoforms are involved in the synthesis of steroid hormones and bile acids, and the metabolism of retinoic acid and fatty acids, including prostaglandins and eicosanoids. Approximately 15 isoforms of P450 are involved in the metabolism of various xenobiotics [12]. The majority of xenobiotics that interact with P450 produce changes in the chemical resulting in easier urinary elimination. However, this system is not perfect. In the case of acetaminophen, a small amount is metabolized by P450 to yield the highly unstable and toxic intermediate *N*-acetyl-*para*-benzoquinone imine (NAPQI). NAPQI will oxidize and conjugate to cysteine groups on proteins [13] as well as DNA and other cellular macromolecules if the concentration of the antioxidant glutathione becomes too low. In addition, NAPQI appears to target mitochondria causing mitochondrial damage. It has been demonstrated with knockout mice that CYP2E1 and to a lesser extent CYP1A2 are the main P450 isoforms responsible for NAPQI formation from acetaminophen [12].

Unlike many other P450 subfamilies, the CYP2E subfamily consists of a single isoform, CYP2E1 which is constitutively expressed in many tissues- hepatic and extra-hepatic. Ethanol is a major inducer of CYP2E1 expression with low levels of ethanol increasing protein stability and high levels of ethanol inducing CYP2E1 mRNA transcription [14-16]. This is the mechanism by which ethanol induces acetaminophen hepatotoxicity. This induction in addition to the poor nutritional status of many alcoholics can make acetaminophen especially dangerous with hepatotoxicity and liver failure occurring even at therapeutic acetaminophen doses. Additionally, acetone and acetal are also known CYP2E1

inducers. Induction of CYP2E1 and metabolism of acetone and acetal are important for the gluconeogenic salvage pathway, which is activated in periods of glucose starvation [10].

In addition to acetaminophen, there are many other substrates for CYP2E1 including nitrosamines, the solvents toluene, benzene, carbon tetrachloride, and ethylene glycol and the anesthetics halothane, isoflurane, and enflurane. The above mentioned solvents and ethylene glycol are also inducers of CYP2E1 [10].

The human CYP1A isoform family consists of CYP1A1 and CYP1A2. While CYP1A1 is mainly expressed extra-hepatically, CYP1A2 is expressed almost exclusively in the liver and is inducible on exposure to cigarette smoke and consumption of charbroiled foods and cruciferous vegetables [10, 17]. Insulin, in diabetics, and the barbiturate phenobarbital are also inducers. Induction of CYP1A2 (and also CYP1A1) is initiated by the cytosolic aryl hydrocarbon (Ah) receptor. A ligand-bound Ah receptor is translocated into the nucleus upon association with the aryl hydrocarbon nuclear translocator protein (ARNT). This complex is then able to bind to the xenobiotic response element (XRE) in the promoter region of the CYP1A gene thus initiating transcription. Ah receptor knock-out mice have lost the ability for CYP1A induction [10]. Additionally, human CYP1A2 protein levels have been shown to vary > 40-fold [10].

CYP1A2 metabolizes nitrosamines and arylamines. In addition to the aforementioned acetaminophen, the NSAID naproxen is also a substrate of CYP1A2. Additionally, caffeine, phenacetin, and theophylline, are also substrates of CYP1A2 which have been used to assay for CYP1A2 activity [10]. Due to the nature of P450 isoforms, there many more known substrates, inhibitors, and inducers of CYP1A2.

1.4.5 Toxicity

Therapeutic doses of ~1 – 4 g/day of acetaminophen are generally considered safe. Taken in doses greater than 150 mg/kg/24 hr (>7.5 g - 10 g), acetaminophen is a well-recognized cause of hepatotoxicity [18, 19]. Acetaminophen poisoning is the number one cause of acute liver failure in the United States as well as United Kingdom [19, 20]. About 20% of untreated patients with acetaminophen poisoning will develop severe hepatic injury. This is defined by an aspartate aminotransferase (AST) level above 1000 U/L [19]. Both AST and alanine aminotransferase (ALT) levels in the blood are good indicators of liver fitness. AST and ALT are two enzymes present in hepatocytes at high concentrations which is leaked into the bloodstream upon liver injury due to hepatocyte necrosis. Therefore, an increase in hepatocyte death due to toxic insult should cause ALT and AST levels in the blood to rise. Increases in ALT and AST levels are commonly caused by chronic events such as hepatitis and alcoholism as well as acute events such as poisoning [21].

The small amount of NAPQI formed from therapeutic doses of acetaminophen by the P450 system usually conjugates with reduced glutathione (GSH). Generally, this is metabolized to mercapturic acid and eliminated [6]. For there to be toxicity to the liver, NAPQI must be present at a concentration above the concentration of glutathione. This can either be due to high levels of NAPQI or low levels of glutathione. High levels of NAPQI formation can happen in an overdose and glutathione depletion can occur because of malnourishment or alcoholism. Excess NAPQI can cause hepatocytes to undergo oxidative stress because NAPQI is unstable and highly reactive. The NAPQI binds to thiol residues of proteins when glutathione concentrations are too low, this is discussed in further detail in

Section 1.4.6 of this dissertation. This oxidative stress can lead to cell death and necrosis of regions of the liver.

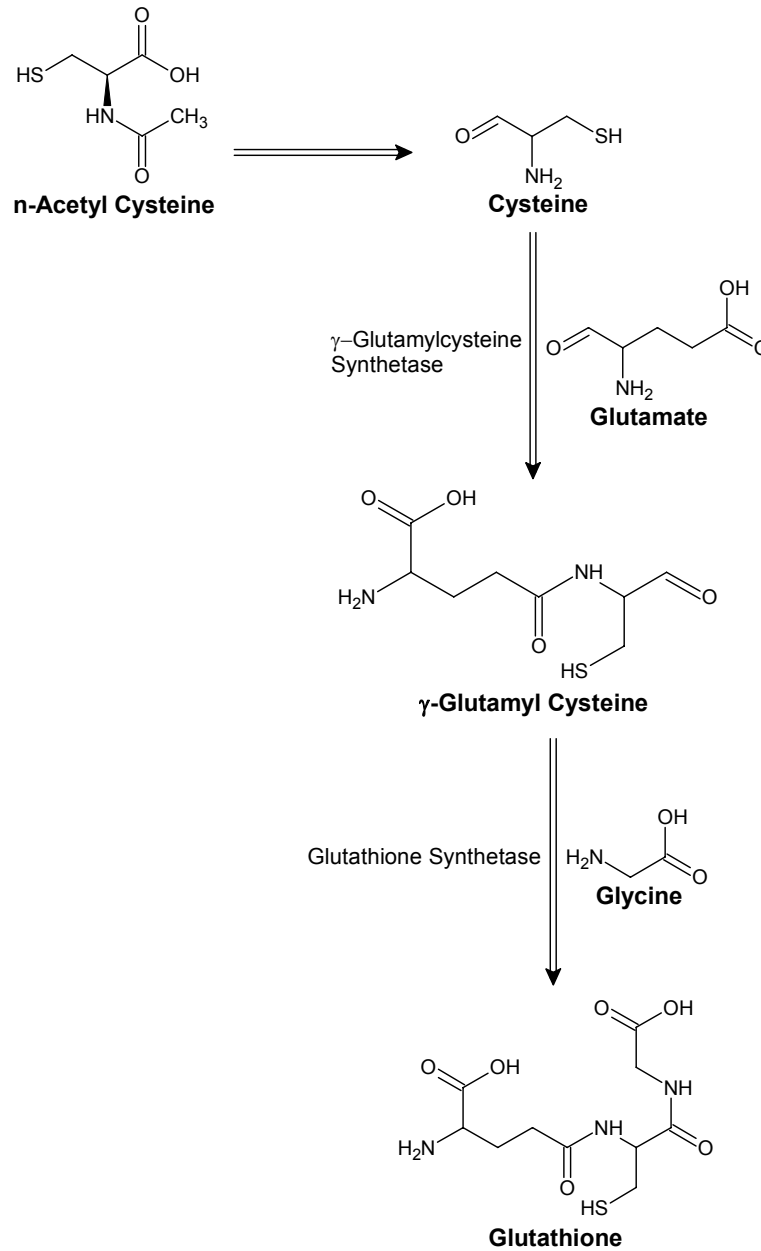


Figure 1-8- In vivo production of glutathione.

Hepatic necrosis is first evident in zone III hepatocytes. This is because periportal hepatocytes (zone I hepatocytes) do not express cytochromes P450. This is fortunate for the mild to moderate overdose victim as the damaged liver may be able to repopulate the dead hepatocytes in zone III. Massive overdoses however can lead to total liver failure.

Early symptoms of acetaminophen poisoning include nausea, abdominal pain, and liver tenderness. Many patients do not experience any of these symptoms [20]. Within 24 hours of overdose, the patient may become jaundiced; hepatic enzyme blood concentration may also increase in this time [20].

The treatment of choice for acetaminophen overdose is administration of n-acetyl cysteine (NAC) [2, 6, 9, 13, 19, 20]. NAC is chosen over glutathione or cysteine because glutathione and cysteine cannot easily enter hepatocytes. NAC is the n-acetylated form of cysteine and both serves as a source of cysteine for glutathione production as well as a substitute for glutathione for conjugating with NAPQI [20]. As an antidote, NAC is most effective if administered within 8 hours of overdose, however clinical evidence has demonstrated that NAC administration from 24h to 72h after overdose is beneficial [20].

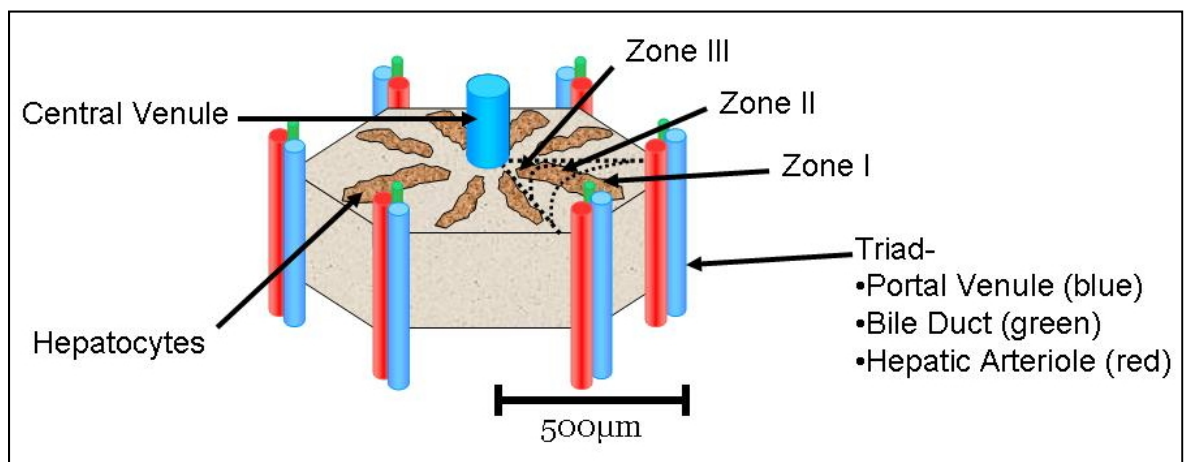


Figure 1-9- The liver lobule [22].

1.4.6 Protein Targets of Acetaminophen

The reactive intermediate of acetaminophen, NAPQI, is highly unstable and usually quickly reacts with glutathione. When there is more NAPQI than glutathione, the NAPQI starts to bind with cellular macromolecules. As mentioned in the previous section, P450 is located in the endoplasmic reticulum and the inner membrane of the mitochondria. Thus, this is where the majority of NAPQI will be produced in the hepatocytes. Since NAPQI is highly unstable and reactive, proteins present in the ER and mitochondria are likely to be the ones arylated by NAPQI. However, it is worth noting that the ER is a large organelle which is intertwined and has contact sites with virtually all of the cellular organelles including the nuclear membrane, mitochondria, peroxisomes, the Golgi apparatus, and the plasma membrane [23]. Some of these proteins arylated by NAPQI have been identified as being Glutamine Synthetase, Lamin A, Selenium-Binding Protein, Glutamate Dehydrogenase, Aldehyde Dehydrogenase, N10-Formyl Tetrahydrofolate Dehydrogenase, and Carbamyl Phosphate Synthetase I [24].

Some potential consequences manifested as changes in metabolite concentrations due to acetaminophen toxicity can be identified. Since glutamine synthetase catalyzes the reaction creating glutamine from glutamate and ammonia and glutamate dehydrogenase catalyzes the reaction deaminating glutamate to form α -ketoglutarate and ammonia, acetaminophen toxicity would likely cause a decreased utilization of glutamate, a buildup of ammonia, and thus a decreased utilization of glutamine (into TCA). This decreased utilization of glutamine may be mitigated by a decreased production of glutamine from glutamate.

| Mass (kDa) | Fraction | Protein | Reaction/Function |
|------------|--------------------------|--|--|
| 29 | Cytoskeleton | Tropomyosin 5 | Actin-binding protein, muscle contraction |
| 32 | Cytosol | 3-Hydroxyanthranilate 3,4-dioxygenase | 3-hydroxyanthranilate + O ₂ <-> 2-amino-3-carboxymuconate semialdehyde |
| 16 | Cytosol | Aryl sulfotransferase | A phenol + 3'-phosphoadenylyl sulfate <-> an aryl sulfate + adenosine 3',5'-bisphosphate |
| 29 | Cytosol | Carbonic anhydrase III | CO ₂ + H ₂ O <-> HCO ₃ ⁻ + H ⁺ |
| 32 | Cytosol | Glycine N-methyltransferase | SAM + Gly <-> SAH + sarcosine |
| 45 | Cytosol | Methionine adenosyl transferase | Met + ATP -> SAM |
| 100 | Cytosol | N-10 Formyl THF dehydrogenase | Folic acid metabolism |
| 28 | Cytosol | Proteasome subunit C8 | Subunit of a proteasome, protein degradation |
| 55 - 58 | Cytosol | Selenium (acetaminophen) binding protein | Antioxidant? |
| 40 | Cytosol | Sorbitol dehydrogenase precursor | sorbitol -> fructose (reaction enzyme precursor) |
| 22 | Cytosol (Macrophages) | Osteoblast-specific factor 3 | Osteoblast recruitment, attachment, and spreading |
| 29 | Cytosol, Microsomes | Thioether S-methyltransferase | SAM + dimethyl sulfide <-> SAH + thiomethylsulfonium |
| 22 | Cytosol, Mitochondria | Glutathione peroxidase | Peroxidase, protects from oxidative damage |
| 23 | Cytosol, mitochondria | Glutathione transferase π | Catalyze GSH conjugation |
| 44 | Microsomes | Glutamine synthetase | Glu + NH ₃ -> Gln |
| 59 | Mitochondria | ATP synthetase α-subunit | Subunit of ATP synthase (ADP + P _i -> ATP) |
| 50 | Mitochondria | Glutamate dehydrogenase | Glu -> αKG + NH ₃ |
| 28 | Mitochondria | Housekeeping protein | Housekeeping protein |
| 54 - 56 | Mitochondria, Cytosol | Aldehyde dehydrogenase | RCHO -> RCOOH |
| 36 | Mitochondria, Peroxisome | 2,4-Dienoyl-CoA reductase | β-oxidation (of unsaturated fatty enoyl-CoA esters) |
| 32 | Not known | Pyrophosphatase | RPO ₄ -PO ₄ -> RPO ₄ + PO ₄ |
| 74 - 75 | Nucleus | Lamin-A | Constituent of nuclear lamina, membrane |
| 35 | Peroxisomes | Urate oxidase | Uric acid -> 5-hydroxyisourate (Enzyme lost in humans?) |
| 46 | Ribosomes | Protein synthesis initiation factor 4A | Involved in binding mRNA to ribosome |

Table 1-1- List of protein targets of NAPQI.[13, 24-26]

The mitochondrial enzyme carbamoyl phosphate synthetase I catalyzes the transfer of an ammonia from glutamine to a phosphorylated bicarbonate resulting in carbamate and glutamate (the carbamate is subsequently phosphorylated to create carbamoyl phosphate for entry into the urea cycle). Inhibition of this enzyme would lead to an increase of ammonia, which has been reported in rats [27] and mice [28]. Ammonia inhibits the catalysis of glutamine to glutamate via glutaminase [29, 30]. In a fed state in organisms and in cell culture, glutamate entering the TCA cycle is derived primarily from glutamine and not proteolysis. Therefore, one would expect an increase in the glutamine:glutamate ratio with increasing NAPQI due to the decreased utilization of glutamine via carbamoyl phosphate and glutaminase. ¹³C-glutamine replacement in culture media is an ideal means to test this hypothesis.

As far as the other proteins, lamin A is a constituent of the nuclear lamina which is a 2D matrix of proteins located next to the inner nuclear membrane. Since it is not an enzyme, acetaminophen binding should not have a significant effect on metabolite concentrations. However, the nuclear lamina is associated with the inner face of the nuclear membrane while the outer face is continuous with the ER. Thus, lamin A is positioned close to the organelle where NAPQI is likely to be formed, the ER. Selenium-binding protein is a protein of uncertain function. It is hypothesized to play a protective role as an antioxidant in the case of glutathione depletion due to its high concentration in the liver and the fact that it is highly nucleophilic [24].

Aldehyde dehydrogenase has many isoforms and the substrates for some of them are unknown. Substrates which could potentially be significant to metabolism (in the sense that they are not vitamins but endogenous metabolites which play key roles in metabolic pathways) are glutamate semialdehyde and methylmalonate semialdehyde. The isoform that metabolizes glutamate semialdehyde (ALDH4A1) catalyzes the second step of the proline degradation pathway, converting 5-carboxylate to glutamate. Inhibition of this enzyme could lead to a decrease in glutamate, further supporting the hypothesis that NAPQI exposure would lead to an increase in the glutamine:glutamate ratio. The isoform that metabolizes methylmalonate semialdehyde catalyzes the conversion of malonate semialdehyde and methylmalonate semialdehyde to acetyl- and propionyl-CoA. Inhibition of this enzyme could lead to a decrease in substrates for the TCA cycle.

Finally, N10-formyl tetrahydrofolate dehydrogenase catalyzes the formation of tetrahydrofolate from N-10-formyl tetrahydrofolate. This is an essential part of folic acid (vitamin B9) metabolism. N10-formyl tetrahydrofolate catalyzes the formation of

tetrahydrofolate from 10-formyltetrahydrofolate [31]. Tetrahydrofolate is then methylated using glycine, serine, or formaldehyde as a methyl donor to form methylene-tetrahydrofolate [32].

It can be seen that many of the proteins which are arylated by NAPQI seem to be a consequence of their cellular location and/or due to their having moieties which can be oxidized by NAPQI. P450 is heavily localized in the ER as well as the mitochondrial membrane [10, 11]. The ER is significantly involved with different cellular organelles, which helps to explain the cellular locations of proteins arylated by NAPQI.

1.5 Metabolism

An overall metabolic scheme which takes place in hepatocytes can be seen in Figure 1-10. The cellular locations of gluconeogenesis, glycolysis, glycogenolysis, glycogenesis, the urea cycle, the citric acid cycle (tricarboxylic acid, TCA, or Krebs cycle), and oxidative phosphorylation can be seen.

1.5.1 Glycolysis

Glycolysis is the process where 6 carbon glucose is broken down to two 3 carbon pyruvate molecules. This process generates energy in the form of ATP and NADH as well as the creation of substrates (via pyruvate) for the TCA cycle.

The series of reactions involved in glycolysis can be seen below in Figure 1-11. The first reaction involves the addition of a phosphate group, catalyzed by a hexokinase (glucokinase in hepatocytes), on the glucose to create glucose 6-phosphate. This first reaction of glycolysis is also the first reaction in glycogenesis. This branching off for

glycogenesis can also be seen in Figure 1-11 (glucose 6-phosphate to glucose 1-phosphate). Glucokinase production is induced by sterol regulatory element binding protein (SREBP) which is released by insulin binding to insulin receptors [33, 34]. Glucokinase is inhibited by glucokinase regulatory protein (GKRP) when glucose and ATP levels are low [33, 34]. This scheme is a key regulatory mechanism of the first step of glycolysis and glycogen production in hepatocytes.

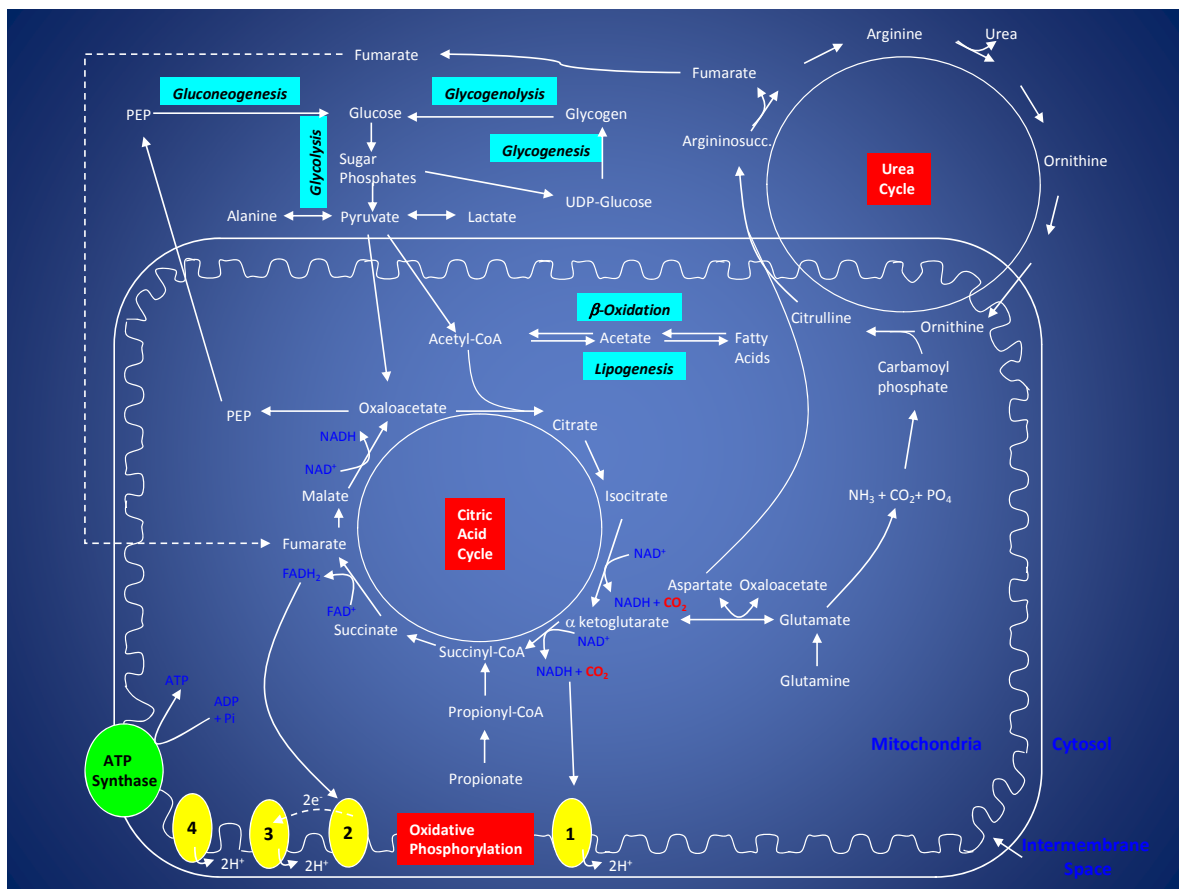


Figure 1-10- Metabolic scheme occurring in hepatocytes.

The glucose 6-phosphate then becomes isomerized to fructose 6-phosphate, which becomes phosphorylated to form fructose 1,6-phosphate. This phosphorylation, by phosphofructokinase I (PFK-1) is the key regulatory mechanism for glycolysis. PFK-1 is

inhibited by ATP, citrate, fructose 1,6-bisphosphate, and glucagon. It is activated mainly by fructose 2,6-bisphosphate, the product of phosphofructokinase II (PFK-2); additionally, PFK-1 is activated by AMP [29, 30]. The 6-carbon glucose 1,6-bisphosphate then becomes split into two 3 carbon molecules, glyceraldehydes 3-phosphate (GADP) and dihydroxyacetone phosphate (DHAP). The DHAP phosphate then isomerizes to yield 2 GADP molecules. However, glycerol production or degradation exits or enters this scheme at DHAP (DHAP to glycerol 3-phosphate), respectively. This can be seen in Figure 1-11. The GADP then becomes phosphorylated, dephosphorylated, isomerized, and dehydrated to form phosphoenol pyruvate (PEP). The PEP is then dephosphorylated to form pyruvate. Pyruvate can then enter the TCA cycle via acetyl CoA or directly in an anaplerotic reaction catalyzed by pyruvate carboxylase (PC). The TCA cycle is discussed in more detail in the following section.

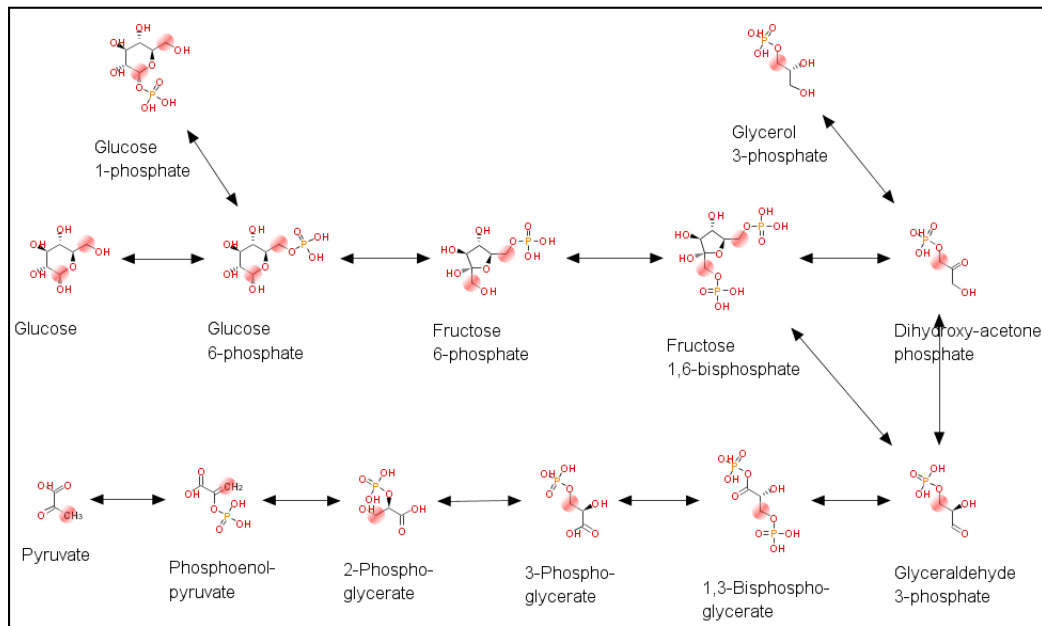


Figure 1-11- Glycolysis (figure created with ARM: Metabolic Map Viewer by M. Arita) [35, 36].

1.5.2 Tricarboxylic Acid (TCA) Cycle

The TCA cycle is the series of chemical reactions which is central to energy production in cells which utilize oxygen for cellular respiration (aerobic respiration). Although the TCA cycle does not use oxygen directly, it is coupled to oxidative phosphorylation, which does utilize oxygen. This occurs in the mitochondrial matrix of eukaryotic cells. Carbohydrates, fats, and proteins provide the substrates for the TCA cycle- a process called anaplerosis [30, 37]. Additionally, the TCA cycle (or parts of it) can be used to provide substrates for carbohydrates, fats, and proteins- a process known as cataplerosis [30, 37]. Figure 1-12 shows the molecules involved in the TCA cycle. Additionally, Figure 1-10 shows the involvement of the TCA cycle in the overall (hepatocellular) metabolism scheme.

Briefly, 4-carbon oxaloacetate becomes acetylated by acetyl-CoA to form the 6-carbon citrate. The citrate is then dehydrated to form cis-aconitate and then rehydrated to form isocitrate. These 2 reactions basically move an -OH from the 3 carbon to the 2 carbon. The 6-carbon isocitrate is then decarboxylated forming 5-carbon α -ketoglutarate and CO_2 . This results in the formation of an NADH from NAD^+ . The 5-carbon α -ketoglutarate is then decarboxylated and binds to CoA to form 4-carbon (not including the CoA) succinyl-CoA and CO_2 . This also results in the formation of another NADH from NAD^+ . The CoA is then cleaved resulting in the formation of symmetrical succinate and an ATP or GTP. Succinate is then oxidized to form fumarate which is hydrated to form malate. The malate is then oxidized to form oxaloacetate. This reaction also results in the formation of a third NADH from NAD^+ . The ATP and GTP formed are used as energy and protein phosphorylation sources. The NADH created are used in oxidative phosphorylation to create ATP molecules

from ADP. Thus, the TCA cycle does not result in much energy production directly; it is the coupling with oxidative phosphorylation which results in the large amount of energy produced compared to anaerobic metabolism only.

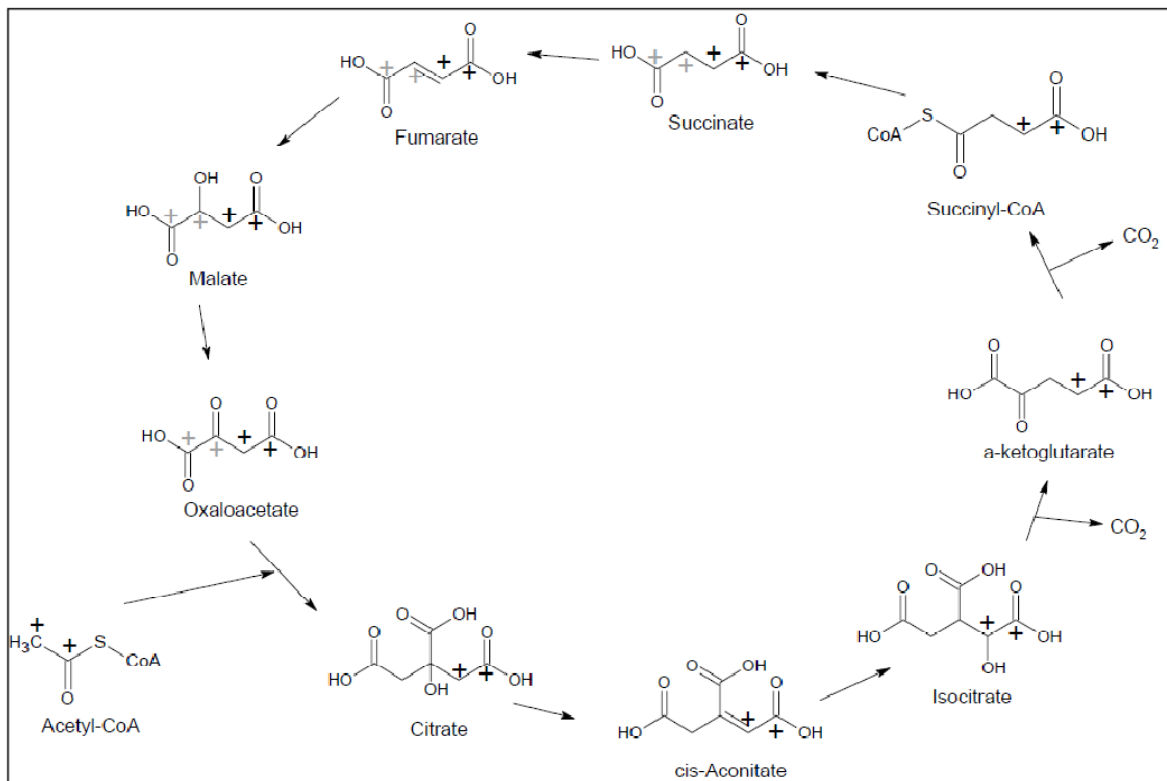


Figure 1-12- The TCA cycle. The two carbon molecules from acetyl-CoA are tracked with plus signs (+). Symmetry of succinate and fumarate lead to scrambling of the carbon molecules at malate and oxaloacetate.

1.5.3 Regulation of Glucose Metabolism

Glucose is the main sugar metabolized for the energy needs of the hepatocyte.

Metabolism of glucose and its key regulatory proteins can be seen in Figure 1-13. The first step for glucose utilization is phosphorylation to glucose 6-phosphate by glucokinase. This allows the sugar to enter glycolysis or form UDP-glucose to allow glycogen or UDP-glucuronic acid synthesis. This enzyme is activated by glucose, ATP, and insulin and inhibited by low glucose concentration, fructose 6-phosphate, and glucagon. Thus, in typical

cell culture conditions consisting of high glucose and high insulin, one would expect phosphorylation of glucose to glucose 6-phosphate allowing glucose to be exposed to the enzymes regulating glycogenesis and glycolysis.

Glycolysis is regulated by the enzyme phosphofructokinase I (PFK-1). This enzyme generally has the opposite activity of phosphoenolpyruvate carboxykinase (PEPCK), the enzyme which regulates gluconeogenesis. This regulatory mechanism ensures that the futile cycle of glucose production and degradation is avoided as this is energetically unfavorable for survival of the organism. PFK-1 is mainly regulated by adenosine monophosphate (AMP) and fructose 2,6-bisphosphate, which is the product of fructose 6-phosphate and phosphofructokinase II (PFK-2). Thus, the regulation of PFK-1 mirrors the regulation of PFK-2. PFK-2 is activated by insulin and fructose 6-phosphate and inhibited by ATP, citrate, fructose 1,6-bisphosphate, and glucagon [38]. Thus, glycolysis is inhibited when there is plenty of energy and TCA cycle activity and activated by low energy (AMP) [38].

As mentioned earlier, the activity of PEPCK is generally opposite that of PFK-1. PEPCK is activated by glucagon and cortisol and inhibited by insulin. However, the activity is mainly regulated by insulin, where its absence activates the enzyme and its presence inhibits it. Thus, in the general cell culture system in high insulin conditions, one would expect this enzyme to be generally inactive. In whole organism studies of human biofluids however, this will depend on the time of the last meal, urination, and blood sampling.

Glycogen synthesis and degradation are regulated by glycogen synthase and glycogen phosphorylase, respectively. Like PFK-1 and PEPCK, the synthesis and degradation of glycogen generally have an inverse relationship so that futile cycles are avoided. Glycogen synthase is activated by glucose 6-phosphate and insulin and glycogen phosphorylase is

activated by AMP, epinephrine, and glucagon. Thus, glycogen is synthesized in the fed state and broken down to supply glucose in the fasted state.

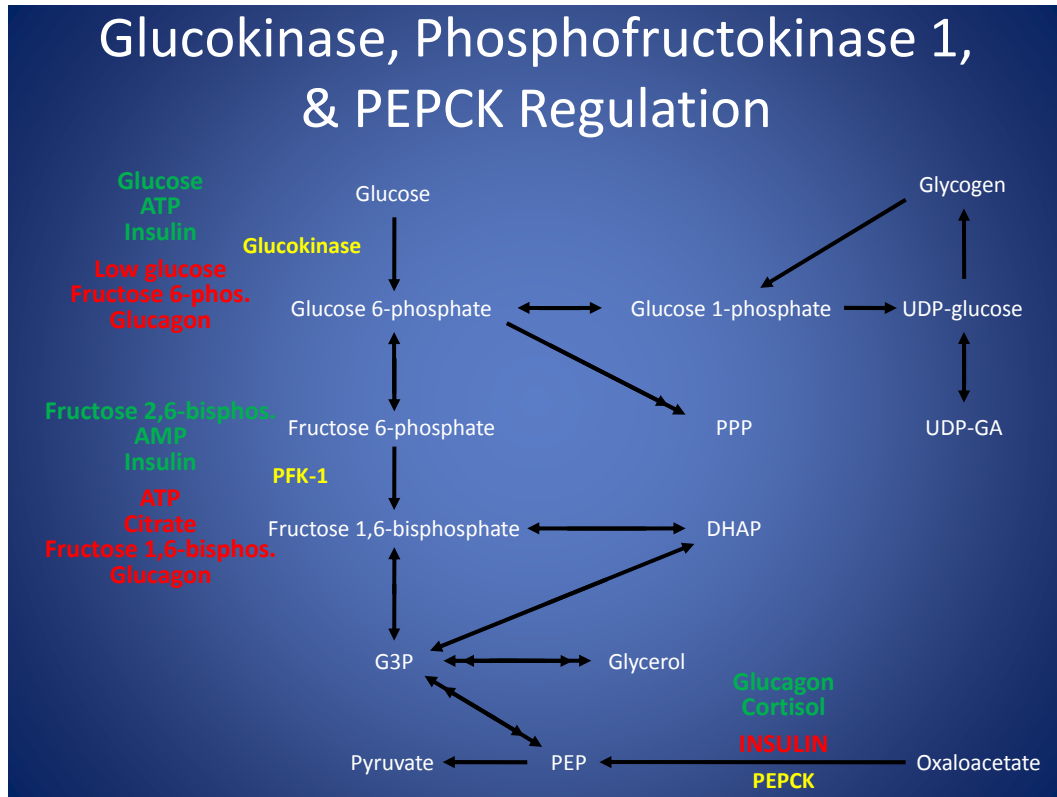


Figure 1-13- Regulation of glucose phosphorylation, glycolysis, and gluconeogenesis in the hepatocyte. Double sided arrows indicate reversible reactions while double arrows indicate multiple steps. Key enzymes are in yellow and the activators and inhibitors of the enzymes can be seen in green and red, respectively. The activators and inhibitors listed work directly or indirectly on the enzyme [29, 30, 37, 38].

1.6 Hepatocyte Cell Culture

The culture of primary hepatocytes was a common laboratory practice since at least the 1960s [39-41]. Use of hepatocyte cultures is invaluable for elucidating metabolic responses of an organism to a xenobiotic. While whole body responses are also important, it can be difficult to deconvolute the data generated from these experiments to determine liver-specific responses. Additionally, scaling up whole animal experiments generally involves the addition of many more animals, eliciting ethical concerns. Since multiple plates of

hepatocytes can be created from one animal, this problem with scaling up is somewhat mitigated. More importantly, stringent experimental controls can be placed on cultured cells which would be impossible with living animals or whole organ perfusions. Additionally, cell cultures can be kept viable for a much longer period of time than whole liver perfusions, but not as long as an intact animal. Thus, animal hepatocyte cultures are an important tool which can be used to elucidate the effects of different drugs which can be used to complement data generated from whole body, whole organ, and cellular fraction (such as mitochondria) experiments.

Hepatocyte culture also allows for the experimental use of human hepatocytes, which is mainly possible by salvaging noncancerous liver tissue from liver resections or the use of livers not suitable for transplantation. These tissues, once considered waste, are now being used as an invaluable tool to researchers allowing for ethical data generation of human metabolism.

1.6.1 History of Rat and Human Hepatocyte Culture

Modern-day monolayer hepatocyte culture was born in 1969 when Berry and Friend developed a perfused liver digestion procedure at the University of California at San Francisco that resulted in 50% viable hepatocytes from rat liver [42]. Since that time, nearly 9,000 studies have been published in peer-reviewed journals with the word “hepatocyte” in the title (PubMed search results). Through the early 1970’s, the isolation procedure was optimized to obtain greater than 95% viability [43]. In the late 1970’s, primary rat hepatocytes, as well as a slew of other species, were cultured on glass or plastic. It was quickly discovered that the hepatocytes dedifferentiate and in the late 1970’s a plethora of

publications on the effects of hormones, such as insulin and glucagon, and various nutrient concentrations were established. This genre of hepatocyte publication peaked in the early 1980's with a couple hundred publications per year on the topics of media factors as well as insoluble factors (such as extracellular matrix) [44] as well as co-cultures [45] and their effects on hepatocyte differentiation. Finally, in the mid 1990's the field of tissue engineering was born, also with interest in hepatocyte culture methods being applied to 3D culture systems [46, 47]. Many of the studies examining the basic effects of culture media and matrix components, and their effects on the metabolome were performed in the late 1970's and not reevaluated for human hepatocyte culture after it was first performed in 1981 [48], likely due to the difficulty and high cost in obtaining human hepatocytes. The hepatocyte culture field was dominated in the 1980's and 1990's with research in growth factors, made possible by new molecular biology techniques.

1.6.2 Dedifferentiation of Hepatocytes in 2D Culture and Media Formulations

Concocted to Attenuate or Reverse this Dedifferentiation

One major problem with cultured hepatocytes is the dedifferentiation that occurs after isolation. Without intervention, hepatocytes in 2D culture typically lose expression of genes for albumin, P450, phase II enzymes (UDP-GT, GST), urea production, start expression of α -fetoprotein, and assume a simple fibroblast like morphology [49-52]. Alpha-fetoprotein is the fetal counterpart of albumin which is minimally expressed in mature hepatocytes. Thus it can be used as a marker of both differentiation and dedifferentiation. High expression of α -fetoprotein is indicative of an immature hepatocyte phenotype, low expression of the protein

is indicative of a mature phenotype, and no expression of the protein is indicative of neither a mature or immature hepatocyte phenotype.

Understandably, researchers have attempted to stop, slow down, attenuate, or otherwise reverse this process of dedifferentiation for hepatocytes [52-58]. Many soluble and insoluble factors have been tested to maintain differentiation, since hepatocytes that have dedifferentiated (and thus no longer act like hepatocytes) are of little use in understanding hepatocyte or liver response to an experimental treatment such as xenobiotic metabolism.

Since it is effective in promoting cell growth and division, serum is frequently added to media for use with cell culture in the form of fetal calf or bovine serum (FCS or FBS, respectively). While hepatocytes exposed to serum can readily grow and divide, dedifferentiation is also facilitated, presumably due to the various and somewhat uncategorized hormones present in the serum. It is thought that one or more of the hormones promotes dedifferentiation. Thus, it is generally agreed that serum-free media is best for the experimentation phase of experiments using cultured hepatocytes [59]. That being said, serum-containing media can, and frequently is used after plating to facilitate cell growth and division [60]. Once attached or confluent, hepatocytes are typically switched to a serum-free hormonally-defined medium prior to experimentation [61].

Additions of high concentrations of amino acids have been shown to facilitate hepatocytes staying in a differentiated state [62, 63]. Additionally, xenobiotics, such as dexamethasone, phenobarbital, and dimethylsulfoxide have also been shown to induce P450 [51, 56, 64, 65], with dexamethasone having multiple effects on maintaining hepatocyte proteins such as the insulin/glucagon receptors [66] and transporters [67]. Thus, these compounds are frequently added to cell culture medium or are already present in media

frequently used for hepatocyte culture. Additionally, phenol red, the near-ubiquitous pH indicator present in many media formulations has been shown to be metabolized by hepatocytes [68, 69]. The metabolism that occurs is the phase II reaction of glucuronidation. However, it is unclear at this time the effects phenol red has on cultured hepatocytes. Reasonable hypotheses would include the decreased capacity for glucuronidation due to the consumption of UDP-GA via conjugation with phenol red or the induction of UDP-GA and UGT production due to the presence of phenol red. If either the former or latter are true, phenol red could also be thought of as a chemical which helps keep cultured hepatocytes differentiated by either increasing the capacity for glucuronidation, with glucuronidation being a normal process occurring in hepatocytes, or by decreasing the capacity for glucuronidation, likely potentiating potential toxic effects of a xenobiotic.

Hepatocytes are generally applied to coated (usually collagen or matrigel) culture plates. After the hepatocytes are applied to the plates and have attached, they are either left uncoated for experimentation or they are coated with another layer of collagen or matrigel. The latter are known as sandwich cultures and have been shown to keep the hepatocytes differentiated and morphologically hepatocytic when cultured longer than a day or two [60, 64, 70]. Thus, sandwich cultures may be best for long term hepatocyte cultures. For cultures of a few days or less, sandwich cultures do not provide a substantial benefit over monolayer cultures. In fact, it appears that monolayer hepatocyte cultures are morphologically better than their sandwich counterparts for short-term experimentation [60]. This is due to the limited movement potential for sandwich cultured hepatocytes. Monolayer cultured hepatocytes are quickly able to spread out and form cellular connections with neighboring cells. This is something that takes longer to occur in sandwich cultures. These cellular

connections lead to the formation of bile cannicular structures between hepatocytes. In longer term cultures, the bile cannicular structures disappear in monolayer culture while they are better preserved in sandwich cultures. This is an important consideration for membrane-bound hepato-proteins and must be considered on an experiment-to-experiment basis.

1.6.3 Cryopreservation of Hepatocytes

Use of human hepatocytes has been hindered by the sporadic and unpredictable availability and oftentimes low numbers of viable cells. Thus, cryopreservation of human hepatocytes would be a desirable way of keeping a more steady supply of hepatocytes available for experimentation. Viability of hepatocytes is poor if no cryoprotectants are added to the cell mixture due to compromised cell membrane integrity caused by expanding ice crystals. A traditional cryoprotectant solution consisted of the addition of 20% DMSO to the culture medium to protect the cells from freezing damage [71, 72]. However, other cryoprotectants have been developed that have been shown to be more effective. In the early 1990s, a vitrification solution consisting of DMSO, acetamide, propylene glycol, and polyethylene glycol was shown to cryopreserve rat hepatocytes better for a week than DMSO [71, 72]. Recently, HyperThermosol and CryoStor solutions have been developed which have been shown to be significantly better than the older cryopreservation solutions at maintaining viability and differentiation during hypothermic and ultra low temperature storage of hepatocytes and other cells and tissues [73, 74].

Viability of cryopreserved hepatocytes is generally lower than fresh hepatocytes. However, quantification of this difference can be difficult due to the different species,

isolation procedures, cryopreservation procedures, and cryopreservation lengths. That being said, viabilities of cryopreserved cells tend to be 50% or less [71]. Additionally, there are generally significant to no decreases in P450 activity in cryopreserved hepatocytes, depending on the P450 isoform, cryopreservation procedures, and culture media, it again can be difficult to quantify the decrease in phase I oxidation. Generally, decreases in P450 activity, glutathione content, and other phase I and phase II proteins are on the order of 0 – 50% [65, 72-74].

1.7 Metabolomics- Stable Isotopes

^{13}C is a non-radioactive isotope of carbon and is naturally present at approximately 1.1% of all carbons. Thus, administration of metabolites enriched with nearly 100% ^{13}C allows for the locational tracking of these metabolites as well as the locational tracking and production of downstream metabolites. ^{13}C enriched metabolites can be differentiated from the “normal” ^{12}C metabolites when samples are measured with NMR spectroscopic or mass spectrometric (MS) technologies. Additionally, administration of deuterated compounds (non-radioactive hydrogen atoms with a molecular weight of 2), such as water (written as $^2\text{H}_2\text{O}$ or D_2O), allows one to assay the origins and flux of different gluconeogenic substrates [75-79].

1.7.1 Previous Isotope Tracking Experiments

Fluxomics has not yet been achieved experimentally even in 2D culture systems, so most of the metabolic fluxes are derived *in silico* using metabolic control analysis [80-85], or metabolic flux analysis [86-89] and limited experimental data. Although comprehensive,

these models depend on isotopomeric analyses of compounds found at branch points in the metabolic network. All existing flux models used for hepatocyte cultures have assumptions, with some of the assumptions being more sound than others, based on the normal whole animal biochemistry [90, 91]. The primary assumption is that the cells are in the fed state due to the nearly four orders of magnitude higher insulin concentration and four-fold elevated glucose concentrations compared to the whole animal plasma concentration in the fed state. The switch from fed to fasted triggers the metabolism of pyruvate from pyruvate dehydrogenase to pyruvate carboxylase, due to conversion of fatty acids to acyl-CoA and then to acetyl-CoA. Additionally, fluxes through certain pathways, such as pyruvate carboxylase (anaplerosis) are assumed to be zero. The reason for these assumptions lies in the type of analyses historically used in these flux studies, wherein either $^{14}\text{CO}_2$ is used as a measure of TCA cycle flux using chromatography and scintillation counters [90, 92-98] or single metabolites are used with ^{13}C isotopomer analysis by mass spectrometry [89, 91, 99-101] or NMR [75-79, 102-107]. Previous chromatographic separation and radioactive quantification analyses of downstream ^{14}C metabolites were unable to obtain a global analysis. Due to the need to analyze what could be separated by chromatographic methods it is necessary to focus output on just control of alanine metabolism [96] or purine metabolism [98], for example. However, NMR spectroscopy is not without its own disadvantages. The major disadvantage of NMR is poor sensitivity. Thus, minor metabolic pathways of low concentrations can be missed making tracer studies of low isotopic enrichment difficult. However, use of the high nutrient concentrations found in culture media with high degree incorporation is ideal for NMR studies since it is innately quantitative and unbiased.

Since at least the 1950's, ^{14}C and ^3H (tritium) isotopes have been used to track metabolism, usually the fate of ^{14}C glucose or ^{14}C acetate [108-110]. Incorporation into glycogen, lipids, ketone bodies, or CO_2 , is generally what was measured in these early analyses. These ^{14}C analyses have stood the test of time as they are still employed to this day.

1.7.1.1 ^{14}C Studies in Rat and Human Hepatocyte 2D Monolayer Cultures

Shortly after the rat hepatocyte mono-layer culture conditions were established, ^{14}C metabolic tracer studies were performed using the recently discovered HPLC to fractionate metabolites, scintillation counting to quantify metabolites of nutrients, and tracer mathematics to model the mass balance of metabolites. These ^{14}C studies utilized ^{14}C -glucose [111-113], U- ^{14}C , 5- ^2H -fructose and U- ^{14}C , 2- ^2H -glyceraldehyde [114], amino acids [115], valine (for protein synthesis) [116], ^{14}C -labeled puines (for nucleotide metabolism) [117], ^{14}C -acetate (for lipogenesis) [118]. In the late 1970's, the effects of glucagon and insulin on ^{14}C -glucose metabolism [119, 120] and β -oxidation using small chain fatty acids (C4 and C8) [121] (C18, C20, C22) [122] were examined. The earliest metabolism studies used ^{14}C tracers to obtain concentrations with the newly developed, higher through-put, HPLC methods just developed rather than the slower thin layer chromatography used in the 1950's and 1960's. An early pioneer of hepatocyte culture, Monte Bissel, published the first metabolomic analysis of media components using paper chromatography and a low concentration of ^{14}C -glucose (5.5 mM) in 1979 [119], after publishing the first drug studies with the cells [123]. The first ^{14}C -labeled acetaminophen study was published in the late 1970's [124].

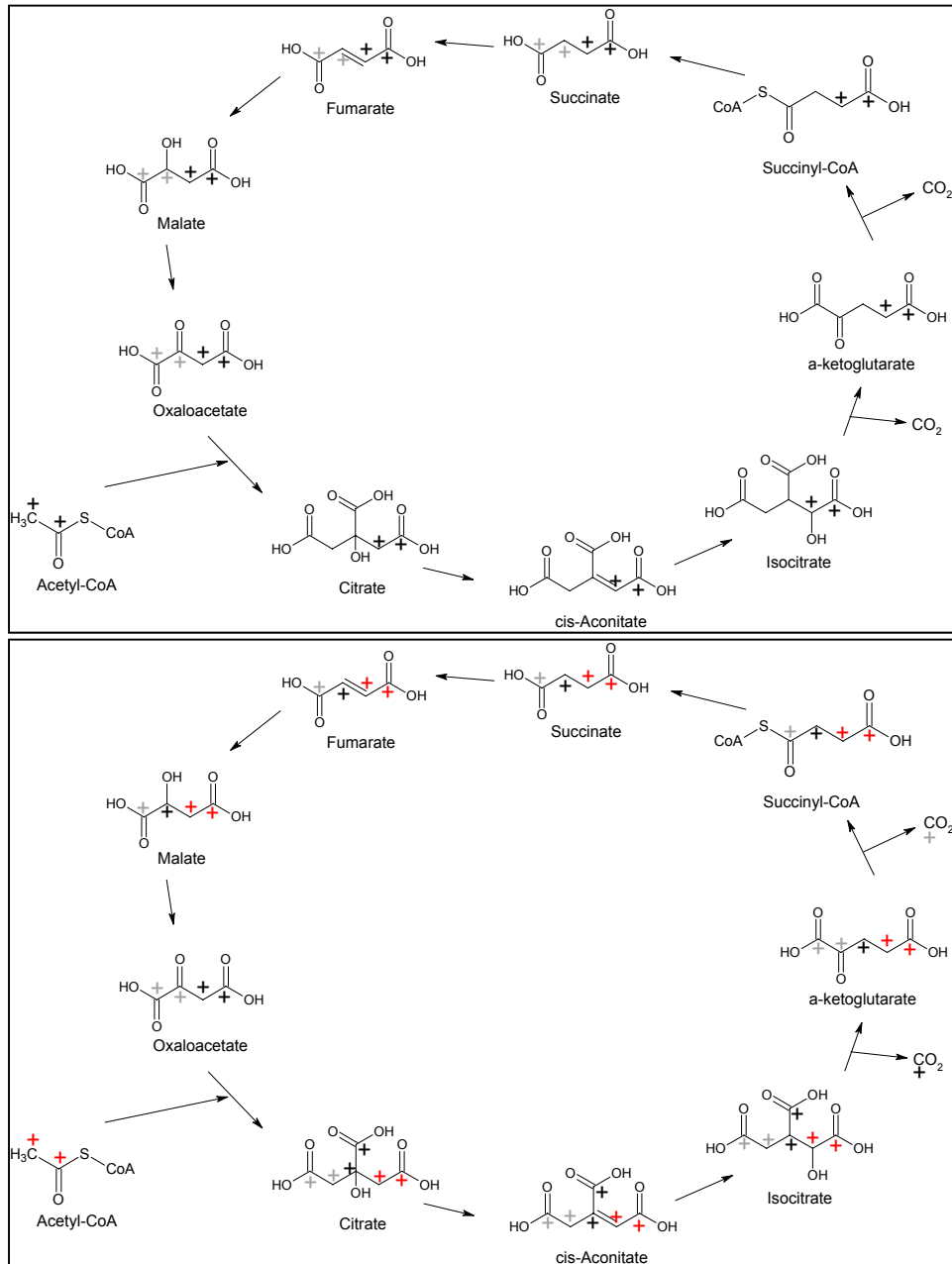


Figure 1-14- Creation of CO₂ in the TCA cycle can be seen. The first cycle through the TCA cycle can be seen in the top part of the figure and the second cycle through the TCA cycle can be seen in the bottom part. Thus, the top part starts at acetyl-CoA and the bottom part starts at oxaloacetate.

One researcher that has still makes great use of this radioactive labeling technique is M. L. Yarmush at Harvard University. His analyses, termed Metabolic Flux Analysis

(MFA), make use of cultured hepatocytes whose metabolites are measured with commercially available assay kits. Additionally, ^{14}C acetate was supplied in the media to the hepatocytes to measure TCA flux. If 1,2- ^{14}C acetate is given to hepatocytes, eventually, $^{14}\text{CO}_2$ will be created via metabolism through the TCA cycle. The places in the TCA cycle *where* CO_2 is created can be seen in Figure 1-11. Figure 1-14 shows the origins of the carbon atoms forming the CO_2 created in the TCA cycle. It can be seen in the figure that it takes 2 cycles through the TCA cycle for the labeled CO_2 to be created.

Using this flux data in addition to static measurements of other key metabolites, Yarmush calculates flux rates for the reactions in the metabolic pathways involved in TCA cycle, urea cycle, pentose phosphate pathway, gluconeogenesis, TG and cholesterol ester oxidation, β -oxidation, amino acid oxidation, ketone body synthesis, glycogen synthesis, and albumin synthesis. In all, flux rates for 74 reactions are calculated [93]. While sophisticated and complex, there are quite a few items of concern. First is that the analysis is performed with static metabolite concentration measurements coupled with 2 active measurements (liberation of $^{14}\text{CO}_2$ from ^{14}C acetate, and O_2 consumption).

Second, derivation of the rates of 74 reactions with only 2 active measurements and a handful of static measurements leaves much open to question. To get around this, 10 assumptions were made, which is another concern. Specifically, the assumptions that flux through pyruvate dehydrogenase is zero, fatty acid synthesis and flux through glycolytic enzymes were set to zero, equal fluxes into pentose phosphate production and glycogen production (because these fluxes were not measured), a single pool of metabolites (therefore the rates represent an average flux, of mitochondrial and cytosolic proteins for instance), the rates of change of the extracellular metabolite pools are assumed to be constant between the

24 hour media changes, and the rate of accumulation of triglycerides was assumed to be constant over the 7 day experiment. The reason for these assumptions is due to the method of analysis, which is generation and analysis of $^{14}\text{C}\text{O}_2$. Since there are multiple entry and exit points for ^{14}C -glucose or ^{14}C -acetate, use of the multiple entries and exits, in addition to recycling, would lead to a scrambling of the ^{14}C -label, affecting the interpretation of the data. This is something which could occur not only with the TCA cycle, but also with the interconnectivity of glycolysis with the pentose phosphate pathway, glycerol metabolism, and fatty acid metabolism.

The third point of concern is the results themselves. The 74 flux rates, which are positive or negative, depending on the direction of the reaction, were calculated for 3 different experimental conditions- hepatocytes exposed to plasma; plasma and amino acids; and plasma, amino acids, and hormones. Approximately 38% of the 222 flux rates (some of which were measured and others of which were derived) had standard deviations of greater magnitude than the flux rates themselves. This means that the direction that these reactions occur is not even certain. It would seem that these overly ambitious experiments made too few measurements, had too many assumptions, and inadequate results.

1.7.1.2 ^{13}C NMR and MS Studies in 2D Rat Hepatocyte Cultures

While these studies can be well suited for short term non human studies, the radioactivity of ^{14}C and tritium makes their utilization in human experimentation ethically impossible. Thus, with the decades of modernization of NMR spectroscopy and mass spectrometry (MS) starting in the 1950's, isotope tracking with ^{13}C compounds became possible. Two main improvements to isotopic tracking with ^{13}C over ^{14}C are the non-

ionising, non-radioactive nature of ^{13}C as well as the positional labeling information available through NMR spectroscopy.

The first ^{13}C study of hepatocytes used NMR spectroscopic isotopomeric analysis to analyze metabolic scrambling of the ^{13}C label (isotopomeric analysis is a term created by the Shulman group at Yale) [103, 125]. These initial studies examined gluconeogenesis in 2D rat hepatocyte cultures [102, 125]. Later, they compared ^{13}C to ^{14}C tracers and found no difference other than the effects of the relatively poor sensitivity of NMR. Later this group would move to examination of mass isotopomers [126, 127]. Mass spectrometry was initially used by Desage and others [128] and they have discovered some limitations compared to the isotopomer method, inherent in ^{13}C NMR [129]. W. J. Malaisse and others published many studies on basic metabolism and the effects of various drugs or factors using ^{13}C tracers and NMR spectroscopy through the 1990's and early 2000's [105-107, 130-137]. The more recent ^{13}C NMR and MS isotopomeric studies have applied metabolic flux analysis which resulted in a comprehensive mass balance output of the two-state rat hepatocyte model where the mass balances of treated cells was compared to those in control conditions [101, 138, 139].

One group that has been working with and refining stable isotopic tracking experiments is A.D. Sherry and C.R. Malloy at the University of Texas Southwestern Medical Center. Their publications on this subject started in the mid 1980's with experiments examining the fate of various ^{13}C compounds involved in the TCA cycle [140-142]. In the mid 1990's, many of their experiments centered on the examination of the different glucose isotopomers formed from U- ^{13}C propionate as well as the dilution of 1,6-

^{13}C glucose [143]. The 1,6- ^{13}C glucose is used to measure glucose carbon skeleton turnover by measuring its dilution.

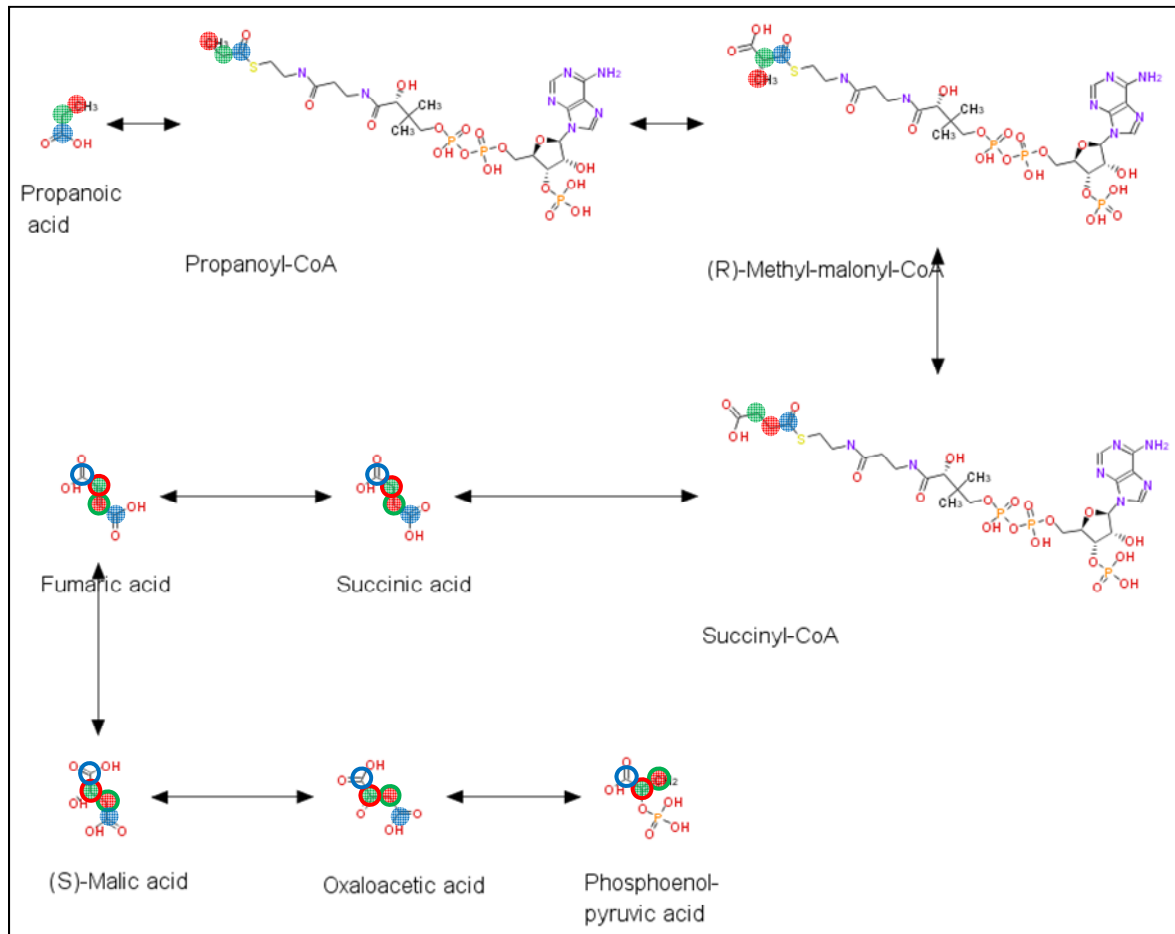


Figure 1-15- Metabolism of propionate through the TCA cycle to PEP. The individual carbon atoms of propionic acid can be tracked. Since succinate is symmetric, scrambling can occur so the 3 tracked atoms will either be blue, red, and green dots or blue, red, and green circles.[35, 36]

Tracking the U- ^{13}C propionate shown in Figure 1-15, one can see that the propionate enters the TCA cycle at succinyl-CoA and exits at oxaloacetate. This results in the labeling of PEP where half of it will be 1,2,3- ^{13}C and the other half will be 2,3- ^{13}C . Gluconeogenesis from these 2 isotopomers will result in the formation of 1,2,3- ^{13}C (and 4,5,6- ^{13}C) and 1,2- ^{13}C (and 5,6- ^{13}C) glucose. This can be seen if tracking backwards in Figure 1-11. Glycolysis

from glucose to PEP and gluconeogenesis from PEP to glucose involve the same intermediates, though not all of the same enzymes are used because they are not all reversible. Further examination of Figure 1-11 reveals that gluconeogenesis involving 2-¹³C pyruvate will result in the formation of 2-¹³C or 5-¹³C glucose and gluconeogenesis involving 1-¹³C pyruvate will result in the formation of 3-¹³C or 4-¹³C glucose. Additionally, glycolysis and gluconeogenesis of 1,6-¹³C glucose will result in the formation of 1-¹³C (and 6-¹³C) glucose. This isotopic labeling of glucose can thus be used to determine flux through the TCA cycle for gluconeogenesis (from the propionate) as well as glucose carbon skeleton turnover (from the dilution of 1,6-¹³C glucose).

1.7.1.3 ¹³C NMR and MS Studies in Human Hepatocytes

Surprisingly, ¹³C NMR studies with human hepatocytes have not (to the best of this author's knowledge) been performed since primary human hepatocyte cell culture was first conducted in 1981 [48]. They have only recently been performed with immortalized human hepatocyte cell lines [99, 144, 145], but not with primary 2D human hepatocyte culture. This is likely due to their sporadic availability, high price, the absence of validated protocols, and the difficulties of extrapolation of *in vitro* data to the *in vivo* situation due to differences in genetics and epigenetics inherent in humans [146-148]. Thus, the interest has mainly been in metabolism of drugs by P450 [149-152] and bioartificial liver support systems [153].

2 The Effects of a Prolonged Standardized Diet on the Normalization of the Human Metabolome

2.1 Introduction

Metabolomic studies employing multivariate statistics generally utilize the analytical technologies of nuclear magnetic resonance (NMR) spectroscopy or mass spectrometry (MS) to measure the low mass metabolic compounds in biological fluids such as urine or serum [154, 155] so that the global metabolic state of an organism can be profiled [156]. The studies then generally use multivariate statistical methods to identify the metabolic changes that result from a particular challenge an organism. These methods have been successfully applied to explain the metabolic alterations resulting from disease states or xenobiotic interventions [157-159], but the applications to nutrition have only recently begun to emerge [160, 161].

Many metabolomic studies employ animal models and toxic or otherwise lethal doses of different xenobiotics, frequently in fasted animals. Understandably, the metabolic changes in these animals can be quite dramatic and therefore easy to see. However, one challenge in performing non toxic or therapeutic xenobiotic interventions in humans is to detect the potentially subtle perturbations in the metabolome due to the experimental intervention through the variability inherent between people. The problem is particularly great when working with human subjects due to the large variability inherent between humans and the ethical necessity for non toxic or minimally toxic experimental intervention. Several metabolomics studies have examined cohorts of healthy human subjects to assess the

variability which can be influenced by genetics, environment, xenobiotics, *et cetera* [162, 163]. In general, these studies found that inter-subject variation was more significant than intra-subject variation- that is, variation of samples between different subjects was found to be greater than the variation of samples from the same subject. This understandable phenomenon indicates that each person has a distinct metabolic phenotype also known as their metabotype [164]. Other studies have looked at the effects of culturally driven dietary influences [165, 166] or specific dietary interventions to assess the extent that diet modulates the metabolome [167-169]. In one study, urine samples from 22 subjects without dietary restriction were collected over a three month period [170]. A standard principal component analysis (PCA) of the data indicated some weak clustering of each subject, but a more advanced statistical modeling was used to identify specific features of the NMR spectra that could be used to identify each individual. This result supports the idea that each person possesses an individual metabotype which is quite heavily masked by inherent variability.

In order to conduct the most informative metabolomics analyses, it would be best to be able to pick out the subtle perturbations resulting from the experimental intervention and ignore the other features. Standardization of diet, environment, and activity could be used to possibly standardize the metabolome. In this study, the question of how much normalization of the human metabolome can be achieved with a prolonged dietary standardization is addressed. Ten subjects were admitted to a clinical research center for two weeks and given a standardized whole food diet. The protocol included daily, early morning fasted serum collections as well as 24 hour pooled urine collections. The results of this study will help inform the design of future studies in order to indicate the highest degree of metabolomic normalization a clinical setting is able to reasonably provide. Additionally, work presented

in this chapter can be used to determine whether or not the clinical study design of the two week acetaminophen study presented in the next chapter (Chapter 3) of this dissertation is valid for a metabolomics analysis.

2.2 Methods

2.2.1 Study Design

This project was approved by the University of North Carolina Institutional Review Board and all participants were consented accordingly and provided with written consent forms. This study involved 65 subjects who were inpatients at the University of North Carolina General Clinical Research Center. Daily urine and serum samples were collected from 10 subjects of this group for the two week period and a single serum sample was collected at a follow-up visit two weeks after the end of the initial study. The remaining subjects were subjected to a shorter three day dietary intervention study.

The two week cohort consisted of seven male and three female subjects. Average subject age was 25.2 with a range from 18 – 42 and average BMI was 25.8 with a range of 19.9 – 32.4. The three day cohort consisted of 55 different subjects. There were 23 females and 32 males. Average subject age was 31 with a range of 18 to 58 and average BMI was 25.8 ranging from 19.1 to 39.6. Subjects refrained from alcohol consumption, medications, vitamins, supplements, or herbs with the exception of birth control pills or antidepressants for at least two weeks prior to admission. Further exclusion criteria included history of abnormal liver enzymes levels, chronic alcohol abuse, chronic liver disease or history of acetaminophen use over the three months prior to screening.

2.2.2 Standardized Diet

Subjects received a constant macronutrient diet composed of common foods for breakfast, lunch, dinner, and bedtime snack rotated on a two-day cycle. Meals were provided at consistent times each day. Thirty-five calories/kg body weight was provided based on actual body weight if BMI was less than 30 or adjusted body weight for obesity if BMI was greater than 30. The macronutrient breakdown was 15% protein, 30% fat, and 55% carbohydrate. Diets were adjusted to maintain body weight by increasing total calories by 300 Cal if weight dropped 1 kg and decreased by 200 Cal if weight increased by 1 kg. No other foods were allowed, with the exception that subjects could consume water, caffeine free diet soda, and decaffeinated black coffee and tea *ad libitum*.

2.2.3 Sample Collection

Daily morning fasted blood samples were drawn at 8:00 a.m. and 24 hour urines were collected and frozen at -80 °C throughout the study. Subjects returned two weeks after discharge for a follow-up visit and fasting blood sample. All samples from days 4 and 11 were collected separately for use in pharmacokinetic analyses and were not available for use with this study.

2.2.4 Sample Preparation

Frozen serum and urine samples were thawed overnight at 4 °C. Aliquots of 540 µL of serum were added to 5 mm NMR tubes containing 60 µL of a D₂O solution containing 26.5 mM formate for a chemical shift reference and 0.2% NaN₃ to inhibit bacterial growth. Aliquots of 540 µL of urine were added to 5 mm NMR tubes containing 60 µL of a 924 mM

phosphate buffered D₂O solution at pH = 6.14 containing 4.6 mM TSP for a chemical shift reference, 92 mM imidazole for a pH reference and 0.2% NaN₃ to inhibit bacterial growth.

2.2.5 ¹H NMR Spectroscopy

All NMR spectroscopy was performed on a Varian INOVA spectrometer (Varian Inc., Palo Alto, CA) operating at 399.80 MHz and 25 °C. A Carr-Purcell-Meiboom-Gill (CPMG) pulse sequence was used to collect the spectra. Serum samples were collected with a pre-acquisition delay of 2.5 s, including 2.0 s solvent presaturation, a 90° pulse followed by a 100 ms CPMG delay time. FID acquisition occurred over 2.56 s with a sweep width of 4389.8 Hz and 16384 points. Urine samples were collected with a recycle delay of 4.1 s, including 4.0 s H₂O presaturation. A 20 ms CPMG delay time was used to narrow the residual water peak. A sweep width of 6388 Hz was digitized with 16360 points leading to an acquisition time of 2.56 s. A total of 256 transients were collected for both serum and urine samples.

2.2.6 Spectral Processing

Processing of all NMR spectra was done in ACD/1D NMR Manager 8.0 (Advanced Chemistry Development, Inc., Toronto). Linear prediction of the first two points, 0.3 Hz exponential line broadening, and zero filling to 32768 points were applied to each spectrum. After Fourier transformation each spectrum was manually phased and baseline correction was applied. The chemical shifts of the serum spectra were referenced to the formate peak at 8.47 ppm and the urine spectra were referenced to the TSP peak at 0.00 ppm. Regions of the spectra upfield of 0.00 ppm and downfield of 10.00 ppm were removed from the analysis as

they contained only noise. The region around the residual water peak from 4.50 – 5.10 ppm was also excluded from the analysis. The urine and serum spectra were then processed as separate groups.

The spectra were integrated using the Intelligent Bucketing method in the ACD software with bin sizes of 0.02 – 0.06 ppm. To reduce the negative impact of noise, the bins containing only noise were excluded. These bins were identified by considering the range of values for a given bin across all spectra. The bins were sorted by increasing bin range and a threshold was determined such that bins with a range less than the threshold were considered noise.

2.2.7 Multivariate Statistical Analysis

The NMR data were imported into SimcaP (version 11.5, Umetrics, Umeå, Sweden). The data were mean centered and scaled to Pareto variance ($1/\sqrt{sd}$). Principal component analysis (PCA) was then performed on the resulting data. The resulting two-dimensional scores plots map out each of the samples on axes that account for the major sources of variance in the data. In this way, similar samples will cluster near one another while disparate samples will be farther apart.

2.3 Results

Typical urine and serum spectra are shown in Figure 2-1 along with some metabolite assignments.

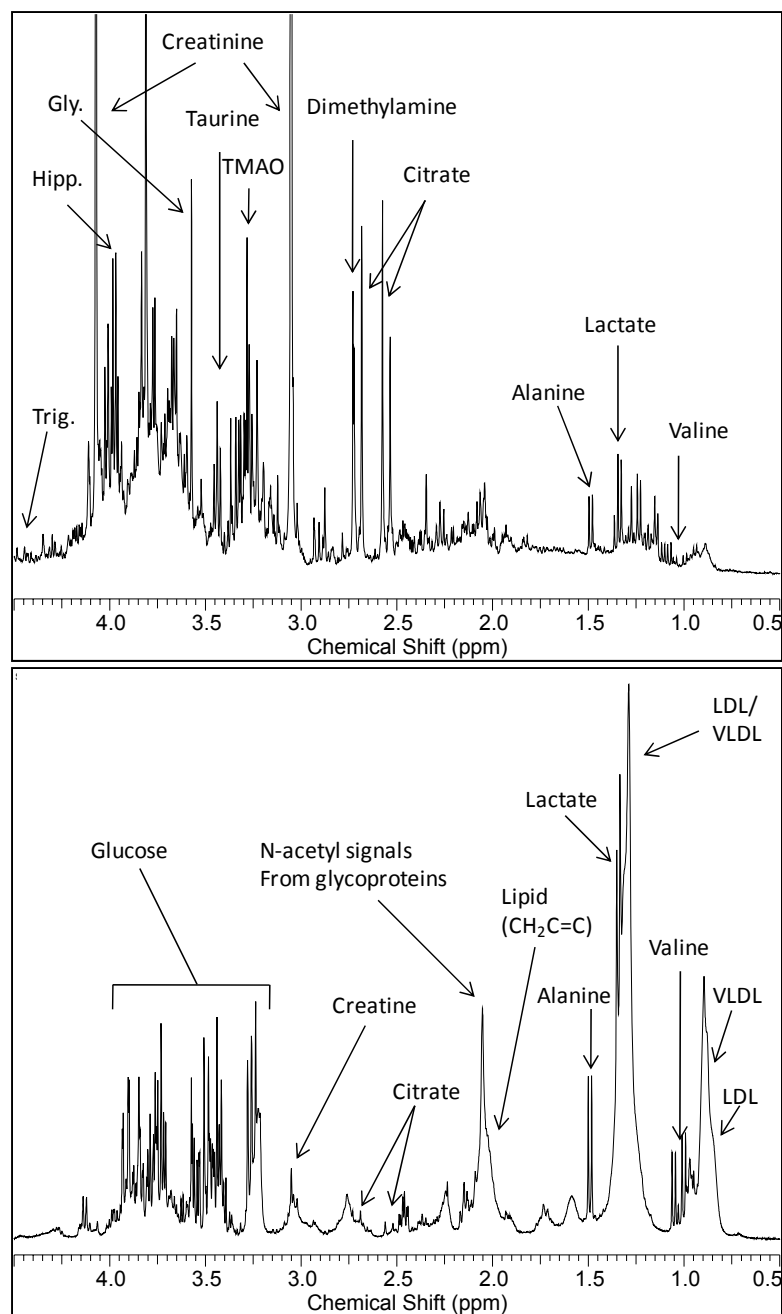


Figure 2-1- Representative spectra from urine (top) and serum (bottom).

2.3.1 Serum

PCA scores plots for the serum data are shown in Figure 2-2. The first two principal components explain over 80% of the variation in the data. The figure shows that, in general, each subject is loosely clustered in a particular region and that these clusters have significant

overlap. Interestingly, five of the subjects possess one or two points that are outliers from the main group. These subjects are highlighted in Figure 2-2 with ellipses around the main group and an arrow pointing either two or from the main group to the outlier. In all cases the outliers are from either the first day or the two week follow-up visit. The samples from the first day were acquired after an overnight fast as were the follow-up visits. The fact that all the other days cluster in the same region suggests that a single day provides all of the normalization possible in human serum with dietary standardization. After the first day, the subjects remain in the same general region of the PCA plot for the remainder of the study. The span of this space is the result of the intra-subject variation inherent between human subjects.

Within each of the clusters, the trajectory of the days across the two weeks was examined for any trends. The samples for each of these subjects were examined to see if a consistent metabolic trajectory could be seen over the two week period. It was clear that aside from the first and last points, no trend is observed. One might have expected that with extended dietary standardization, the metabolome of each of the subjects would tend to normalize and thus move toward the same region of the PCA scores plot, but this is not the case and the trajectory does not appear to move with any order.

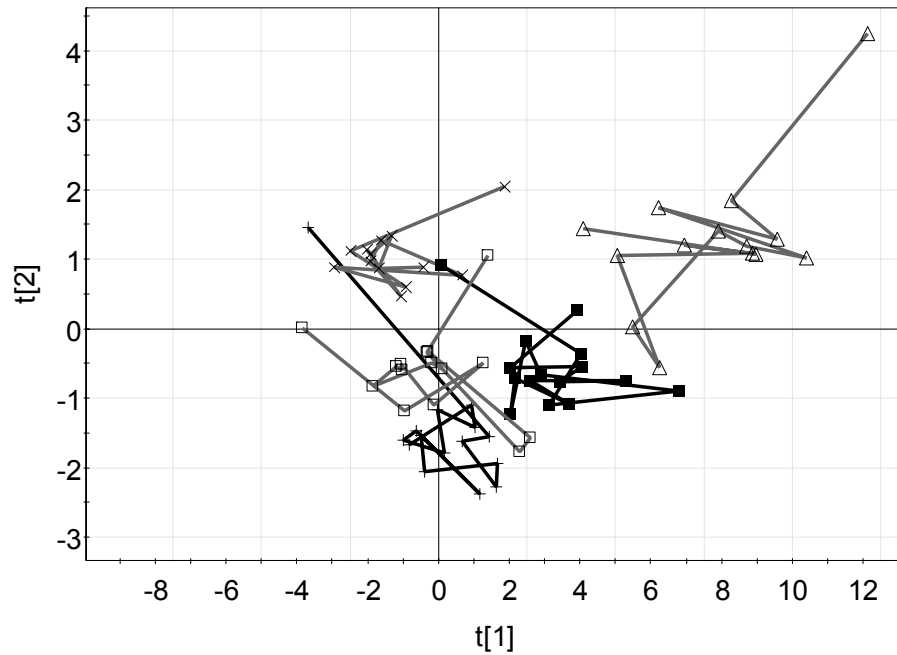
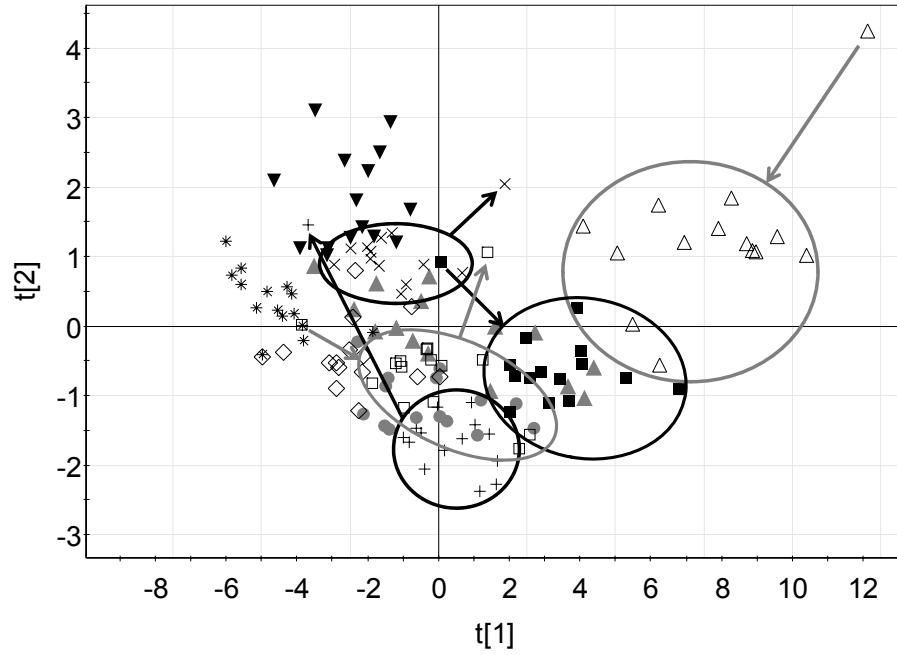


Figure 2-2- PCA scores plot of the serum samples. All samples are shown on the top, with day 1 or day 13 samples shown outside of the circles. Trajectories for selected subjects are shown on the bottom.

2.3.2 Urine

The PCA scores plot of the urine data is shown in Figure 2-3. In this model, all of the samples from one subject were outliers from all of the other samples from the rest of the subjects due to the presence of glucose in the urine. Since this abnormal occurrence is indicative of diabetes or glucose intolerance, the samples from this subject were excluded from further analysis. The spectra from two additional samples were also excluded due to poor quality. Since all urine samples were pooled 24 hour collections and this type of collection was not possible for the two week follow-up, urine samples from the two week follow-up were not used. In general, the scores plot shows less overlap between the subjects indicating a higher degree of inter-subject variation. The more diffuse subject groupings indicate that intra-subject variation is higher in the urine samples than in the serum. There were only 2 subjects which demonstrated day 1 samples that were outliers from the main group.

Since the previous data suggest that any metabolomic standardization due to controlled diet occurs within one day, urine samples from 55 subjects with only three days of dietary standardization were also examined. Additionally, a large amount of potential standardization is likely to occur in the first three days of diet standardization than three days later in the diet standardization study. Serum samples for all subjects were not available for this part of the study. It was thought that by increasing the number of samples, the more subtle changes in the metabolome may be detectable and thus some faint normalization effects of the three days of dietary standardization would be revealed. The PCA scores plot for this data is shown in Figure 2-4. It is clear that there is no significant separation of the samples from days one, two or three. A supervised partial least squares model for this data

was constructed (data not shown) and the results confirmed that there is no statistically valid separation of the days.

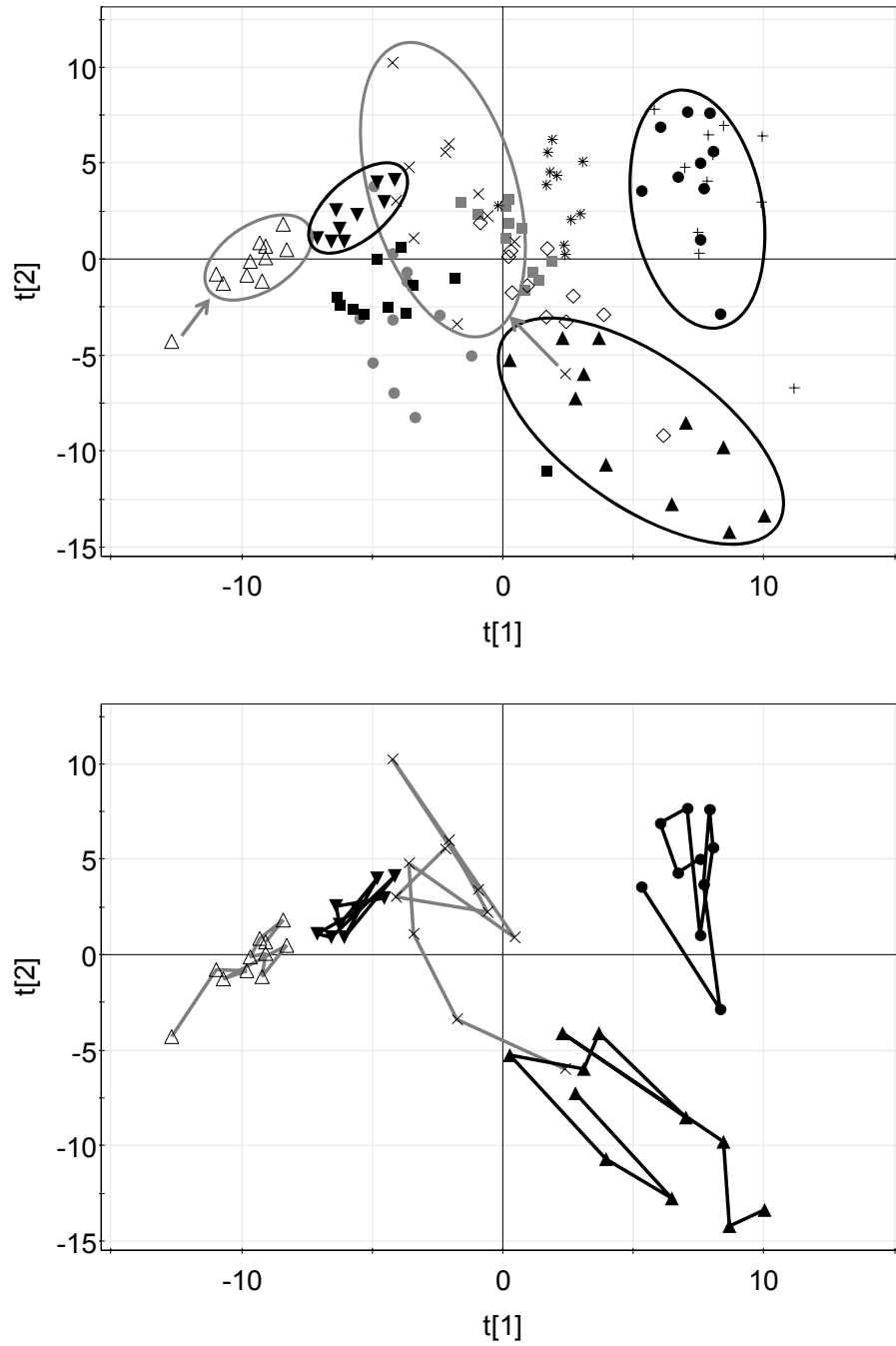


Figure 2-3- PCA scores plot of the urine samples. All samples are shown on the top, with day 1 or day 13 samples shown outside of the circles. Trajectories for selected subjects are shown on the bottom.

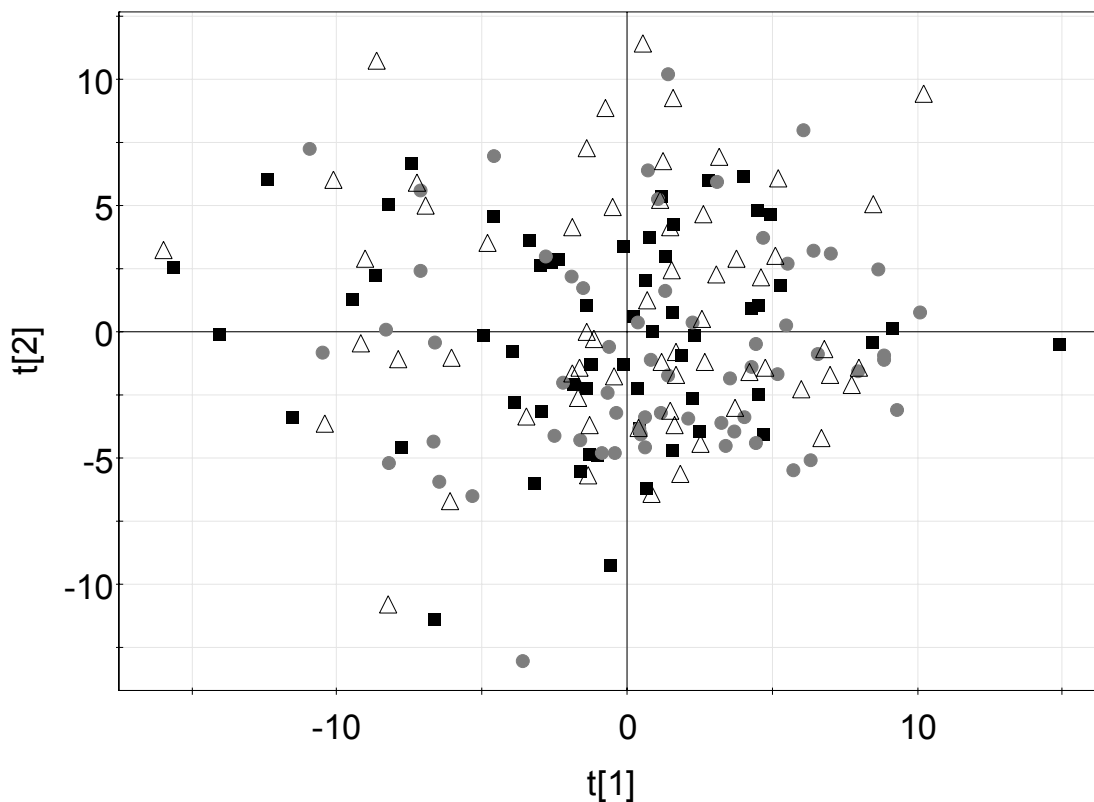


Figure 2-4- PCA scores plot of urine samples from days 1 - 3 for 65 subjects.

2.4 Discussion

This study was designed to address the question of how much normalization can be achieved in the human metabolome by carefully controlling diet and environment. For the serum metabolome, previous studies [167, 168] concluded that dietary standardization on the day prior to, or day of sample collection resulted in no observable normalization. By extending the dietary intervention our results show that for almost half of the subjects, an appreciable normalization of the metabolome is achieved with a single day of a standardized diet. The calorie controlled, standardized diet appears to have created a new homeostasis of the metabolome after 24 hours. There are several possible reasons why this effect was seen

in our study and not the other two. First, by extending the length of time that the diet was standardized, we were able to obtain a clearer picture of each person's metabolic space and therefore the outlier days are more distinct. Second, the more stringent dietary and environmental controls of an inpatient study may allow the observation of these subtle effects.

In the studies by Walsh and Lenz, detectable normalization of the urinary metabolome was observed after an acute dietary standardization, yet only minor standardization was observed in our study [167, 168]. This does *not* refute the other studies since we collected pooled 24 hour urine samples, whereas the other studies analyzed the much more variable samples from first void, morning, and evening collections. It is reasonable that acute dietary effects are more distinct in these time focused samplings. Essentially, these effects are averaged or diluted out by our 24 hour collections. The fact that the extended dietary standardization showed very little additional normalizing effect on the urinary metabolome shows that, as with serum, the normalizing effect of the diet is essentially complete after 24 hours.

To our knowledge this study provides the highest degree of dietary and environmental control in a human metabolomics trial to date. This study was carried out using global NMR-based profiling and therefore the inherent sensitivity limitations of NMR must be considered. It is possible that some low concentration components such as vitamins or minerals could be detected using analytical methods other than NMR. In future metabolomics studies, it appears that an inpatient, standardized diet lasting one to two days should be sufficient to provide all of the normalization that can be achieved in the human metabolome. These results, when applied to the study design of the two week

acetaminophen study presented in the next chapter of this dissertation (Chapter 3) indicate that the clinical design of the study is valid for a metabolomics analysis. Therefore, the subjects will be metabolically standardized and thus, the effects of acetaminophen administration will not be convoluted with the effects of dietary standardization.

3 Early Prediction of Acetaminophen-Induced Hepatotoxicity with Pharmacometabolomics

3.1 Introduction

Acetaminophen overdose is the primary cause of acute liver failure in the United States and the United Kingdom [19, 20]. This contrasts with the generally safe attitude many have towards the drug. Drug-induced liver injury (DILI) is the major adverse event that leads to regulatory actions on drugs, including failure to receive marketing approval, restricted clinical indications, and withdrawal from the marketplace [171]. It is not always possible to identify the susceptible patients due to the sometimes idiosyncratic nature of DILI, many patients who could take the drug safely may be denied treatment [172]. While genetic factors are sometimes the reason for DILI from certain drugs, frequently they don't fully explain the DILI [173]. This reflects the importance of non-genetic factors influencing susceptibility to DILI. Age, environment, nutrition, and other factors may play significant roles as discussed in the previous chapter (Chapter 2) of this dissertation and elsewhere [160, 161].

In a recent study, rats were given a single toxic-threshold dose of acetaminophen. Using NMR-based metabolomics, it was found that the pattern of endogenous metabolites in urine collected 48 to 24 hours prior to dosing could distinguish which animals would go on to develop severe DILI [174]. These authors proposed the term “pharmaco-metabonomics” which they defined as “the prediction of the outcome of a drug or xenobiotic intervention in an individual based on a mathematical model of pre-intervention metabolite signatures”.

Additional support for the pharmaco-metabonomic approach was reported in another rodent study in which the pre-dose urinary metabolomes could be used to predict which rats would develop diabetes after administration of a xenobiotic inducer of diabetes [175]. Finally, an article recently came out using a systems biological approach to characterize the differences in response as well as homeostatic differences between humans that experience hepatotoxicity and those that do not when given the drug ximelagatran [176].

A major goal in the application of pharmaco-metabolomics is to predict susceptibility of humans to adverse drug reactions. Among the challenges for this goal are to see the metabolic differences between responders and non-responders while only supplying the patients with therapeutic doses. This presents a two-fold problem. Generally, therapeutic doses do not elicit the usual more extreme metabolic responses of toxic sub-lethal or lethal doses. Additionally, effects from non toxic experimental interventions can be difficult to see in humans (see the previous chapter for more information on this). In this study, we have examined the potential of pharmaco-metabolomics to predict the outcomes of recurrent therapeutic dosing with acetaminophen in a human trial.

There are large inter-individual differences in susceptibility to acetaminophen-induced liver injury. It has recently been shown that about one in three healthy adult volunteers receiving the maximum recommended daily doses of acetaminophen (4 g/day) will develop mild liver injury as evidenced by elevations in serum alanine aminotransferase (ALT), aspartate aminotransferase, and α -glutathione-s-transferase [177]. Thus, human acetaminophen administration presents the ideal opportunity to test the idea of pharmacometabolomics in humans.

3.2 Methods

3.2.1 Clinical Trials

This study was composed of a cohort of 71 healthy adult males and females, aged 18-58 that were admitted inpatient for 14 days to the General Clinical Research Center at the University of North Carolina Hospitals. A genetic analysis of these subjects has been reported and this manuscript contains a more complete description of the protocol [178]. After three days on a controlled whole food diet, 58 subjects received 4 g (1 g, *qid*) daily for seven days and 13 subjects were placebos. Urine was continuously collected each day and pooled in 24 hour collections for metabolomics analysis (except for days 4 and 11 when urine was pooled in several collections for pharmacokinetic analyses). Serum was also obtained each morning for standard liver chemistry tests, including ALT.

3.2.2 Sample Preparation

Urine samples were removed from -80 °C storage and allowed to thaw at 4 °C overnight. Samples were vortexed to redissolve any precipitates due to freezing. Since the pH of urine can be variable, 540 µL of urine was added to NMR tubes containing 60 µL of a 900 mM phosphate buffer (pH = 6.2) solution in deuterium oxide (D₂O). In addition to the phosphate buffer, the D₂O solution contained 90 mM imidazole for pH reference, 4.6 mM trimethylsilyl-propionic acid (TSP) for concentration and chemical shift reference and 0.2% NaN₃ to act as a preservative.

3.2.3 NMR Spectroscopy

NMR experiments were performed on a 9.8 T Oxford magnet (Oxford Instruments, Plc, United Kingdom) controlled by a Varian Inova console (Varian Inc., Palo Alto, CA). The spectra were collected with a pulse sequence consisting of a 100 ms d1 delay, 4.0 s of presaturation, 20 ms CPMG delay, 90° pulse, and 2.6 s of acquisition. The free induction decay (FID) was acquired over a sweep width of 6387.7 Hz with 32720 complex points.

3.2.4 Data Processing and Analysis

The NMR data was processed with ACD NMR Processor, version 11 (Advanced Chemistry Development, Toronto, Canada). The FIDs were zero filled to 32768 real points and a 0.5 Hz exponential decay window was applied to the FIDs before Fourier transformation. The resulting spectra were then manually phased by a single person and baseline corrected with a 6th degree polynomial. All spectra were referenced such that the TSP peak was set to 0.00 ppm. Areas upfield of -0.20 and downfield of 10.00 ppm were omitted from further analysis. In addition, 4.60 – 6.30 ppm was excluded from analysis due to the residual water and urea peaks being in this area. The resulting areas of the spectra were binned using the Intelligent Bucketing routine with buckets ranging in width from 0.02 – 0.06 ppm in the ACD software. This routine uses an algorithm to place bin boundaries at areas of consensus local minima to avoid splitting peaks into more than 1 bin. The bins were then integrated to find the area under the spectra. Each bin integral represents the concentration of the metabolite or metabolites which have peaks in that bin.

The resulting integrals were exported and bins containing imidazole and TSP were excluded from further analysis. The resulting bins were normalized such that the sum of all

remaining integral values was assigned a value of 100. This was done to remove variance in the data resulting from urine dilution. Finally, the bins were sorted by average bin value. A threshold was found below which, bins only contained noise. These bins were excluded from further analysis and resulted in the loss of approximately 0.5% of total integral value per spectrum. The remaining 137 bins were then exported to Simca-P version 11.5 (Umetrics, Umea, Sweden) for multivariate analysis.

3.2.5 Multivariate Statistical Analysis

PCA analysis was performed on the samples to determine outliers which were excluded from further analyses. This resulted in slightly differing numbers of samples in each of the models. OPLS-DA models were generated using the Simca-P software. Cross-validation statistics for the OPLS-DA models were generated by the software using a leave one-subject-out cross-validation data procedure. The model statistics for the OPLS-DA models are: day 9 – 10- $R^2X = 0.471$, $R^2Y = 0.526$, $Q^2 = 0.452$; day 5 – 6 $R^2X = 0.432$, $R^2Y = 0.544$, $Q^2 = 0.451$; and day 2 – 3 $R^2X = 0.227$, $R^2Y = 0.560$, $Q^2 = 0.240$. The cross validation results for the three models are, 73.5%, 71.0% and 65.2% respectively.

3.3 Results

Figure 3-1 shows the ALT levels of the subjects over the two week study. Subjects who experienced peak ALT elevations greater than 2.0X their baseline level were considered “responders” (n=17) and those with levels less than 1.5X their baseline were considered “non-responders” (n=18). The intermediate responders (n=15), with ALT levels between

1.5X and 2.0X baseline, were not included in these analysis, in order to maximize differences between the responder and non-responder phenotype.

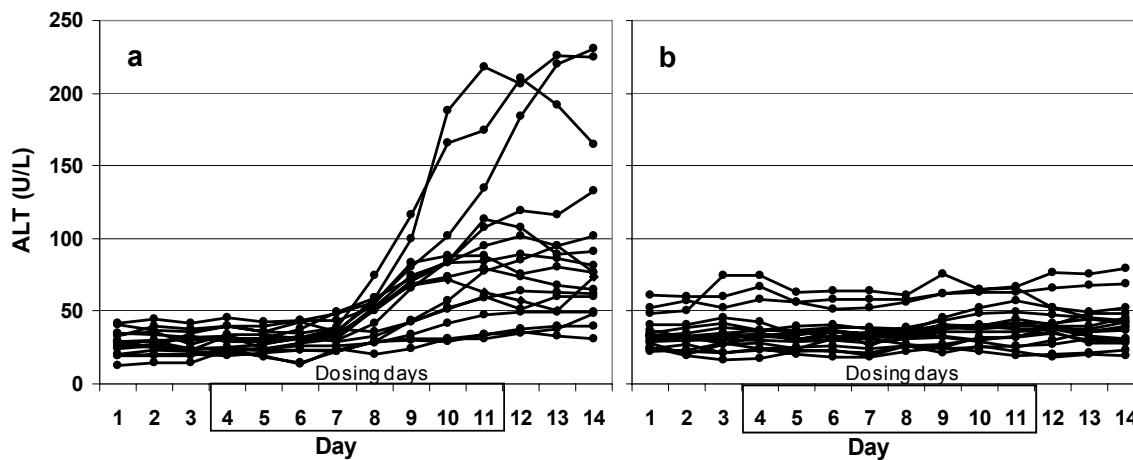


Figure 3-1- ALT levels for the responders (left) and non-responders (right).

The hypothesis of this study is that the human urinary metabolome contains sufficient information to discriminate the responders from the non-responders. As an initial test of this hypothesis, principal component analysis (PCA) was performed on binned NMR spectra obtained from all urine samples collected from days 5 through 10, which are all dosing days, on all of the responders and non responders. The PCA scores plot in Figure 3-2 shows each of the samples plotted on the two most significant axes. It can be seen that there is a clear distinction between the responder and non-responder groups.

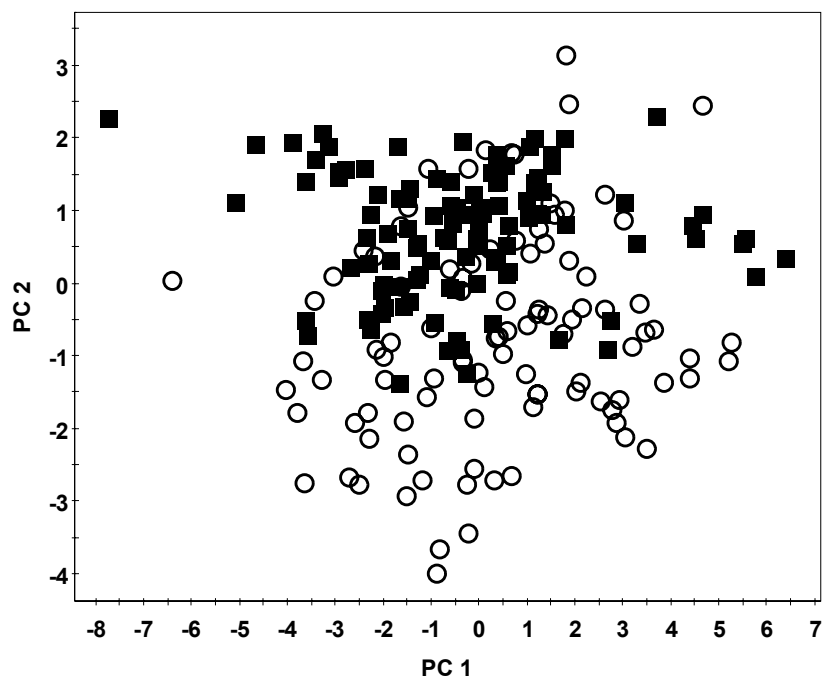


Figure 3-2- PCA scores plot for all responders (black) and non-responders (white) for days 5 - 10.

Next, a series of orthogonal partial least squares-discriminant analysis (OPLS-DA) models [179] were created using the data obtained at different time points during the study. Initially, samples from days 9 and 10 were analyzed, because the ALT levels of all of the responders had risen by this time and it seemed likely that there would be maximal discrimination between the two groups. Figure 3-3 displays the results of the OPLS-DA analysis for days 9 and 10, showing an appreciable separation of the two groups. The model statistics, R^2X , R^2Y and Q^2 indicate that the model is robust and not the result of statistical over-fitting. The R^2 values describe how well the models fit the NMR data (X data) and the responder/non-responder status data (Y data). The Q^2 values describe the predictive capacity of the model. The predictive accuracy of the model was calculated using a leave-one-subject-out cross validation procedure and was calculated as being 73.5%.

Figure 3-3 shows the OPLS-DA loadings coefficients which highlight the spectral bins that are most significantly different between the groups. The magnitude of the coefficients is related to the importance of that bin to the group separation and the error bars are the 90% confidence intervals derived from cross validation. Metabolite assignments for these bins are annotated on the plot. It is seen that a mixture of both endogenous and exogenous metabolites are important for the model discriminating the responders from non-responders.

The next step in the analysis was to determine if the urinary metabolome could distinguish the responders from non-responders after acetaminophen dosing, but prior to any rise in ALT levels. In this way, pharmaco-metabolomics is being used to monitor the initial perturbations in the metabolome after dosing has begun but before the evoked phenotype-rise in ALT. Samples from days 5 and 6 were analyzed and the OPLS-DA model is shown in Figure 3-3. As with the days 9 and 10 data, significant separation of the responders and non-responders is observed. The cross validation statistic of 71.0% correct sample classification is very similar to those for the model from days 9 and 10.

Finally, the metabolome present in urine obtained prior to dosing was examined to determine whether it contained enough information to discriminate the responders from non-responders. For this analysis, samples from days 2 and 3 of the study (the final pre-dosing days) were modeled. The validation statistics indicated a much less robust model with a Q^2 value of 0.240. The cross-validation procedure yielded a prediction accuracy of 65.2%, indicating that the pre-dose samples do not contain significant information to distinguish responders from non-responders.

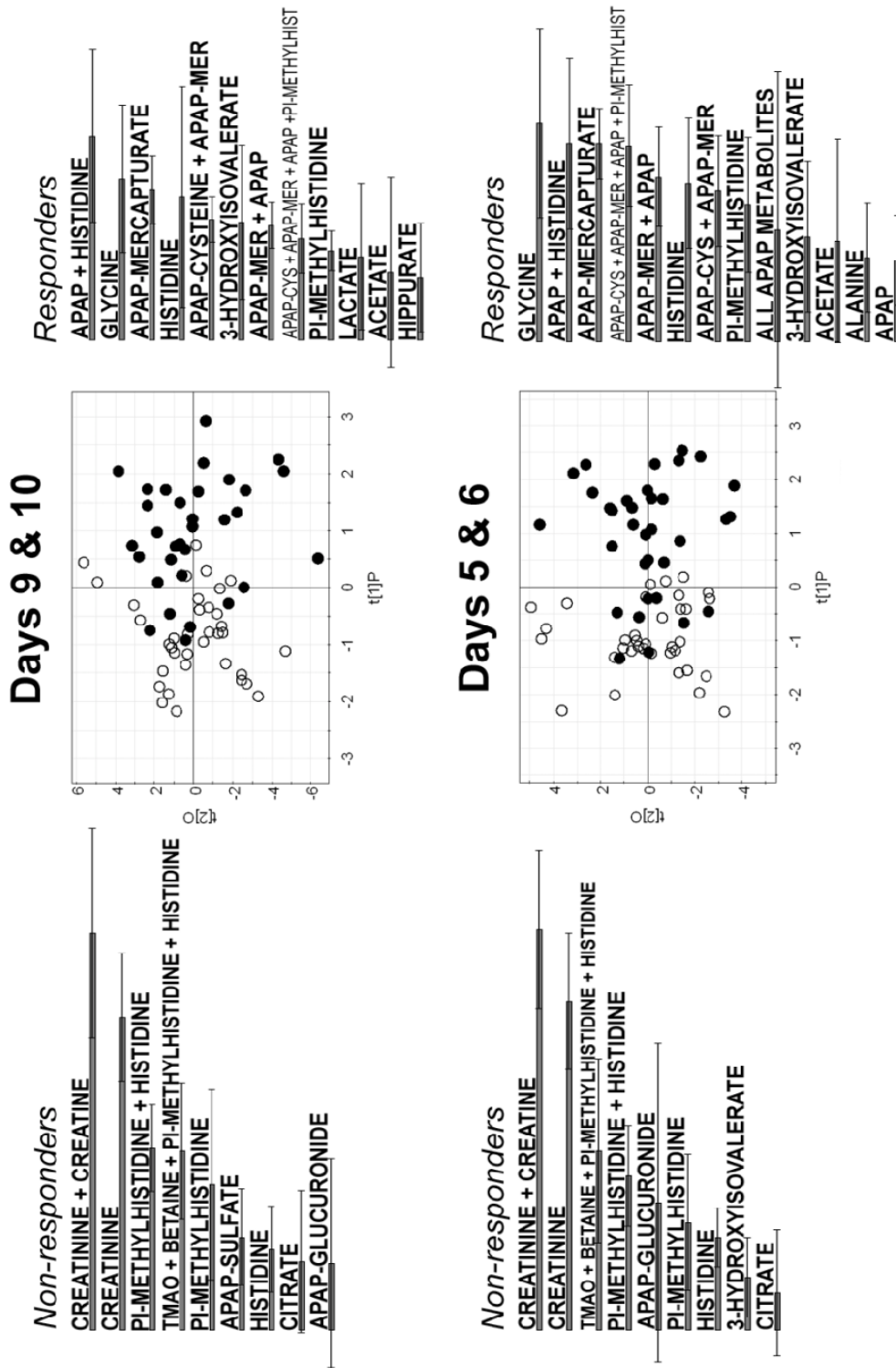


Figure 3-3- OPLS-DA scores plots for days 9 - 10 (top middle) and days 5 - 6 (bottom middle). The responder subject samples are the black dots and the non-responder subject samples are the open circles. Significant bins are identified to either side of the scores plots. The magnitude and confidence of significance are indicated by the magnitude of the bar and the size of the 90% confidence line, respectively.

| Days 9 - 10 | <i>Predicted</i> | |
|--------------------|------------------|---------------|
| <i>Actual</i> | Responder | Non-responder |
| Responder | 10 | 5 |
| Non-responder | 4 | 14 |
| Accuracy | 72.7% | p = 0.010 |
| Days 5 - 6 | <i>Predicted</i> | |
| <i>Actual</i> | Responder | Non-responder |
| Responder | 12 | 5 |
| Non-responder | 4 | 14 |
| Accuracy | 74.3% | p = 0.004 |
| Days 2 - 3 | <i>Predicted</i> | |
| <i>Actual</i> | Responder | Non-responder |
| Responder | 9 | 7 |
| Non-responder | 6 | 12 |
| Accuracy | 61.7% | p = 0.179 |

Table 3-1- Confusion matrices for the day 9 – 10 (top), 5 – 6 (middle), and 2 – 3 (bottom) OPLS-DA models.

We next compared the early-intervention pharmaco-metabonomic model obtained from days 5 and 6 with the model from days 9 and 10 to determine if the same or different metabolic perturbations led to the discrimination. To address this, a shared and unique structures (SUS) plot [180] was created, Figure 3-4. In this figure, the model components that are most highly correlated to the responder/ non-responder status from days 5 and 6 are plotted against those of days 9 and 10. Since the points lie predominantly along the diagonal, the significant components of each of the two models were quite similar. It is seen that the predictive bins contain acetaminophen metabolites as well as endogenous metabolites. It is of note that the cysteine and mercapturate conjugates of acetaminophen tended to be higher in the urine of responders than non-responders. This is consistent with expectation since these are the major derivatives of N-acetyl paraquinone imine (NAPQI), the known hepatotoxic metabolite and thus responders tended to make more NAPQI than the non-responders.

To determine if the prediction of the responders and non-responders was mainly driven by the acetaminophen metabolites, models for both days 5 and 6 and days 9 and 10 were created using quantitative measurements of the parent acetaminophen together with all measured acetaminophen metabolites- the glucuronide, sulfate, cysteine, and mercapturate conjugates, (data not shown). The separation between the groups is much less clear and the Q^2 values of 0.09 for days 9 and 10 and 0.16 days 5 and 6 are much weaker and indicative of no significant predictive capacity. Models generated using only the endogenous components, excluding all acetaminophen metabolites, were similar in appearance to those created with all of the data and the cross validation and predictive capacity calculations were also very similar (data not shown). Given the fact that the number of bins corresponding to acetaminophen metabolites is less than 10% of the total number of bins used in the model, it is not surprising that the model did not change appreciably, but the fact that the acetaminophen metabolites were significant in the OPLS-DA loadings coefficients plots indicates that the combination of endogenous and exogenous metabolites is important for the prediction of the responder/non-responder status of a subject. Additionally, the fact that the removal of the acetaminophen (and conjugates) bins did not negatively impact the model, as well as the fact that the acetaminophen (and conjugates) are elevated and lowered in the expected groups (responder or non-responder) is an indication that the information contained in the acetaminophen (and conjugates) bins is redundant or linked, directly or indirectly, with other endogenous bins.

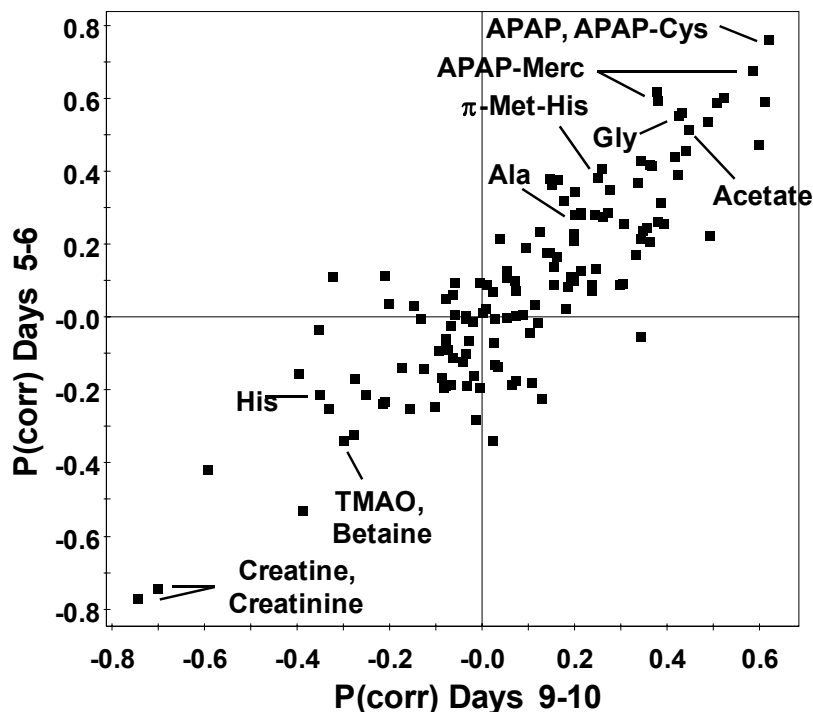


Figure 3-4- Shared and unique structures (SUS) plot generated from the first component of the day 9 - 10 and day 5 - 6 OPLS-DA loadings plots. The location of the bins along the bottom left to the top right diagonal indicate similar model characteristics between the day 9 – 10 and 5 – 6 models.

3.4 Discussion

A significant amount of research on acetaminophen-induced liver injury has been conducted, but most of it involves toxic doses in animal models or clinical examinations of accidental or deliberate human overdoses [181-190]. Although an extensive identification of specific metabolic perturbations was not possible in this study, several of the identified metabolites are consistent with previous studies. Elevated levels of the cysteine and n-acetyl cysteine (mercapturate) conjugates of acetaminophen were observed in the responders. This is consistent with the increased formation of the toxic intermediate, NAPQI, in those subjects. The cysteine and mercapturic acid conjugates are breakdown products of the glutathione conjugated acetaminophen [191, 192]. Several amino acids including glycine,

alanine, and histidine were found to be elevated in the responders at both days 5 – 6 and 9 - 10. Glycine is a precursor of glutathione, which is required to detoxify NAPQI. A perturbation in the synthesis of glutathione in the responders may lead to less efficient utilization of glycine and thus more excreted in the urine. Additionally, glycine has been hypothesized to have hepatoprotective effects not involving glutathione synthesis by attenuating fatty acid β -oxidation interference related hepatotoxicity [193].

Two possible mechanisms which could account for the high amounts of glycine in the responders involve creatine synthesis and glutathione conjugate degradation. In humans, approximately half of stored creatine originates from food and half is synthesized [194]. The first step in the synthesis of creatine, the rate limiting step, involves the transfer of an amidino group from arginine to glycine forming guanidinoacetate (and ornithine). This is catalyzed by arginine-glycine amidinotransferase (AGAT). Next, the guanidinoacetate is methylated by the methyl donor s-adenosyl methionine (SAM) forming creatine (and SAH, s-adenosyl homocysteine). This reaction is catalyzed by guanidinoacetate methyltransferase (GAMT). Thus, one would expect a negative correlation between glycine and creatine, which is what we see in this case. The responders have higher glycine and the non-responders have higher creatine/creatinine.

Glutathione is used to conjugate and detoxify, in a phase II reaction, the NAPQI created in a phase I reaction by P450. Higher levels, or increased production of, glutathione could be a mechanism to mediate the NAPQI toxicity. The first step in glutathione synthesis involves the formation of γ -glutamylcysteine from glutamate and cysteine via the enzyme γ -glutamylcysteine synthetase. This is the rate limiting step in glutathione production. Next, glycine is added to the c-terminus of the cysteine via the enzyme glutathione synthase. Since

cysteine is the rate limiting amino acid in glutathione, up regulation of cysteine synthesis may allow for up regulation of glutathione synthesis which may allow for greater detoxification of NAPQI.

Cysteine synthesis involves the formation of cystathione from homocysteine and serine via the enzyme cystathionine β -synthase. Next, the cystathione is cleaved to yield α -ketobutyrate and cysteine via the enzyme cystathionine γ -lyase.

To create the homocysteine necessary for cysteine synthesis, SAM is demethylated to create SAH which has the adenosine hydrolyzed to create homocysteine. A methyl acceptor is necessary to create the SAH from SAM and one such acceptor is guanidinoacetate. Methylation of guanidinoacetate forms creatine. Guanidinoacetate is formed from glycine (and arginine). This is one mechanism linking glycine with creatine and APAP-mercapturate (via GSH via cysteine synthesis). It is postulated that the upregulated cysteine synthesis allows for better detoxification of NAPQI and therefore less (or no) hepatotoxicity from APAP. One of the byproducts of the cysteine synthesis would be depleted glycine and increased creatine. This is observed in the non-responders and has been demonstrated before [195, 196].

Another possible mechanism for the increased glycine seen in the responders involves the fact that glutathione conjugates are generally not excreted in the urine. The γ -glutamate-cysteine bond is broken by γ -glutamyltransferase (GGT), located on the surface of hepatocytes and at the surface of brush border cells on the proximal tubules of the kidney [192], and the glutamate is released. In humans, unlike rodents, the specific activity of GGT is higher in the liver than the kidney [192]. This would lead to the formation of APAP-Cys-Gly from APAP-GSH as the APAP-GSH leaves the hepatocyte into circulation. The brush

border membranes of the kidney are also rich in cysteinylglycine dipeptidase. This is the enzyme which cleaves glycine from cysteine-glycine conjugated molecules. The resulting APAP-Cys is either excreted or absorbed by the brush border cells and acetylated on the nitrogen of the cysteine by the intracellular enzyme, n-acetyltransferase. This forms the n-acetyl-cysteine conjugate, also known as the mercapturic acid conjugate. The cleavage of the glycine in the proximal tubule is a likely candidate for the increased glycine excreted in the urine of the responders.

Several bins contained metabolites that are often attributed to gut flora, including TMAO, betaine, and hippurate, which tended to be present in lower levels in the responder group. Differences in the pre-dose profile of TMAO and betaine were also observed in the original pharmaco-metabonomic paper in rats by Clayton, *et al* [174]. Perhaps the gut flora has an effect on absorption of acetaminophen or enterohepatic circulation of the drug. These effects may attenuate or intensify acetaminophen toxicity and these flora-specific metabolites may be a way to evaluate these effects. Unfortunately, further development of this hypothesis is beyond the scope of this study.

To our knowledge, this represents the first application of the pharmaco-metabolomics concept in the study of an adverse drug reaction in humans. As noted in the original description [174], the success of the pharmaco-metabolomic approach would be expected to vary based on the particular drug, dosage and metabolic perturbation imposed by the treatment. We were unable to detect patterns in the pre-dose urine metabolome that would significantly separate responders from non-responders, although this might have been possible had a larger number of subjects been studied, or had the study been conducted with an animal model. However, significant separation was achieved once the subjects began

treatment with acetaminophen and before DILI occurred. In this study the endogenous changes including possible perturbations in glutathione synthesis could only be observed once the acetaminophen dosing begun.

Since serious DILI is often a delayed phenomenon, occurring weeks to months after starting therapy [171], this early intervention pharmaco-metabolomic approach, if confirmed in studies of other medications, could represent a practical method to identify susceptible patients soon after starting drug treatment but before they are at risk of developing DILI.

4 Stable Isotope Resolved Metabolomics of Acetaminophen Toxicity Reveals an Apparent Stressed Phenotype Exhibited in Primary Human Hepatocytes

4.1 Introduction

Some experiments are well suited for multivariate statistical examinations, such as the one described in Chapter 3 of this dissertation. However, these multivariate statistical analyses do have their limitations. The main limitation is the fact that metabolite measurements are all static and derived from the central compartment (i.e. blood or urine) and metabolic effects of the experimental intervention are surmised based on known mechanisms. Thus, it may not be possible to determine specific anomalous mechanisms resulting in the increase or decrease of the observed metabolites.

Changes in the concentration of a metabolite can be due to increased or decreased production or consumption of that metabolite. These things cannot be conclusively determined with concentration alone. Additionally, shifts in metabolism- where a compound is being produced from a different pathway or compound, cannot be determined with concentration alone. This is especially important when there are multiple branch points in a metabolic pathway, like with the multiple entry and exit points of the TCA cycle. These points provide sources of energy from different pathways, such as glycolysis, glutaminolysis, and fatty acid β -oxidation. Understanding shifts in metabolism, as well as in the transcriptome and proteome, are important parts of fully understanding the effects that different xenobiotics have on an organism or cell type. In consideration of these deficiencies

in human metabolomic studies of biofluids, this study focuses on the metabolomic aspects of acute acetaminophen exposure and toxicity to human hepatocytes.

It was seen in the previous chapter of this dissertation (Chapter 3) that there were significant elevations in lactate, alanine, and acetate in the responders compared to the non-responders. These are the metabolites out of the entire cohort which have a significant liver/energy relationship. Additionally, data from whole human studies can be difficult to deconvolute due to multiple organ interactions, temporal effects, and the heterogeneity of the human population. Therefore, the use of stable isotope enriched glucose and octanoic acid media formulations with cultured human hepatocytes may allow for metabolic analysis of the pathways pertinent to the three significant metabolites identified in the previous chapter. Lactate and alanine are the end-products of glycolysis via glucose catabolism, and acetate is the end-product of fatty acid (i.e., octanoic acid) catabolism via β -oxidation. This ^{13}C fluxomic method has recently been called stable isotope resolved metabolomics (SIRM) [197].

The experiments presented in this chapter were conducted with fresh primary human hepatocytes, cryopreserved primary human hepatocytes, and fresh primary rat hepatocytes. Initial experiments were conducted with fresh human hepatocytes to determine the sub-toxic to minimally toxic effects of acetaminophen on human hepatocytes. It was initially intended to be a similar exposure concentration to the acetaminophen dose given to the humans in the previous study described in Chapter 3. This was conducted in an attempt to generate more data to complement the experiment and subsequent analysis. Previous experiments have shown the 24 hour LD_{50} of acetaminophen in cultured primary human hepatocytes to be 28.2 mM [198]. Thus, exposing human hepatocytes to 1 and 10 mM acetaminophen for 2 hours

should elicit sub-toxic or minimally toxic effects what will be detected as shifts in substrate utilization in the metabolome.

The first experiments with the fresh hepatocytes involved dosing them with 1 or 10 mM acetaminophen in DMEM + 10% FBS containing either U-¹³C glucose (which can assay for lactate and alanine) or U-¹³C octanoic acid (which can assay for acetate). The addition of these two compounds was intended to probe the metabolic origins of the biomarkers found in the human study described in the previous chapter. The paradigm of acetaminophen toxicity is that the TCA cycle is inhibited due to oxidative stress related inhibition of oxidative phosphorylation resulting in a lower ATP:ADP ratio [187-189]. It is thus hypothesized that this uncoupling of oxidative phosphorylation leads to a high NADH:NAD⁺ ratio which leads to a decrease in TCA cycle activity and a compensatory increase in anaerobic glycolysis to correct the redox state as well as produce ATP [199]. This increase in glycolysis will likely result in accumulation of the anaerobic glycolytic end products of lactate and alanine, derived from glucose [188]. In fact, an increase anaerobic respiration due to acetaminophen toxicity has also been demonstrated [199], and an early term defined the phenomenon as “chemical hypoxia” [188]. Additionally, arguments can be made for an increase in acetate or a decrease in acetate due to the uncoupling of oxidative phosphorylation and the TCA cycle. An increase, which was observed in the experiment in Chapter 3, could be due to a buildup of acetate caused by it being less utilized as a result of the impairment in TCA cycle activity. Or acetate could decrease if the impairment in TCA cycle activity causes fatty acid β -oxidation to decrease.

In addition to glycolysis, it is hypothesized that acetaminophen toxicity will have an inhibitory effect on glutamate (and therefore glutamine- found in the culture media) entry

into the TCA cycle due not only to the decrease in TCA cycle activity, but also because the reactive intermediate of acetaminophen, n-acetyl-p-benzo-quinone imine (NAPQI), has been shown to bind to glutamate dehydrogenase and glutamine synthetase (see Table 1.1 in Chapter 1.4.6 of this dissertation). Thus, it is hypothesized that due to acetaminophen toxicity, there will be decreased glutamine utilization for the TCA cycle. Thus, it is hypothesized that upon exposure to acetaminophen, there will be a shift towards the creation of ^{13}C -labeled metabolites of the U- ^{13}C glucose-derived glycolytic end products of lactate or alanine (see Figure 1-11) and a decrease in U- ^{13}C glutamine entry into the TCA cycle (see Figure 1-12).

As will be discussed in further detail in the results section, it was determined that the cultured human hepatocytes do not metabolize glucose to a significant degree, even in the presence of high concentrations of glucose and insulin. This unexpected non-utilization of media glucose led to another set of experiments to compare the basal metabolism of rat hepatocytes with the human hepatocytes. Many of the human hepatocyte cultures were from liver resections. The human stress response to injury and surgery (the surgical trauma in addition to exposure to certain anesthesia) has been documented to induce a considerable stress response [200, 201].

In light of these studies showing the effects on metabolism of surgery and anesthesia, an experiment to determine whether or not the block in glycolysis observed in the human hepatocytes could be overcome by depletion of ATP via mitochondrial oxidative stress by the use of hepatotoxic administration of acetaminophen. Cryopreserved human hepatocytes were used to test the effect of a higher dose of acetaminophen over a two-fold longer period

of exposure to ensure toxic inhibitory effects on the TCA cycle and ultimately up-regulate glycolysis and the metabolism of glucose (U-¹³C glucose in this case).

4.2 Methods

4.2.1 Human Hepatocyte Isolation and Cultures

Primary fresh human hepatocytes were isolated from living donors, plated, and cultured for one to two days to allow attachment. They were then shipped to the authors via overnight delivery. After they were received, they the hepatocytes were cultured for another day to allow for media acclimation prior to experimentation. Six 6-well plates were received five times for five different experiments. The 1 male and 5 female subjects ranged in age from 24 – 71 and were not steatotic.

Primary cryopreserved human hepatocytes were isolated from an approximately 18 month old male and cryopreserved using standard hepatocyte cryopreservation procedures. After thawing, the hepatocytes were cultured in a DMEM-based media supplemented with FBS and cultured for 1 day to allow attachment. They were then acclimated to the new media for 12 hours.

4.2.2 Rat Hepatocyte Isolation and Cultures

All animals were humanely treated and housed in accordance with the guidelines set by the Institutional Animal Care and Use Committee (IACUC) of the University of North Carolina (protocol 08-130.0A). Male Sprague Dawley rats (Charles River, Frederick, MD) were housed in a 12-h light-dark cycle and allowed water and food *ad libitum*. The rats were anesthetized for surgery with pentobarbital (0.5 µg/g body weight), and the hepatocytes were

isolated following collagenase perfusion of the liver. After isolation, the hepatocytes were incubated at 37 °C in Krebs-Ringer-HEPES (KRH) (116 mM NaCl, 5 mM KCl, 1mM KH₂PO₄, 2.5 mM MgSO₄, 2.5 mM CaCl₂, 25 mM HEPES, 1% BSA, pH 7.4) for 10 min. While at 37 °C, the cells were gently mixed every 2 min. The hepatocytes were then allowed to settle for 15 min on ice and the top layer was removed. Then, the cells were washed in KRH and spun and pelleted at 50 x g three times. After the last spin, the hepatocytes were re-suspended in KRH and cell number and viability was assessed by trypan blue exclusion. Hepatocyte viability was 85% or greater. The hepatocytes were plated into 14 cm collagen coated plates (BD PharMingen, San Diego, CA) at a density of 20 x 10⁶ cells/plate and incubated at 37 °C in 5% CO₂ for 24 h at 37 °C in 5% CO₂ prior to experimentation.

4.2.3 Hepatocyte Treatments

Upon reception of the fresh hepatocytes, media was changed to a high glucose (25 mM) DMEM media containing 10% FBS, 4 mg/L insulin, 100 nM water-soluble dexamethasone, and penicillin-streptomycin. The fresh hepatocytes were allowed to acclimate to the new media (and shipping effects) for 24 hours in a 37 °C, 5% CO₂ incubator. Each experiment had a control, a vehicle control (0.1% DMSO), a low dose (1 mM) acetaminophen treatment, and a high dose (10 mM) acetaminophen treatment. The 3 experimental conditions each used six wells of one 6-well plate. Thus, each of the conditions was performed in a pooled sextuplet. For each experiment, the fresh hepatocytes were exposed to media containing U-¹³C glucose instead of the regular ¹²C glucose for 2 hours, or media supplemented with 1 mM U-¹³C octanoic acid for 2 hours.

Upon reception of the cryopreserved human hepatocytes, the media was changed to high glucose serum free DMEM containing 4 mg/L insulin, 100 nM water-soluble dexamethasone, and penicillin-streptomycin. The cryopreserved hepatocytes were allowed to acclimate to the new media for 8 hours in a 37 °C, 5% CO₂ incubator. All experiments were performed in a pooled triplicate with 3 wells of a 6 well plate being pooled. Experimental conditions were used to examine vehicle control (0.1% DMSO), exposure to a low dose of acetaminophen (10 mM), and exposure to a high dose of acetaminophen (40 mM). For each experiment, the hepatocytes were exposed to media containing either U-¹³C glucose or U-¹³C glutamine substituted for the regular ¹²C glucose or glutamine.

With the intent on eliciting a response due to acetaminophen toxicity, higher doses of acetaminophen were used in the cryopreserved human hepatocytes (10 mM and 40 mM vs. 1 mM and 10 mM). Additionally, the cryopreserved hepatocytes were exposed to acetaminophen for 4 hours instead of the 2 hours that the fresh hepatocytes were exposed. Finally, the cryopreserved hepatocytes were given a hormonally-defined serum-free medium, instead of a serum containing medium, like the fresh hepatocytes were given, since it has been shown that the presence of serum in media promotes down regulation of P450 and hepatocyte dedifferentiation [59, 60].

After the rat hepatocytes were isolated, they were given a media formulation consisting of high glucose (25 mM) DMEM media containing 10% FBS, 4 mg/L insulin, 100 nM water-soluble dexamethasone, and penicillin-streptomycin. The hepatocytes were allowed to adhere to 100 mm plates for 24 hours in a 37 °C, 5% CO₂ incubator. For each experiment, consisting of 4 – 5 replicates, the hepatocytes were exposed to media containing U-¹³C glucose instead of the regular ¹²C glucose, U-¹³C glutamine instead of the regular ¹²C

glutamine for 2 hours, or media supplemented with 1 mM U-¹³C octanoic acid for 2 hours. These conditions were tested with both insulin and glucagon separately.

4.2.4 Metabolite Isolation

Metabolites from the human hepatocytes were extracted with a modified cold methanol extraction procedure [202-207]. First, wells were washed 2 times with 2 mL of ice cold phosphate buffered saline (PBS). Next, 500 µL of methanol-water (65:35), stored in dry ice, was added to the wells. The cells and liquid were then scraped from the wells and removed. The wells were then rinsed with another 500 µL of ice-cold methanol-water (35:65). The cells and liquid was again removed and kept. The samples were then shaken and frozen in liquid N₂. Once thawed, the samples were vortexed and frozen again in liquid N₂. The mixture was then centrifuged to separate the pellet from the methanol-water solution, which was drawn off and kept. One mL of ice cold methanol-water (this time at 50:50) was added to the pellet which was then vortexed to separate the pellet from the bottom of the tube (due to the centrifugation) and frozen in liquid N₂. Once thawed, the samples were again centrifuged to separate the pellet from the methanol-water which was drawn off and added to the initial extraction. The extractions were then dried overnight in a room-temperature speed vac.

Metabolites from rat hepatocytes were extracted by a slightly modified Folch method [208]. First, plates were washed 2 times with 12 mL of cold PBS. Next, 5 mL of ice-cold methanol was added to the plates. The cells were then scraped from the plates and removed. The plates were then rinsed with another 5 mL of ice cold methanol and scraped again. The methanol was again removed and kept. Ten mL of ice cold water and 13 mL of chloroform

was added to the methanol-cell mixture. After the samples were mixed, they were allowed to separate into aqueous and organic phases overnight at 4 °C. Samples were then centrifuged at 500 x g for 15 minutes and the two phases were separated and dried under vacuum.

4.2.5 NMR Sample Preparation

The aqueous extract samples from the human hepatocytes were removed from -80 °C storage and reconstituted with 240 µL deuterated water containing trimethylsilyl propionic acid (TSP) which serves as a concentration and chemical shift reference and 0.02% NaN₃ to act as a preservative. Fresh hepatocyte extracts were reconstituted as pooled sextuplets and the cryopreserved extracts were reconstituted as pooled triplicates.

Media samples from both the human and rat hepatocytes were mixed 5:1 with D₂O (200 µL media with 40 µL D₂O) containing TSP and 0.2% NaN₃. Organic extract samples were reconstituted with 240 µL of a 50% deuterated methanol, 50% deuterated chloroform solution containing 0.05% trimethylsilane (TMS) which serves as a concentration and chemical shift reference.

Aqueous extract samples from the rat hepatocytes were removed from -80 °C storage and reconstituted with 240 µL deuterated water containing 1.0 mM trimethylsilyl propionic acid (TSP) which serves as a concentration and chemical shift reference and 0.02% NaN₃ to act as a preservative. Organic extract samples were reconstituted with 240 µL of a 50% deuterated methanol, 50% deuterated chloroform solution containing 0.05% trimethylsilane (TMS) which serves as a concentration and chemical shift reference.

4.2.6 NMR Spectroscopy

Aqueous cell extract and cell media NMR experiments for the human hepatocytes were performed on a 17.1 T Oxford magnet (Oxford Instruments, Plc, United Kingdom) controlled by a Varian Inova console (Varian Inc., Palo Alto, CA). The spectra were collected with a pulse sequence consisting of a 100 ms d1 delay, 2.0 s of presaturation, acquisition pulse at the Ernst angle, and 3.64 s of acquisition. The free induction decay (FID) was acquired over a sweep width of 8999.9 Hz with 64k complex points.

NMR spectroscopy of organic cell extracts from the rat hepatocytes was performed on the same spectrometer as above. The spectra were collected with a pulse sequence consisting of 2 ms d1 delay, acquisition pulse at the Ernst angle, and 3.64 s of acquisition. The FID was acquired over a sweep width of 8999.9 Hz with 64k complex points.

4.2.7 Data Processing and Analysis

The NMR data was processed with ACD NMR Processor, version 11 (Advanced Chemistry Development, Toronto, Canada). The FIDs were zero filled to 64k real points and a 0.5 Hz exponential decay window was applied to the FIDs before Fourier transformation. The resulting spectra were then manually phased and baseline corrected by a single person. All spectra were referenced such that the TSP peak was set to 0.00 ppm. Metabolite concentrations were calculated by either integrating or fitting peaks of interest and comparing those peak areas to the area of the TSP peak.

4.2.8 Statistics

The concentrations and fractional enrichments were shown as mean \pm standard error of the mean and were compared for significance using an unpaired Student's t-test with $p < 0.05$. Microsoft Excel 2007 (Redmond, WA) and GraphPad Software, Inc. (La Jolla, CA) were used for all statistical calculations.

4.3 Results

Representative spectra of hepatocyte extract showing fractional enrichment of aspartate, alanine, lactate, fumarate, and glycogen from U-¹³C glucose is shown in Figure 4-1. From the respective ¹H spectra displayed in this figure, the metabolic products of the media glucose (as well as octanoic acid and glutamine, though not shown) can be easily seen and discriminated from the other metabolites not created from the media glucose, as well as the ¹³C satellite peaks used to calculate the fractional enrichment.

The time to reach ¹³C isotopic steady state was determined using by observing the change in fractional enrichment of lactate over time as well as other metabolites of relatively slower turnover rate. This can be seen in Figure A-1 in Appendix A. Additionally, the isotopomeric scrambling scheme of U-¹³C pyruvate derived from U-¹³C glucose and forming the isotopomers represented by the respective peaks in the ¹H spectra shown in Figure 4-1 is shown in Figure A-2 in Appendix A. More details on this are in Appendix A.

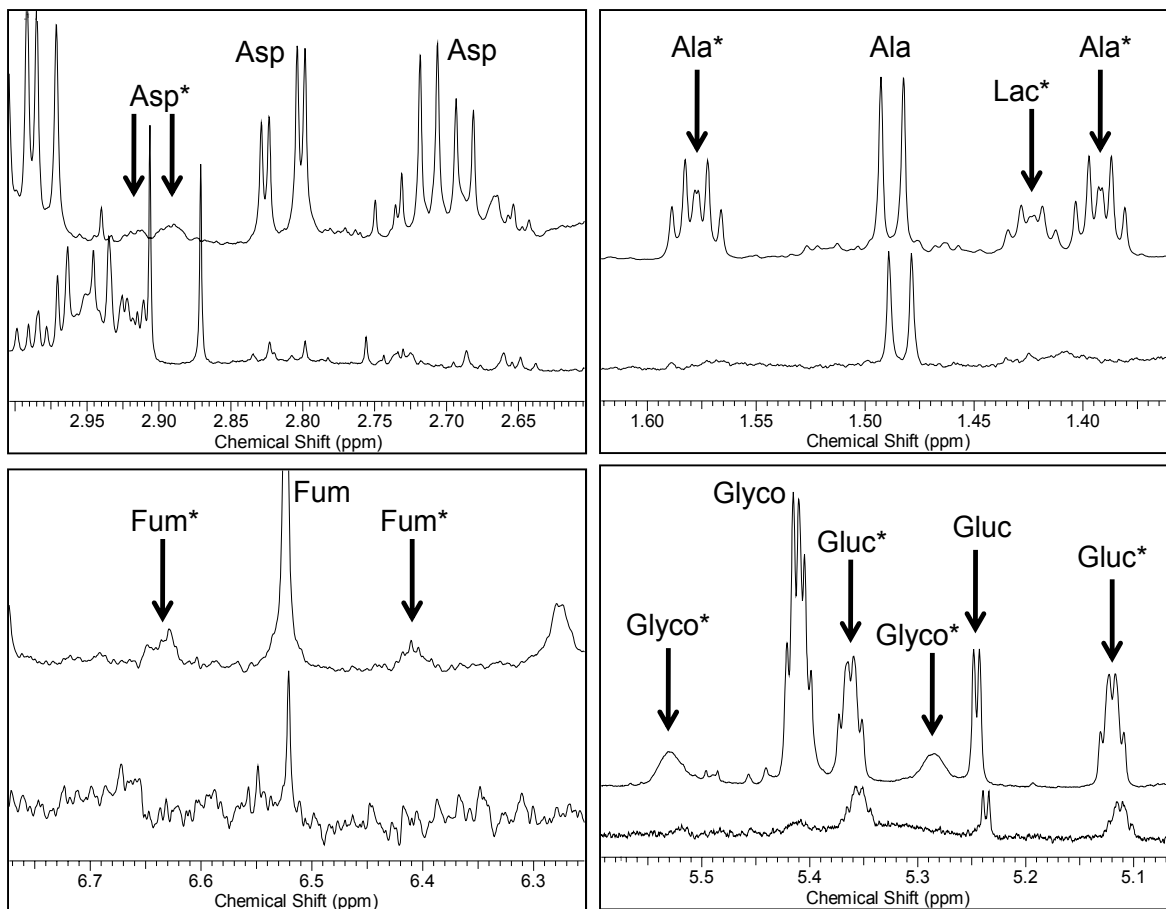


Figure 4-1- Comparison of representative primary human hepatocyte (bottom spectra) and primary rat hepatocyte (top spectra) extracts from hepatocytes given ^{13}C glucose enriched media. Asp = aspartate, Ala = alanine, Lac = lactate, Fum = fumarate, Glyco = glycogen, and Gluc = glucose. ^{13}C metabolites are marked with an asterisk (*). It can be seen that there is production of lactate, alanine, glycogen, aspartate and fumarate in the rat hepatocytes, but not in the human hepatocytes.

The most striking observation is the fact that human hepatocytes do not metabolize media glucose or glutamine for energy needs to any detectable level over the 2 hour (fresh hepatocytes) or 4 hour (cryopreserved hepatocytes) exposure period. This is evident due to the lack of metabolic products of the media ^{13}C glucose in fresh and cryopreserved human hepatocytes as well as media ^{13}C glutamine in cryopreserved human hepatocytes in the intracellular extracts or media.

While the U- ^{13}C glucose and U- ^{13}C glutamine do not seem to be metabolized for energy to a significant degree in the fresh human hepatocytes, the free fatty acid, octanoic

acid is metabolized (via fatty acid β -oxidation) to the ketone bodies acetate and β -hydroxybutyrate as well as the TCA cycle intermediate fumarate. Thus, it appears that the human hepatocytes are in a fasted or even a stressed metabolic state due to the presence of fatty acid β -oxidation, and the lack of glycolysis and glutaminolysis for energy needs even in the presence of high media glucose and insulin concentrations.

Examination of metabolism in cultured primary rat hepatocytes was conducted to determine if they metabolize glucose, octanoic acid, and glutamine to the same extent as human hepatocytes. Since the human hepatocytes appeared to be in a fasted or stressed state, rat hepatocytes were cultured under the same conditions to compare the metabolism to the human hepatocytes. Thus, high glucose DMEM formulations containing insulin and the different ^{13}C -enriched compounds substituted for the normal ^{12}C compounds were tested in rat hepatocytes. When the rat hepatocytes were incubated with DMEM containing U- ^{13}C -glucose, U- ^{13}C -glutamine, and U- ^{13}C -octanoic acid, fractional enrichment of acetate, acetoacetate, aspartate, alanine, fumarate, glycogen, and β -hydroxybutyrate (β -HB) was detected. The fractional enrichments of the above mentioned metabolites are observed as ^{13}C satellite peaks, which can be seen in the ^1H NMR spectra shown in Figure 4-1. From the detection of the ^{13}C fractional enrichment in the rat cellular extracts it is concluded that they metabolized the media glucose, while the lack of detectable ^{13}C fractional enrichment in the human hepatocytes demonstrates that they do not consume media glucose. Aerobic metabolism of glucose, glutamine, and octanoic acid as well as anaerobic metabolism of glucose, ketosis of octanoic acid, and glycogen synthesis from glucose is all observed. Thus, the rat hepatocytes rely on sugars, amino acids, and free fatty acids (FFA) as substrates for aerobic energy production.

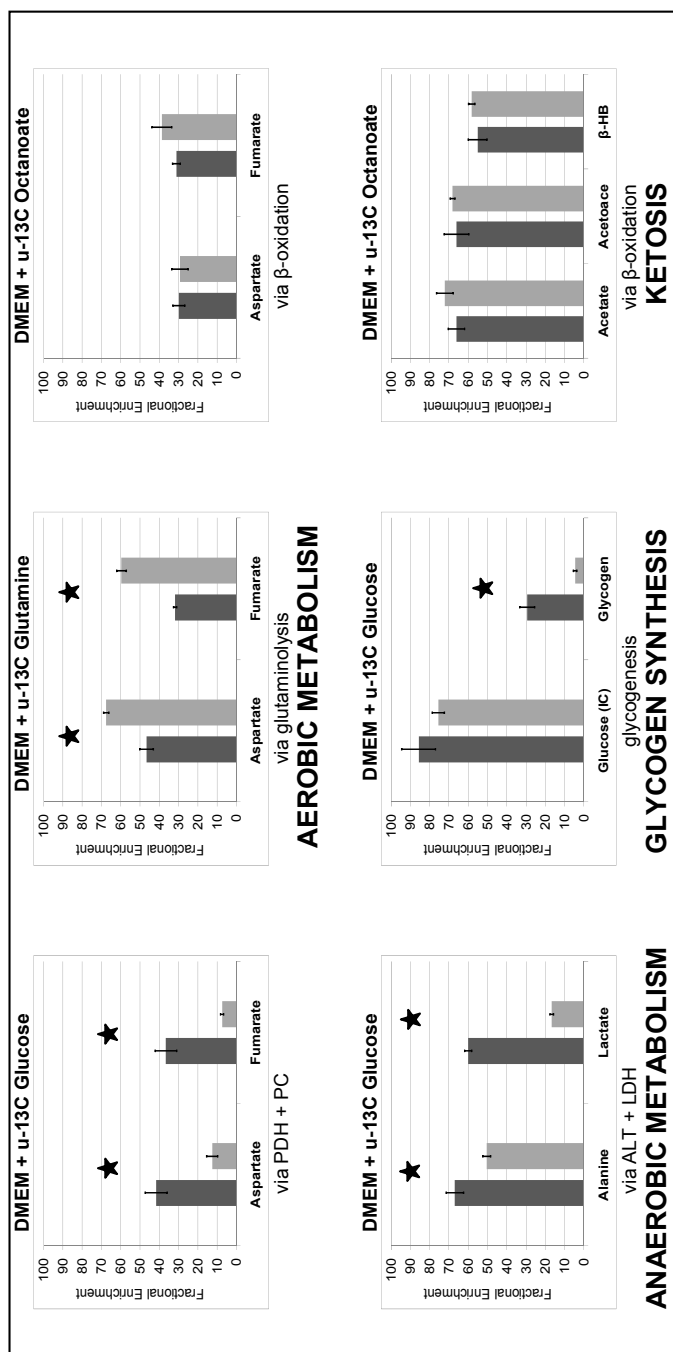


Figure 4-2- Fractional enrichment of metabolites created by rat hepatocytes supplied with media containing insulin (dark gray) or glucagon (light gray). Bar graphs show ^{13}C fractional enrichments as well as the standard error of the mean for the measurements. Star indicates $p < 0.05$.

It is quite apparent upon examination of Figure 4-1 that the utilization of media glucose is quite different between the two species. Two main regulators of glycolysis are the enzymes glucokinase (hexokinase IV) and phosphofructokinase 1 (PFK-1). Glucokinase phosphorylates glucose allowing it to enter the first step of both glycolysis and UDP-glucose

synthesis, from which glycogen and UDP-glucuronic acid are synthesized. Thus, it is likely that the block in metabolism is either with glucokinase or PFK-1 or both.

With the intent to examine the hepatocytes under starved conditions, experiments were conducted as above with glucagon substituted for insulin to determine if this induced starved phenotype in the rat hepatocytes is similar to what is observed in the human hepatocytes. These results are shown in Figure 4-2. Aerobic and anaerobic metabolism of glucose was observed to decrease with glucagon by noting the decrease in fractional enrichments of fumarate and aspartate, and alanine and lactate, respectively. Additionally, a small decrease in intracellular glucose fractional enrichment and a large decrease in glycogen fractional enrichment are observed with glucagon supplemented media. Glutaminolysis to provide TCA cycle intermediates was shown to increase when glucagon is added to the media. This is apparent by noting the increase in fumarate and aspartate fractional enrichment.

Addition of octanoic acid to the media gives the hepatocytes a source of free fatty acids to metabolize. It is apparent that the both the human and rat hepatocytes readily metabolize the octanoic acid to the TCA cycle intermediate of fumarate as well as the ketone bodies of acetate and β -hydroxybutyrate. The availability of higher concentrations of rat hepatocytes (and also likely the greater metabolic rate) makes it possible to see fractional enrichment of aspartate and acetoacetate in the rat cultures. When the insulin in the media was switched to glucagon to simulate a starved phenotype in the rat hepatocyte cultures, there was not a significant increase in the fractional enrichment of downstream metabolites of the octanoic acid, as one would expect [30, 209]. This is likely due to the hepatocytes being in a state of maximal fatty acid β -oxidation, regardless of insulin, glucagon, or glucose

exposure, or because of the significant water and lipid solubility of the octanoic acid allowing easy passage through cell membranes. Thus, the hepatocytes exhibit an affinity for fatty acid β -oxidation regardless of whether they are in insulinic or glucagonic conditions.

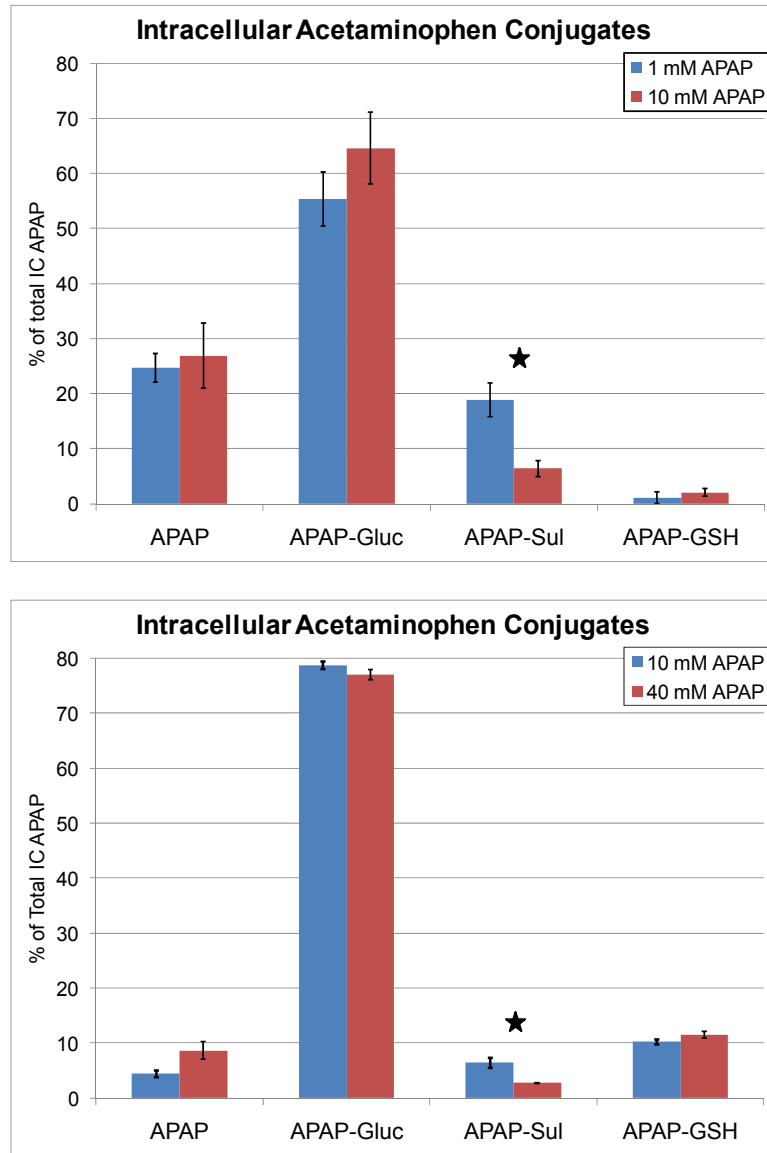


Figure 4-3- Intracellular acetaminophen conjugates present in primary fresh (top) and cryopreserved (bottom) human hepatocytes. Values are expressed as percentage of total acetaminophen, conjugated or unconjugated and the error bars are the standard errors of the measurements. APAP = unconjugated acetaminophen, APAP-Gluc = acetaminophen-glucuronide conjugate, APAP-Sul = acetaminophen-sulfate conjugate, APAP-GSH = acetaminophen-glutathione conjugate. Star indicates $p < 0.05$

When both the fresh and cryopreserved human hepatocytes were given 1, 10, and 40 mM acetaminophen, the parent drug, the glucuronide, sulfate, and glutathione conjugates were detected in the intracellular extracts. The ratios of the intracellular acetaminophen conjugates for both the fresh and cryopreserved hepatocytes can be seen in Figure 4-3. In the fresh human hepatocytes, one can see a decrease in the sulfate conjugate and increases in the glucuronide and glutathione conjugates going from a low dose (1 mM) to a high dose (10 mM) of acetaminophen. This is as expected as it fits the paradigm of sulfation and glucuronidation. The sulfation pathway is high affinity and low capacity while the glucuronidation pathway is the opposite. It appears that the sulfation pathway becomes overwhelmed and consequently, there is an increase in glucuronidation. Additionally, glutathione conjugate formation is P450- and glutathione-dependant. As the concentration of acetaminophen in the media is increased, one would expect the concentration of the glutathione conjugate to increase. For more information on this mechanism, see Chapter 1, Section 1.4.5 of this dissertation.

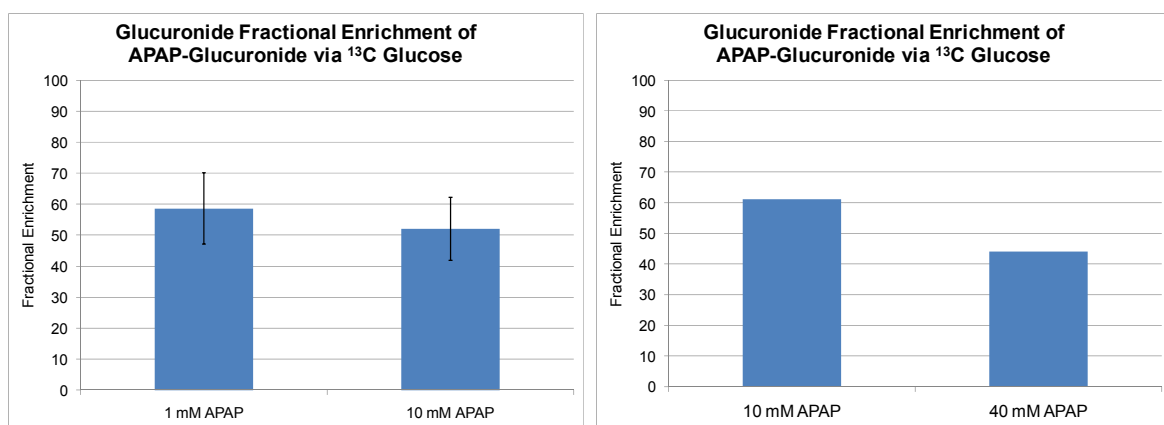


Figure 4-4- ¹³C Fractional enrichment of glucuronide (via U-¹³C glucose) in the acetaminophen-glucuronide conjugate for fresh primary human hepatocytes (left) and cryopreserved human hepatocytes (right). Error bars are standard error of the mean.

There is a slightly different response than expected from the cryopreserved hepatocytes. Generally, there is a higher degree of glucuronidation, lower sulfation, and lower glutathione conjugation in the cryopreserved hepatocytes, the trends going from low to high dose acetaminophen stay the same with the exception of the acetaminophen-glucuronide conjugate. There was a minor decrease in the glucuronide conjugate, a moderate decrease in the sulfate conjugate, and a minor increase in the glutathione conjugate. Thus, it is likely that at this higher dose and longer exposure, the glucuronidation pathway is becoming overwhelmed as well. The concentration of both the parent acetaminophen and the glutathione conjugates are observed to increase with increasing doses in both the fresh and cryopreserved hepatocytes. This is as expected since higher acetaminophen concentrations allow for more of the parent compound to enter the hepatocytes making more of it available to be metabolized by P450. This oxidation of acetaminophen creates NAPQI which directly binds glutathione.

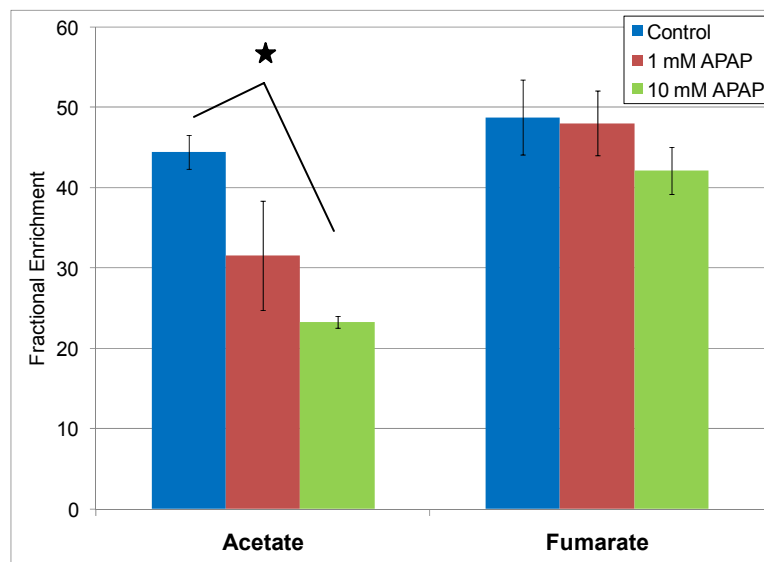


Figure 4-5- Fractional enrichments of acetate, fumarate, and β -hydroxybutyrate in fresh primary human hepatocytes given media supplemented with $U\text{-}^{13}\text{C}$ octanoic acid. Error bars indicate standard error of the mean. Star indicates $p < 0.05$.

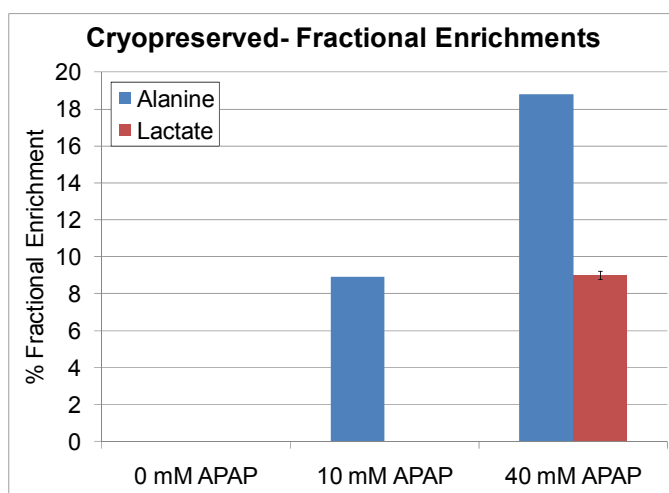
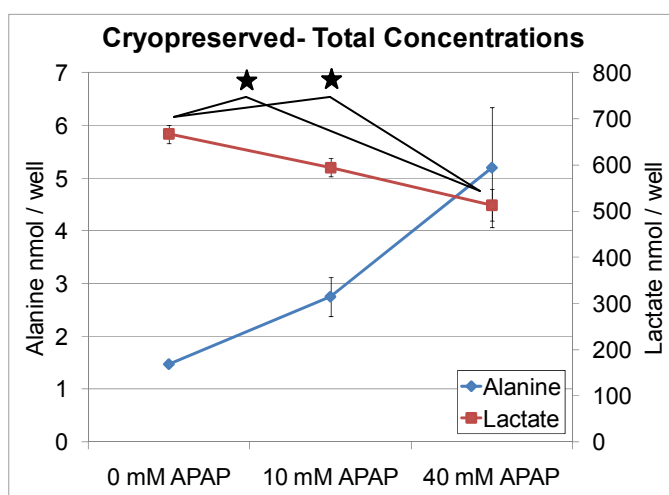
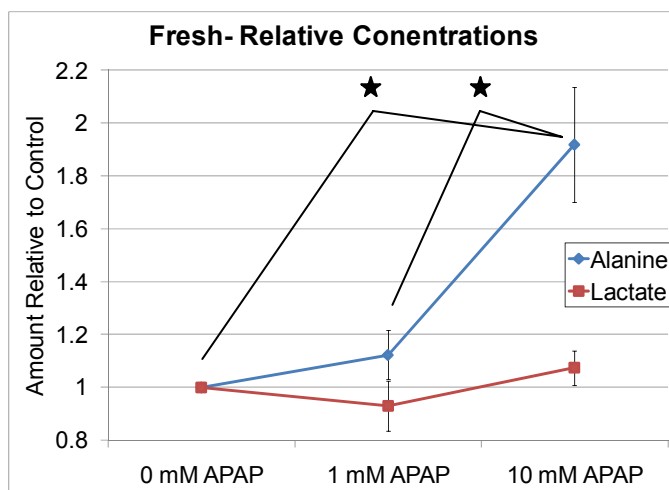


Figure 4-6- Relative alanine and lactate concentrations in the fresh and cryopreserved human hepatocytes (top), alanine and lactate concentrations in the cryopreserved human hepatocytes (middle), and alanine and lactate fractional enrichments in the cryopreserved human hepatocytes (bottom). All fractional enrichments are from media U-¹³C glucose, alanine measurements are intracellular, and lactate measurements are from the media. Since all the ¹³C alanine is seen in the cell extracts, which are pooled triplicates, there are no error bars for the fractional enrichment chart. Error bars indicate standard error of the mean. Star indicates p < 0.05.

While it was stated earlier that metabolism of glucose for energy was not detected in the human hepatocytes, glucose was metabolized in the presence of acetaminophen (not in an energy-production pathway though). Figure 4-4 shows the fractional enrichments of the glucuronide moiety of the acetaminophen-glucuronide conjugate. The fractional enrichment is due to the creation of UDP-glucuronide from the media U-¹³C glucose. It is thus apparent that glucokinase is active since glucose must be phosphorylated to glucose 6-phosphate to eventually create the UDP-glucuronic acid, which is used to glucuronidate acetaminophen. The fractional enrichments trend downwards as the acetaminophen dose increases (Figure 4-4).

Figure 4-5 shows the decrease in fractional enrichment, upon acetaminophen dosing, of acetate and fumarate created from media U-¹³C octanoic acid. Noting the fumarate fractional enrichment, it can be concluded that TCA activity trends downwards with increasing acetaminophen dose. With a decrease in TCA activity, one would expect decreases in the supply of TCA intermediates, which is observed with the decrease in acetate fractional enrichment. This ¹³C acetate is created through fatty acid β -oxidation of octanoic acid, and therefore, β -oxidation decreases with increasing acetaminophen dose.

When the cryopreserved hepatocytes given the U-¹³C glucose enriched media were exposed to toxic concentrations of acetaminophen (at 10 and 40 mM), evidence of glucose metabolism to supply energy is observed. Figure 4-6 shows that alanine becomes fractionally enriched at both acetaminophen doses and lactate becomes fractionally enriched at the high acetaminophen dose. As the acetaminophen dose increases, the total amount of alanine (¹²C plus ¹³C alanine), ¹³C alanine, and fractional enrichment of alanine all increase.

However, the total amount of lactate decreases with increasing dose, while fractional enrichment of lactate is only observed at (and thus increases with) the highest acetaminophen dose. It is worth noting that all of the measured alanine is intracellular alanine and the vast majority of the lactate (>99.8%) is extracellular, which is not unexpected. Thus, the measured alanine may be more of a result of a dynamic pool of alanine while the lactate may be a less dynamic pool, in the sense that it is created, excreted into a significantly larger pool (the media), and less likely to be remetabolized.

4.4 Discussion

One of the most striking results from this analysis is the serendipitous discovery using ^1H NMR spectroscopy, of no detectable metabolic products of the media ^{13}C glucose in the human hepatocytes until high concentrations of acetaminophen were added to the media. Specifically, there was no detectable ^{13}C fractional enrichment of lactate, alanine, fumarate, aspartate, or glycogen produced in the media or cell extract from the U- ^{13}C glucose or U- ^{13}C glutamine in the media. Thus, media glucose and glutamine were not used as an anaerobic or aerobic energy substrate nor was it used as an energy storage substrate via glycogen at the detection level of the ^1H NMR spectra obtained at 16.4 T. To the best of this author's knowledge, this non-utilization of glucose and glutamine in human hepatocyte cultures has not been reported in the scientific literature.

4.4.1 NMR Sensitivity and Calculation of ^{13}C Fractional Enrichment and Concentration between Samples from Humans and Rats

NMR spectroscopy benefits from the inherent quantitative and unbiased nature of analysis, ease in data interpretation, chemical and structure identification, and spectral reproducibility. However, NMR is not as sensitive of an analytical method as others, such as mass spectrometry or HPLC. Thus, to increase the NMR sensitivity per unit time, 1D ^1H NMR spectroscopy was performed instead of the more complex, higher information content analyses of 2D NMR spectroscopy carried out by others working in the field of stable isotope metabolomics [197, 210]. Additionally, it would not have been entirely necessary to perform 2D analyses because any gains from the enhanced resolution would have been negated by decreased sensitivity, unless an extraordinary amount of time was spent on data acquisition. This would have been especially problematic with the cryopreserved and fresh human hepatocyte extract samples due to the small sample sizes compared to the rat hepatocyte samples, comprising $\sim 3 \times 10^6$ and $\sim 6 \times 10^6$ hepatocytes versus $\sim 20 \times 10^6$ hepatocytes, respectively. This results in an approximately 11 and 44 fold longer acquisition time for the fresh and cryopreserved human hepatocyte extracts than the rat hepatocyte extracts, respectively, to obtain the same signal to noise ratio.

4.4.2 The Observed Metabolic State of the Rat Hepatocytes

Figure 4-2 shows the change in metabolism the rat hepatocytes undergo when they go from the fed (insulin) to the fasted (glucagon) state. These results demonstrate that the normal biochemical effects of insulin and glucagon were observed. In addition, the cells appear to heavily utilize β -oxidation as an energy source, as supported by the ^{13}C

incorporation from octanoic acid into the TCA intermediate, fumarate, and the TCA anapleurotic product, aspartate, as well as the ketone bodies excreted into the media- acetate, β -hydroxybutyrate, and acetoacetate. The extensive metabolism of U- ^{13}C octanoic acid suggests that the rat hepatocytes are primed for fatty acid β -oxidation, which is indicative of a starved metabolic state. However, it is also likely that the amphipathicity of the molecule is the cause of the high metabolic rate of octanoic acid. Octanoic acid has significant water and lipid solubility and thus can passively diffuse across cell membranes without it being necessary to be transported via acyl-carnitine transferase thus enhancing β -oxidation-derived acetate into the TCA cycle [211], which is likely the reason for its metabolism not being modulated by the hormones of insulin and glucagon [212].

4.4.3 The Observed Stressed Phenotype in the Human Hepatocytes Compared to Rat Hepatocytes

There are similarities and striking differences when comparing the phenotypes present in the human hepatocytes given media supplemented with insulin and rat hepatocytes in the induced starved state (media supplemented with glucagon). While the human hepatocytes did not metabolize media glucose or glutamine, they were seen to metabolize octanoic acid. When switched from insulin to glucagon, the rat hepatocytes had a large decrease in aerobic and anaerobic metabolism of glucose and glycogen synthesis and saw no change in octanoic acid metabolism, while there was an increase in the aerobic metabolism of glutamine (Figure 4-2). The *decreased* glucose metabolism and increased glutamine metabolism seen in the glucagon-induced starved metabolic phenotype of the rat hepatocytes do not quite match the absence of glucose and glutamine metabolism seen in the human

hepatocytes. Thus, it is likely that the human hepatocytes are in a metabolic state past the starved state; it appears that they are in a stressed metabolic state.

As mentioned in the Introduction (Chapter 1), the human stress response to injury and surgery (the surgical trauma in addition to exposure to certain anesthesia) has been documented to induce a considerable stress response [200, 201]. This response results mainly in the release of the hormones epinephrine, cortisol, and glucagon [200]. The combination of the three hormones results in an insulin resistant, starved metabolic state, which is manifested by glucose intolerance, a negative nitrogen balance, glycogenolysis, gluconeogenesis, increased alanine production, and increased fatty acid β -oxidation [201, 213]. While hypothesized to be a natural response to allow injured animals to survive by catabolizing their fuel reserves, it has been argued that this response is no longer necessary with modern surgical and convalescent methods [213]. In fact, patients can become hypoglycemic upon anesthesia and surgery, necessitating the use of a dextrose/saline infusion. Working on this hypothesis, other researchers have conducted research to prevent the response due to the anesthetic and surgery instead of treating the symptoms (prophylactic vs. curative care) [200].

This stress response well describes the phenotype that is being seen with the human hepatocytes. The human hepatocytes appear to be in a more than just in the starved metabolic state, they appear to be in the insulin resistant, glucose intolerant state. The lack of glutamine metabolism could be explained by inhibition of glutaminolysis due to the negative nitrogen balance since ammonia is an inhibitor of glutaminase and glutamate dehydrogenase. Inhibition of these enzymes would inhibit glutamine metabolism. This stress hormone exposure may drive the metabolic state of the resulting human hepatocyte cultures and thus,

rat hepatocyte cultures may allow for the examination of an unstressed hepatocyte phenotype for comparison.

4.4.4 A Comparison of Acetaminophen Metabolite Distribution in Human

Hepatocytes and *In Vivo* Human Biofluids

The ratios of the acetaminophen conjugates in the fresh hepatocytes (Figure 4-3) are not unexpected as it matches the known paradigm of sulfation being a low capacity, high affinity process and glucuronidation being a high capacity, low affinity process. This has also been demonstrated in previous acetaminophen studies with rat [214-221] and human hepatocyte cultures [222, 223]. Additionally, an increase in the parent acetaminophen and the glutathione conjugate as media acetaminophen concentration is increased is expected due to the greater amount of acetaminophen present to undergo phase I metabolism via P450. However, the ratios of the acetaminophen conjugates for the cryopreserved hepatocytes are somewhat surprising. The slight decrease in the glucuronide conjugate may be due to the glucuronidation pathways becoming overwhelmed, leading to the decrease in the glucuronide conjugate fraction seen with the increasing acetaminophen concentration.

Acetaminophen metabolites were not seen in the media due to either the acetaminophen not being released into the media or the amount released not being measurable above the background (noise as well as other metabolites, including acetaminophen). Since all of the acetaminophen was intracellular, the breakdown metabolites of acetaminophen-glutathione were not seen. Glutathione conjugates are typically excreted from hepatocytes into the bile canaliculi where glutamate is cleaved from the glutathione tripeptide by the canicular membrane bound γ -glutamyl transpeptidase

creating the cysteine-glycine dipeptide conjugate and free glutamate [192]. This conjugate makes it from general circulation to the proximal tubule of the kidney where the glycine is cleaved by membrane bound cysteinyl-glycine dipeptidase as it is taken into brush border cells creating the cysteine conjugate and free glycine. Inside the brush border cells the cysteine of the amino acid is acetylated creating the n-acetyl cysteine, or mercapturic acid conjugate which is excreted [192]. Thus, in this 2D hepatocyte culture system, the cysteine or n-acetyl cysteine conjugates are not seen.

It can be seen that the cryopreserved human hepatocytes have a significantly higher fraction of intracellular acetaminophen as the glutathione conjugate than the fresh hepatocytes in comparing the 10 mM acetaminophen dose. Figure 4-3 shows that 10.3% and 11.5% of the acetaminophen in the cryopreserved hepatocytes exposed to 10 mM and 40 mM acetaminophen is in the form of the glutathione conjugate. This is greater than the 1.1% and 2.1% acetaminophen-glutathione found in the fresh hepatocytes exposed to 1 mM and 10 mM acetaminophen.

Generally, the fresh primary human hepatocytes were isolated and then incubated for 24 – 48 hours. They were then shipped overnight for use. Thus, the hepatocytes were 48 – 72 hours old before they were received. After the hepatocytes are given approximately 24 hours to acclimate to the new environment and recover from shipping, experiments would take place. This would be approximately 72 – 96 hours after isolation. Cryopreserved hepatocytes were received for experimentation less than 48 hours after isolation, not counting the amount of time they were cryopreserved. This minimization of time is one way in which dedifferentiation is attenuated. Additionally, serum, which has been shown to induce dedifferentiation [59, 60, 224], was removed from the cryopreserved hepatocyte media 12

hours prior to the end of experimentation. One could expect greater toxic effects of acetaminophen with more differentiated hepatocytes, which is seen in the cryopreserved hepatocytes. Although the donor of the cryopreserved hepatocytes was a child (~18 months), all phase II enzymes are present at birth and will change with age [225], however, it was demonstrated that the cryopreserved hepatocytes possessed significant P450 activity (CYP2E1 and/or CYP1A2), as well as intact glucuronidation and sulfation pathways.

4.4.5 Fractional Enrichment of Acetaminophen-Glucuronide and Its Relationship with Glycolysis

Evidence that the glucuronidation pathway becomes overwhelmed in the human hepatocytes at high acetaminophen doses may be seen in Figure 4-4. At first glance, the data in this figure may seem to be unexpected. It shows that the fractional enrichment of acetaminophen-glucuronide, indicative of the amount of UDP-glucuronic acid produced from media glucose, trends downwards as the acetaminophen concentration increases. Since the starting fractional enrichment (the fractional enrichment at the lowest acetaminophen concentrations) is around 60%, and the hepatocytes are not exposed to media containing U-¹³C glucose until the time that they are also exposed to acetaminophen, the conclusion can be made that up-regulation of production of UDP-glucuronic acid is fast, and it relies mainly on media glucose as the principal substrate. Thus, since the fractional enrichment of acetaminophen-glucuronide trends downwards with increasing dose, the subsequent increase in up-regulation of UDP-glucuronic acid production must also rely on substrates other than glucose. We are hypothesizing that it is a consequence of the increase in glycolysis, evident by the increased production of ¹³C alanine and ¹³C lactate which can be seen in Figure 4-6.

Hence, glucose is being redirected from UDP-glucuronic acid production for glucuronidation, to glycolysis for energy production. This is to compensate for the decreased oxidative phosphorylation and TCA cycle activity.

This fractional enrichment of acetaminophen-glucuronide also provides support for glycogen synthesis. Acetaminophen-glucuronide excretion in urine and measurement of glycogenesis was first reported in dogs in 1995 [226], then later in humans in 2001 [75]. The pathways for both glycogen and UDP-glucuronic acid synthesis from glucose are nearly the same. Glucose becomes phosphorylated to glucose 6-phosphate (which is also the first step in glycolysis), glucose 6-phosphate becomes converted to glucose 1-phosphate which then becomes attached to uridine diphosphate (UDP) to create UDP-glucose. This UDP-glucose is used to create UDP-glucuronic acid by the enzyme UDP-glucose 6-phosphate dehydrogenase, which converts the hydroxyl moiety on the 6 carbon of the glucose to a carboxylic acid. However, UDP-glucose is the form of glucose directly used for glycogen synthesis. In fact, acetaminophen has previously been shown to stimulate glycogen synthesis by increasing UDP-glucose [227]. Most importantly, the method of acetaminophen-glucuronidation in combination with ^{13}C nutrient administration probes the glucose 6-phosphate pool.

It has been previously reported that glucokinase activity in human hepatocytes is approximately 20 fold lower than rat hepatocytes [228]. The data presented here showing greater than 50% fractional enrichment of acetaminophen-glucuronide from media U- ^{13}C glucose indicates > 50% fractional enrichment of UDP-glucuronic acid, and working backwards, > 50% fractional enrichment of glucose 6-phosphate. This indicates significant glucokinase activity in humans. Additionally, it shows that the block in glucose metabolism

in human hepatocyte metabolism is controlled by phosphofructokinase-1 (PFK-1) and PFK-2, and not glucokinase (see Figure 1-13). The release in the block is likely due to the decrease in the ATP/ADP ratio due to acetaminophen toxicity allowing PFK-2, and thus, PFK-1 activity since ATP inhibits both proteins (see Chapter 1.5.1 for more on this).

4.4.6 Fatty Acid Metabolism in Rat and Human Hepatocytes and the Effects of Acetaminophen

It is evident upon examining Figure 4-5, that cultured human hepatocytes have a high affinity for fatty acid β -oxidation of octanoic acid, and that the mitochondrial aerobic metabolism system is in working order even though they do not metabolize glucose or glutamine. When the hepatocytes are given U- ^{13}C octanoic acid supplemented media, approximately 50% of the acetate and fumarate present in the cell extracts was the ^{13}C analog. Thus, approximately half of the ketone bodies and anapleurotic substrates for the TCA cycle come from the supplied octanoic acid. It appears that the cultured human hepatocytes are in a metabolic state primed for fatty acid β -oxidation, and not glycolysis or glutaminolysis, even in a high glucose, high insulin environment.

When the U- ^{13}C octanoic acid supplemented hepatocytes are given acetaminophen, it can be seen in the same figure (4-5) that the fractional enrichments of both acetate and fumarate decrease. This is likely due to a decrease in oxidative phosphorylation and compensatory decreases in the TCA cycle and fatty acid β -oxidation as a consequence of the acetaminophen dose. Evidence supporting a decrease in oxidative phosphorylation in humans due to acetaminophen administration has been described previously [187-189, 199]. Impairment in oxidative phosphorylation would lead to an uncoupling of the TCA cycle due

to the redox state of the cell shifting towards NADH as a result of its production in the TCA cycle and its buildup by not being oxidized to NAD^+ by the uncoupled oxidative phosphorylation.

4.4.7 Enzyme Inhibition Due to Acetaminophen Toxicity

Inhibition of oxidative phosphorylation would lead to a condition similar to what is seen in bacterial fermentation or increased anaerobic metabolism due to heavy exercise. With acetaminophen toxicity however, the TCA cycle and oxidative phosphorylation activity is decreased due to protein arylation instead of low $[\text{O}_2]$. Therefore an increase of the anaerobic products of alanine and lactate from media glucose, to regenerate NAD^+ in addition to ATP, upon increased acetaminophen supplementation is expected and in fact observed (Figure 4-6).

The total concentration ($^{13}\text{C} + ^{12}\text{C}$) of intracellular alanine as well as the ^{13}C alanine, indicative of alanine produced from all sources and alanine produced from media glucose only, respectively, increased in the cryopreserved hepatocytes as they were exposed to increasing toxic acetaminophen concentrations. Additionally, the intracellular concentration of alanine in the fresh hepatocytes (^{13}C alanine was not observed) increased with increasing acetaminophen dose. The increase in the ^{13}C alanine concentration is indicative of an increase in glycolysis, and the increase in total alanine concentration is indicative of an increase in alanine transaminase (ALT, the enzyme which catalyzes the formation of alanine from pyruvate) activity.

The total concentration of extracellular lactate in the cryopreserved hepatocytes, on the other hand, decreases with increasing toxic acetaminophen concentration. However, the

^{13}C lactate can only be seen in the media at the highest acetaminophen concentration and thus increases (from zero) with increasing acetaminophen concentration. The increase in ^{13}C lactate indicates that there is an increase in glycolysis and the decrease in total lactate could indicate that there is a decrease in lactate dehydrogenase (LDH) activity. Additional evidence for a decrease in LDH comes from the fractional enrichments of lactate and alanine. Upon exposure to 40 mM acetaminophen for 4 hours, alanine is 18.8% fractionally enriched and lactate is 9.0% fractionally enriched. Since both of these metabolites are created from pyruvate, they should have similar fractional enrichments, if the activity of ALT and LDH does not change over the 4 hour exposure. However, the lower fractional enrichment of lactate than alanine indicates that LDH also decreases (or decreases more than ALT) with acetaminophen toxicity.

The literature has contradictory information regarding cellular LDH activity after toxic acetaminophen exposure. Although it is well known that acetaminophen produces chemical hypoxia and a lactate/pyruvate ratio increase, total lactate often does not increase at higher acetaminophen doses [229, 230]. In fact, one study showed lower LDH activity (released into the media) due to the interaction of NAPQI with cell proteins in hepatocytes exposed to acetaminophen [230].

Examination of the literature as well as the data generated here brings up the prospect of LDH arylation by NAPQI. This has not been reported in the literature, however an earlier study found an approximately 130 kD protein in the cytosol [231-233] and also the mitochondria [28] which was arylated. This is the same mass as LDH, bringing up the possibility of LDH arylation.

4.5 Conclusions

Cultured human hepatocytes do not rely on media glucose or glutamine for energy, however they do readily metabolize octanoic acid, even in the presence of high glucose and insulin. Rat hepatocytes do metabolize the three metabolites in the presence of both insulin or glucagon, exhibiting the fed and fasted phenotypes, respectively. The human hepatocytes were not in the fed or fasted phenotype, they displayed a stressed phenotype.

When acetaminophen was added to the culture medium, human hepatocytes formed the sulfate, glucuronide, and glutathione conjugates from the parent drug. Media glucose was heavily utilized to create the UDP-glucuronic acid used for acetaminophen glucuronidation. Acetaminophen toxicity demonstrated that the block in glycolysis was caused by PFK-1 and not glucokinase. Additionally, the block in glycolysis was released, and inhibitions in LDH, the TCA cycle, and fatty acid β -oxidation were demonstrated with acetaminophen toxicity.

5 Conclusions and Perspectives, Pitfalls, and Future Directions

5.1 Conclusions and Perspectives

Most rigorous experiments utilize a top-down or a bottom-up approach, with the former involving the breaking down of a system through successive experiments. The latter involves the piecing together of small systems through successive experiments. For a more complete understanding of the effects of acetaminophen, its global effects were examined as well as its liver-specific effects. Thus, this dissertation was conducted in a top-down approach with the effects of acetaminophen examined in human subjects first. This was followed by an examination of acetaminophen on cultured human hepatocytes. This top-down approach has resulted in the creation of a pharmacometabolomic early intervention model which has identified biomarkers predictive of acetaminophen hepatotoxicity. Furthermore, the hepatotoxic effects of acetaminophen on hepatocyte energy metabolism pathways have been better elucidated and confirms existing paradigms of toxic mechanisms. Through the efforts put forth in this research, additional discoveries were made, namely the time and degree of human urinary and blood metabolome normalization due to controlled diet as well as the discovery of the apparent stressed metabolic state of human hepatocytes in culture. It is likely that this latter serendipitous discovery in human hepatocytes is the most important scientific finding of this dissertation. The stressed phenotype non-utilization of media glucose seen in Chapter 4 has the potential to impact many areas of research including- hepatocyte cryopreservation, extracorporeal liver bioreactors, and liver transplantation.

The use of cryopreserved human hepatocytes has become a popular alternative to fresh human hepatocytes due to the sporadic availability of human hepatocytes. By using cryopreserved hepatocytes, researchers are able to utilize a steady supply of fully characterized (i.e. P450 activity) hepatocytes at the time and amount of their choosing, which is quite difficult or even impossible to do with fresh human hepatocytes. The process of hepatocyte cryopreservation, understandably, can be quite detrimental to hepatocyte viability. Perhaps the addition of a short chain fatty acid, such as octanoic acid, will improve hepatocyte viability by increasing metabolism of substrates for energy allowing the stressed hepatocytes to remain viable long enough to recover from the stresses of isolation and cryopreservation. This same idea could be applied to the fields of extracorporeal liver bioreactors and liver transplantation. Perhaps the administration of octanoic acid and glucagon supplemented medium or high glucose medium after isolation will allow hepatocytes to better utilize fatty acid β -oxidation for energy as well as utilize the fatty acids as a substrate for gluconeogenesis and glycogenesis. This could help the human hepatocytes increase, or at least retain, their glycogen content, which was seen to be quite low in the human compared to the rat hepatocytes. Furthermore, although not measured, it is likely that the lipid and free fatty acid content of the hepatocytes was quite low due to their utilization for energy. Administration of octanoic acid could help to attenuate the depletion of endogenous lipids and free fatty acids reserving them for membranes and extracellular matrix, improving attachment and viability.

5.2 Pitfalls

As with most studies, there are ways in which these studies could have benefited with different study designs. One thing that could have helped all three of the experiments discussed in Chapters 2 – 4 would have been larger sample sizes. However, this comes at a price, as added cost and time. The pharmacometabolomics study in Chapter 3 would most benefit from larger sample numbers, however, this would be extremely cost prohibitive due to the two week inpatient hospital requirement. The analyses in this section of the dissertation suffered most from poor statistical significance, largely due to the nature of human diversity as well as the relatively minor xenobiotic influence of therapeutic doses of acetaminophen. Furthermore, the analysis as a whole would likely have benefited greatly if a higher field NMR spectrometer were used to analyze the urine samples. This would have resulted in spectra of substantially higher resolution and sensitivity. It would be expected that higher quality spectra would have resulted in higher quality statistical analyses. In addition, mass spectrometric analysis of the urine samples would have made it possible to assay for the low concentration metabolites, potentially uncovering the effects of acetaminophen on many more metabolites not measured by NMR spectroscopy, making it possible to analyze additional metabolic pathways. Finally, administration of ^{13}C enriched compounds would have allowed for a superior analysis of metabolic pathways. For more information on the advantages of using ^{13}C compounds, see sections 1.7 and 4.1.

There were a few drawbacks with the hepatocyte culture experiments described in Chapter 4. A relatively easily remedied drawback of this chapter is the number of samples (human subjects) used. There were only primary human hepatocyte cultures from two subjects exposed to the U- ^{13}C octanoic acid media formulation. This experiment should be

repeated a third time to increase statistical significance. Also, the cryopreserved human hepatocyte experiments were only performed with hepatocytes from one subject. This should be repeated two more times to allow for statistical examination of some of the results.

A major drawback of the experimental procedure of Chapter 4 involves the manner in which the replicates for the rat hepatocyte culture experiments were performed. To the chagrin of this author, the experiments were replicated such that there were approximately 4 – 5 replicates per experimental intervention and media formulation (such as U-¹³C glucose DMEM with insulin) where the replicates were plates of cultured hepatocytes isolated from the *same* rat. This resulted in extremely consistent measurements within replicates (i.e. small error bars), but necessitated the use of fractional enrichments instead of absolute concentrations. This was due to the inability to reliably normalize data between hepatocyte cultures isolated from different animals for the number of viable hepatocytes on each culture plate. Being able to accurately track absolute production rather than relative production (via fractional enrichment) would have allowed for better metabolic pathway analysis. Another method which would have facilitated improved metabolic pathway analysis would have been to utilize positional-labeled ¹³C substrates instead of uniformly-labeled ¹³C substrates (isotopologues versus isotopomers). This would have allowed for improved atomic tracking and improved elucidation of specific entry points into the TCA cycle, such as at oxaloacetate or citrate (via pyruvate carboxylase or pyruvate dehydrogenase, respectively) as well as determination of TCA cycling. For a better explanation of this, see Figure A-2.

Finally, the integration of transcriptomics and proteomics techniques to the analysis would have permitted an enhanced understanding of what was happening in the hepatocyte

culture system through the use of a systems biology approach. This integration of the three ‘omics technologies will be discussed in further detail in the next section.

5.3 Future Directions

The diet standardization study in Chapter 2 was somewhat surprising that only a single day was required to normalize the urine. Future work could be performed in a larger metabolomic examination of the effects of different diets, such as region- or ethnicity-specific diets or vegetarianism, for example. An important part of metabolomics is the measurement of changes in the metabolome, and so metabolome standardization is quite important. As far as the two week acetaminophen study discussed in Chapter 3, serum samples were collected. Analysis of the serum samples has begun. Once finished, this should complete the multivariate statistical metabolomic analyses for this study.

There are quite a few directions to be taken with the experiments in Chapter 4. The rat hepatocyte experiments should be tested with xenobiotics which have potential to challenge the metabolome, such as acetaminophen. This could act as a validation of the method. Then, the importance of stable isotope metabolomics for drug toxicity testing may be shown to be an integral part of the analysis, much like the other ‘omic technologies of proteomics and transcriptomics. Furthermore, additional ^{13}C or ^{15}N enriched compounds could be administered to the hepatocytes to track other metabolite changes. For instance, ^{15}N enriched ammonia could be added to the media to better observe the urea cycle and energy state of the cell via the ATP:ADP ratio, respectively. Other ^{13}C compounds could also be used to probe other metabolic pathways, such as propionate to observe anaplerosis and gluconeogenesis. With the easy availability and low cost of rat hepatocytes for

experimentation, multiple proofs of concept experiments could be conducted for method validation using rat hepatocytes. Once refined, the methods can be translated for use with human hepatocytes. Finally, ^{31}P studies, using an NMR-compatible bioreactor could be conducted to determine the effects of acetaminophen toxicity on hepatocellular bioenergetics and pH.

Additionally, acetaminophen administration to the rat hepatocytes could allow for the examination of hepatocyte response to the toxic effects of hepatocytes in the fasted or fed state, instead of the apparent stressed-fasted state of the human hepatocytes. Evidence describing impairment in glutaminolysis due to acetaminophen toxicity was described in Chapter 4. Since the rat hepatocytes exhibited significant glutamine entry into the TCA cycle while in the fed or fasted states, this protein arylation impairment of glutamine-related enzymes could be tested. This was attempted with the human hepatocytes, but was not possible due to the undetectable amount of glutaminolysis, presumably due to the ammonia-induced inhibition of glutamine dehydrogenase presumably due to the stress-induced negative nitrogen balance. However, the discovery of a decreased lactate concentration due to acetaminophen toxicity uncovered some contrasting data in the literature regarding LDH and possible arylation by NAPQI. Thus, standard proteomic analysis of protein adducts could be utilized to determine the degree of LDH (and other proteins) arylation by NAPQI.

The serendipitous discovery of this apparent stressed phenotype exhibited by the human hepatocytes deserves further investigation. Perhaps the administration of epinephrine, cortisol, and glucagon to rats prior to hepatocyte isolation or addition of the above compounds to media formulations given to rat hepatocyte cultures could be conducted in an

attempt to replicate the metabolic state of the cultured human hepatocytes in cultured rat hepatocytes.

The underlying caveat of ‘omics analyses (transcriptomics, proteomics, and metabolomics) is that in genetic disorders, disease states, age, or exposure to toxicants there is a shift in the relative mass balance (transcripts, proteins, and metabolites) from that of “normal”. This fingerprint can serve as a phenotype of that particular state. The interaction between the transcriptome, proteome, and metabolome can be seen in Figure 5-1. For transcriptomics, that shift is evaluated by measuring changes in mRNA transcripts of the different genes. For proteomics, that shift is evaluated by measuring changes in protein concentrations in addition to post translational modifications. Changes in production or degradation of mRNA or proteins are not what are important, *per se*. What is important are the concentrations of the transcripts or proteins as it is the concentrations that have the biggest downstream effects. This is because the transcripts or proteins themselves are generally not metabolized or transformed to something else, like metabolites are. Thus, concentrations of metabolites are not suitable by themselves to fully explain changes in metabolism.

An experiment conducted using all three of the ‘omics technologies to determine the specific signaling pathways involving the activations and inactivations of the enzymes involved in glycogen synthesis and PFK-1-mediated glycolysis should be conducted to conclusively determine the exact mechanisms keeping cultured human hepatocytes stuck in the stressed state. In doing so, one could identify ways to attenuate or inhibit this phenomenon, thus creating hepatocyte culture conditions where the hepatocytes display a more natural, *in vivo* phenotype rather than the stressed phenotype.

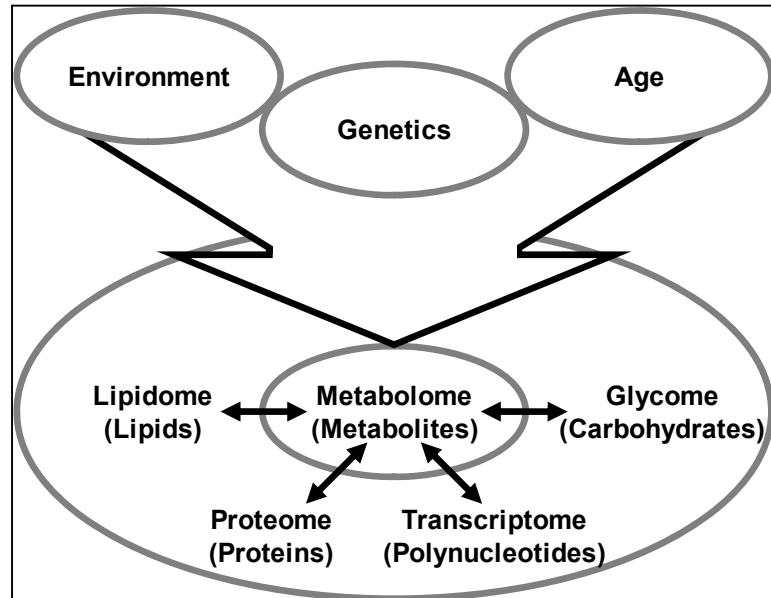


Figure 5-1- Diagram showing the various ‘omics sciences (left) and the TCA cycle (right) with some of the metabolites that feed into it. The switch from fed to fasted states can be seen in the figure as well as some of the ¹³C compounds that are used in the experiment (grey italics).

Thorough analyses probing the mechanistic underpinnings of the efficacy or toxicity of xenobiotics should consist of a combination of the ‘omics technologies. Thus, the effects of acetaminophen (or of any xenobiotic for that matter) should fully be probed using all of the 3 ‘omics technologies- transcriptomics, proteomics, and metabolomics. These analyses could be done in a way where two of the techniques anchor, or validate, another technique. For instance, experiments such as those conducted in Section 4 of this dissertation could be conducted. The results of those experiments could show some potential perturbations in metabolism. Then proteomic and transcriptomics methods could be conducted such that proteins and transcripts involved in those metabolic changes are examined to see if they validate the metabolomic results. Or perhaps, transcriptomic experiments could be conducted such that statistical methods are used to identify the potential up or down regulated genes upon exposure to acetaminophen. Then, proteomic or metabolomic methods

could be used to interrogate the pathways involving the up or down regulated genes. These types of thorough integrated, anchoring 'omics analyses should be conducted to fully explain the effects of xenobiotic interventions or disease state examinations.

To summarize, the major conclusions from each of these studies is- (1) just one day of dietary standardization is required to normalize the human urinary and blood metabolome, which has the potential to reduce the cost of future metabolomic studies; (2) one of the first examples of pharmaco-metabolomics in humans was presented; (3) the discovery of the stressed phenotype in cultured (and possibly isolated) human hepatocytes may lead to the discovery of media additives which may inhibit this phenotype, possibly increasing liver transplant survivability and hepatocyte cryopreservation viability.

Appendix A- Creation of a Stable Isotope Metabolomic Model Applied to Rat Hepatocyte Cultures

It was shown previously (Section 4 of this dissertation) that human and rat hepatocytes can be given media supplemented with ^{13}C metabolites which can be used to track production of different metabolites involved in the TCA cycle. Additionally, shifts in energy and phase II metabolism can be seen. This method can easily be added to existing cell culture experiments and can be combined with standard proteomic or transcriptomic experiments to make a more complete assay of hepatocyte response to xenobiotic intervention. This is due to the integration of all three 'omics sciences- metabolomics, proteomics, and transcriptomics, thus allowing these complementary technologies to anchor each other. However, there were some problematic issues that came up with the implementation of this method in human hepatocytes. Primarily, human hepatocytes are expensive, they can be difficult to obtain, and they can be difficult to culture- especially cryopreserved hepatocytes. Additionally, it was difficult to get much (or any) fractional enrichment of downstream metabolites from glucose. Thus, it is now necessary to refine and implement a minimal-assumption stable-isotope metabolomic model for use with cheap and easy to obtain primary rat hepatocytes. Experiments were performed to determine which media components are metabolized for short-term energy needs, which as a consequence would allow for the tracking of metabolic changes due to the presence of the downstream metabolic products of stable isotope enriched media.

The cell culture system is ideal for the demonstration of this global analysis, which becomes increasingly complex as one adds the various cell types comprising tissues, and the various tissues of intact organisms. Primary rat hepatocyte cultures were used in this study

since they have been a validated model of toxicity testing since the early 1980's [234-236], and liver is the metabolic hub of the body through which most metabolites and xenobiotics must pass. Metabolite tracking studies using ^{13}C isotopomers have been performed with transformed cells using ^{13}C -labeled nutrients and found that glycolysis and glutaminolysis are the primary carbon source [237]. Surprisingly, similar studies using stable isotopes have not been performed to fully characterize primary liver cultures, despite decades of development [197, 238, 239]. Perhaps the overriding problem is that primary hepatocyte cultures undergo a complex change in phenotype during the isolation and plating process that affects metabolism [52, 240, 241]. Surprisingly, this dedifferentiation process has not been fully characterized using ^{13}C or ^{14}C nutrients. The dedifferentiation process and steps taken to halt or reverse it are explained in Section 1.6.1 of this dissertation.

To demonstrate this minimal-assumption stable-isotope metabolomic model method, rat hepatocytes were cultured in media containing various ^{13}C -labeled nutrients at the same concentration as in the respective ^{12}C basal media. In addition, the effects of a free fatty acid was investigated whereby octanoic acid was included in the media formulation to induce β -oxidation [242, 243], and observe its effects on glycolysis and gluconeogenesis [211, 244], ketone body production, lipogenesis [94], mitochondrial hyperpolarization [245-247]. The goal of this method is to stream-line NMR analysis to create a high information output describing metabolic perturbations so that increased through-put preclinical metabolomic analyses of xenobiotics can be performed.

To do this, rat hepatocytes were isolated, cultured, and exposed to media supplemented with $\text{U-}^{13}\text{C}$ glucose, $\text{U-}^{13}\text{C}$ glutamine, or $\text{U-}^{13}\text{C}$ octanoic acid. Media and cell

extracts were examined by NMR spectroscopy to determine the downstream metabolites created from these ^{13}C metabolites.

In order to determine whether a dynamic approach to quantify flux [98, 248] would be possible, and what temporal resolution would be required, hepatocytes were exposed to U- ^{13}C glucose enriched media for a variable amount of time, from 15 minutes to 8 hours. Isotopomers of lactate were examined to see how total fractional enrichment and fractional enrichment of the different isotopomers change over time. The results of the analysis of this media can be seen in Figure A-1. Within minutes, lactate, a glycolytic end-product, reached isotopic ^{13}C fractional enrichment steady-state, with the ratio of $^{12}\text{C}/^{13}\text{C}$ isotopomers not changing after 15 minutes. However, an exposure period long enough to reach ^{13}C fractional enrichment steady-state for TCA cycle intermediates (fumarate, aspartate), gluconeogenesis (APAP-glucuronide, glucose), fatty acid β -oxidation (acetate, acetoacetate, β -hydroxybutyrate), pentose phosphate pathway (NDP-ribose), and urea cycle (arginine), must be chosen. Therefore, the results of previous rat hepatocyte $^{14}\text{C}/^{13}\text{C}$ tracer studies were considered [111-114, 119-122, 125-137, 139]. Glycogen synthesis can reach steady state by 1 - 48 hours after plating depending on the stress state [125-137]. In fact, longer time course studies over the course of 48 hours showed that glycogen content increased over 48 hours (Appendix 2, Figure A-1), and were likely not in metabolic or ^{13}C isotopic steady state over the 2 hour ^{13}C exposure period. Protein synthesis can range from 20 minutes for insulin to weeks [32, 116, 117], while fatty acids have a similar range depending on whether they are involved in signaling (phosphatidylinositol) or part of the nuclear membrane [117, 123, 138]. Therefore, 2 hours was chosen for the ^{13}C dosing period and since the turn over rates of glycogen, lipid, protein, and polynucleotide pools are significantly longer than their

monomer pool, such as UDP-¹³C-glucose, amino acids, acetate, and ribose, respectively, these monomer can be used to sample intermediary metabolism as supported by decades of ¹⁴C and ¹³C research in rat hepatocyte and perfused organ studies [111-139].

The lactate isotopomers are formed by metabolism of U-¹³C glucose-derived pyruvate via the TCA cycle [249]. They can be used to determine the amount of TCA flux through PDH and PC as demonstrated in Figure A-2. Isotopomeric analysis is a powerful method for quantifying flux [210, 248, 250, 251]. The dynamic method requires multiple time points and therefore requires nearly an order-of-magnitude more effort, although it is more robust than the static method since actual flux rates for the various metabolic pathways can be obtained. The static method for quantification of fractional enrichment of metabolites comprising the various metabolic pathways has been used extensively and focuses on the objective of this method- to be high through-put [248, 252]. Although isotopomeric analysis is possible with this method, absolute fractional enrichments were obtained to streamline analysis with the intent of up scaling so that they can be attached to other experiments to provide better mechanistic information regarding cell metabolism.

To determine the effect of glucose and glutamine concentration on net flux, DMEM formulations containing insulin and three concentrations of U-¹³C-glucose (2.5, 12.5 and 25 mM) were substituted for the normal ¹²C glucose and tested at 24 h after plating. For reference, low glucose DMEM is approximately 5.5 mM and high glucose DMEM is approximately 25 mM. It was discovered that at 12.5 mM glucose and below, no glycogen was synthesized. This is the highest amount of glucose found in the normal range of serum which should induce the insulinic response of glycogen synthesis *in vivo*. It was not until the hepatocytes were given high glucose (25 mM) media that glycogen was synthesized (Figure

A-4). The most glycogen was synthesized with normal glutamine concentrations (4 mM) found in DMEM (data not shown). Since a normal metabolic response was desired, a high glucose medium with normal glutamine concentration was used for the experiments, even though higher levels of lactate and alanine were formed with this formulation (data not shown). In the body, the liver is involved in the Cori cycle, converting lactate and alanine to glucose via gluconeogenesis. However, in the high glucose medium, lactate accumulated intracellularly as well as in the media. The excess lactate during this period could serve as an energy source for the brain or muscles, but the static nature of the media in 2D cultures allows metabolites transported out of the cell to accumulate.

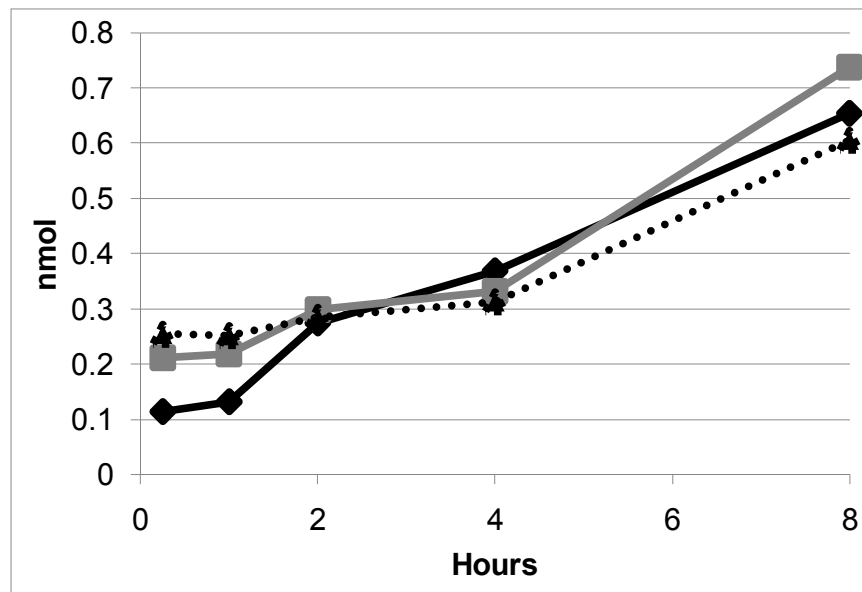


Figure A-1- Short time course study describing the amounts of normal lactate and ¹³C enriched lactate produced upon incubation with DMEM containing ¹³C glucose substituted for regular glucose. ¹²C lactate (black diamonds), ^{3-¹³C lactate (gray squares), and ^{2,3-¹³C lactate (black dots) can all be seen.}}

The lipid fractions were analyzed for significant changes and none were detected over the 48 h (data not shown). Representative lipid fraction spectra can be seen in Figure A-3.

Additionally the lipid fraction was analyzed for incorporation of the ¹³C label and glucose

was the only substrate that formed the glycerol backbone of lipids, however, the fractional enrichment was minor compared to the entire lipid pool since there were no ^{13}C satellite peaks found in the ^1H NMR spectra of the chloroform extracts (data not shown). Although the lipids showed very little incorporation, lipogenesis may be important for future studies and this method could be used to analyze this fraction in more detail as previous ^{13}C NMR methods have described [253].

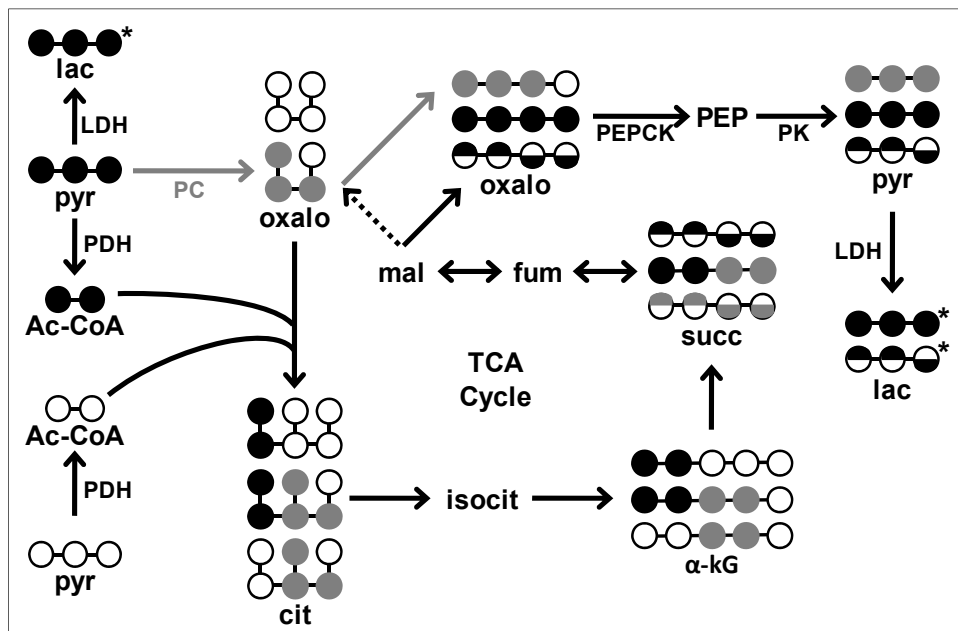


Figure A-2- Labeling patterns of lactate and TCA cycle intermediates. White circles are unlabeled and black and gray circles are labeled. Half black half white circles indicate that a symmetrical molecule has been labeled which makes half of the downstream metabolites labeled one way (1,2- ^{13}C oxaloacetate for instance) and half another (3,4- ^{13}C oxaloacetate).

Many preliminary studies were performed to correlate this ^{13}C method with the many previous ^{14}C and ^{13}C studies on the optimization culture media for rat hepatocytes primarily performed in the late 1970's. Several early studies varied the concentration of glucose and monitored the effects of glucagon and insulin on ^{14}C -glucose metabolism ^{14}C -glucose [111-113, 119, 120], amino acids [115], and the effect of fatty acids [121] [122]. Basically, it was

concluded that 25 mM glucose and 500 - 1000X insulin concentration best mimicked the fed state [111-113, 119, 120]. Similar results on glucose concentration as previously reported [111-113, 119, 120] were discovered using 2.5, 5, 12, and 25 ^{13}C -glucose with 1000X insulin. At 12 mM there was a switch to a fasted metabolic phenotype with no glycogen synthesized and little lactate (Figure A-4). At 2.5 mM, the rat hepatocyte cultures died by 48 hrs, and at 5 mM, they were in a starved phenotype, similar to the 1979 results of Monte Bissel [119, 120].

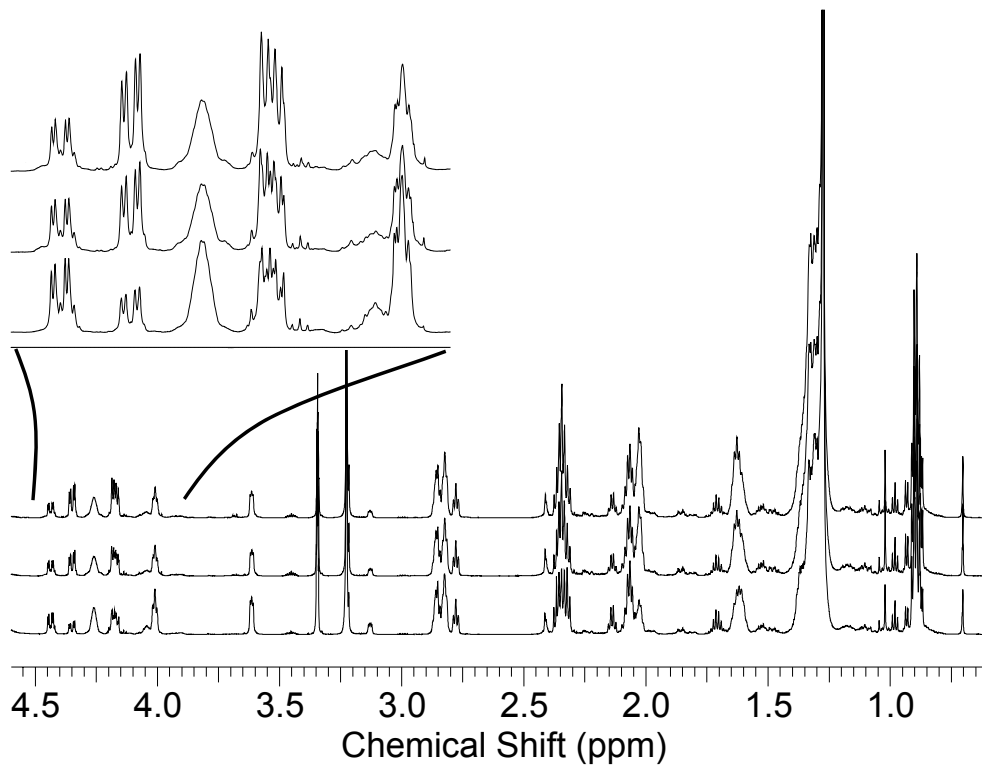


Figure A-3- Chloroform extract (lipid) fraction from representative cell extracts at 2 h (bottom), 24 h (middle), and 48 h (top).

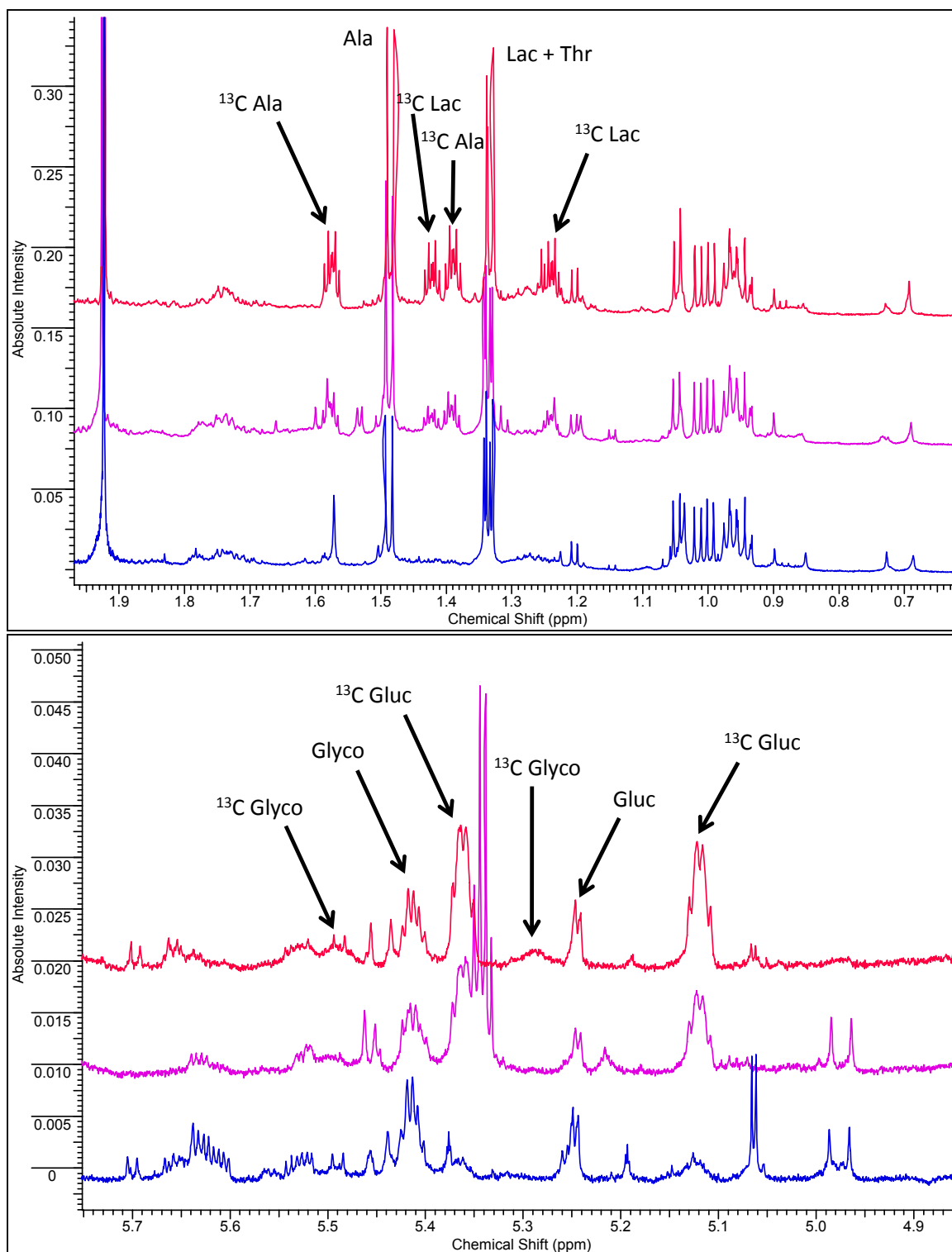


Figure A-4- Spectra from rat hepatocytes exposed to DMEM containing 25 mM (red), 12.5 mM (pink), and 2.5 mM (blue) glucose for 2 hours. It can be seen that lactate and alanine production does not occur at the low concentration glucose medium and the glycogen production only occurs in the high concentration glucose medium.

Appendix B- Temporal Effects on Cultured Rat Hepatocytes

Additional longer-term time course studies were done to examine the changes hepatocyte metabolism undergoes over the first 48 hours after plating. Hepatocytes were exposed to DMEM containing insulin and ^{13}C glucose substituted for regular glucose for 2 hours at 2, 24, and 48 hours after plating. These results can be seen in Figure B-1. Due to the method in which this data was collected, absolute production rates (instead of fractional enrichments) were able to be obtained. There were increases in production of (from ^{13}C glucose) and total concentration of aspartate, fumarate, lactate, intracellular glucose (uptake, not production), and glycogen; and an increase in alanine production. Total concentrations of the ketone bodies- acetate, acetoacetate, and β -hydroxybutyrate remain relatively steady over the 48 hours. These studies indicated that 24 hours was the earliest point that studies should be performed. In order achieve the increased through-put goal of the method, as well as minimizing dedifferentiation of the hepatocytes, the 24 hour time point may be a good time point for experimentation.

A general increase in metabolism (aerobic and anaerobic) was seen when the incubation period for the hepatocytes was increased from 2 to 24 to 48 hours. When designing experiments involving hepatocytes, however, one must also keep in mind the dedifferentiation (or transdifferentiation) that hepatocytes undergo with time after isolation and plating. Thus, one should strike a balance between metabolic activity and dedifferentiation or culture their hepatocytes in media formulations conducive to hepatocyte differentiation. These aspects are discussed in detail in the introduction section of this dissertation.

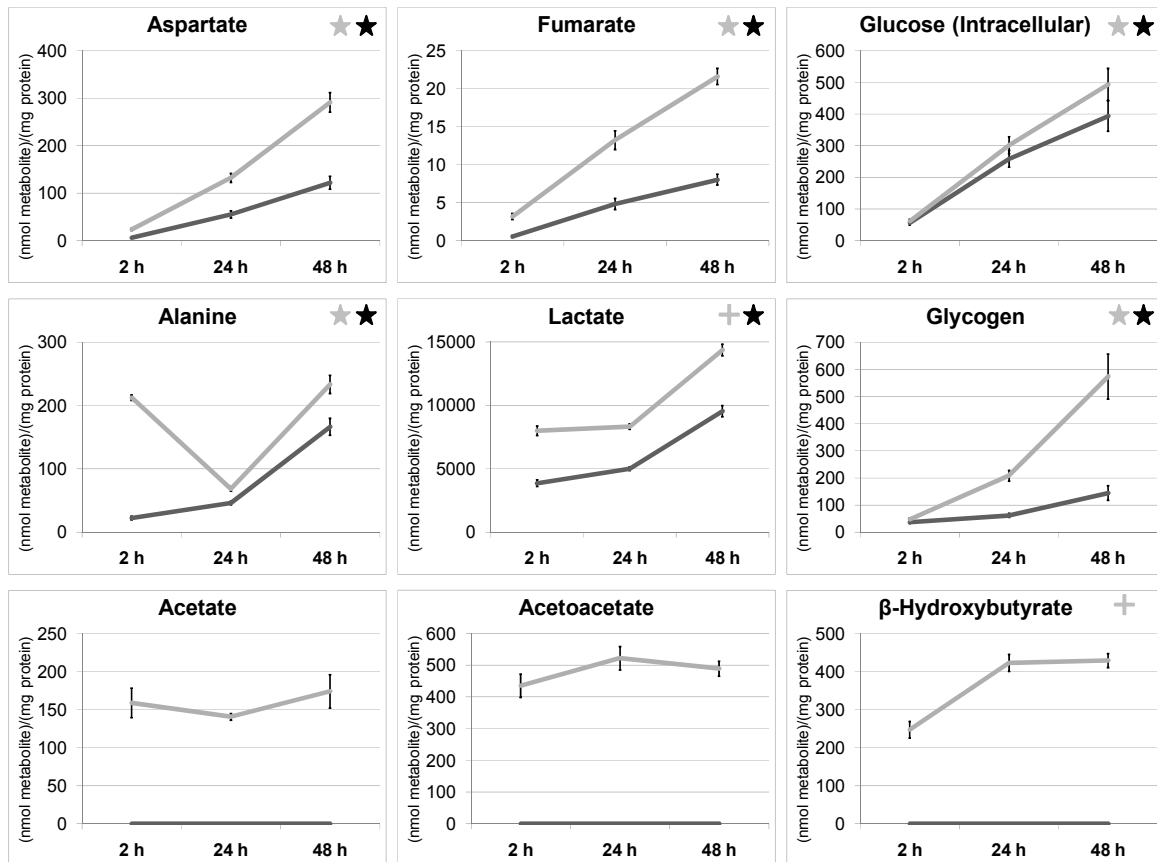


Figure B-1- Graphs describing the change in metabolites 2, 24, and 48 hours after plating upon exposure to DMEM containing ¹³C glucose and insulin for 2 hours. The graphs show both ¹³C enriched (black) and total amounts (¹²C + ¹³C, grey lines) of metabolites standardized per milligram protein. The error bars indicate standard error of the mean. The black star indicates p < 0.05 between all three ¹³C time points, the grey star indicates p < 0.05 between all three ¹²C time points, and the grey cross indicates p < 0.05 between the first and third ¹²C time points.

References

1. Claridge, T.D., *High-resolution NMR techniques in organic chemistry*. 1st edition ed. 1999, Amsterdam: Pergamon.
2. Evers, A.S. and M. Maze, *Anesthetic pharmacology: physiologic principles and clinical practice: a companion to Miller's Anesthesia*. 2004, Philadelphia: Churchill Livingstone.
3. Foegh, M.L. and P.W. Ramwell, *Basic and clinical pharmacology*, B.G. Katzung, Editor. 2004, Lange Medical Books: New York
4. Seibert, K., Y. Zhang, K. Leahy, S. Hauser, J. Masferrer, W. Perkins, L. Lee, and P. Isakson, *Pharmacological and biochemical demonstration of the role of cyclooxygenase 2 in inflammation and pain*. Proc Natl Acad Sci U S A, 1994. 91(25): p. 12013-7.
5. Botting, R.M., *Mechanism of action of acetaminophen: is there a cyclooxygenase 3?* Clin Infect Dis, 2000. 31 Suppl 5: p. S202-10.
6. Hardman, J.G. and L.E. Limbird, *Goodman & Gilman's The pharmacological basis of therapeutics*. 10th ed ed. 2001, New York McGraw-Hill Medical Pub.
7. Bales, J.R., P.J. Sadler, J.K. Nicholson, and J.A. Timbrell, *Urinary excretion of acetaminophen and its metabolites as studied by proton NMR spectroscopy*. Clin Chem, 1984. 30(10): p. 1631-6.
8. Amar, P.J. and E.R. Schiff, *Acetaminophen safety and hepatotoxicity--where do we go from here?* Expert Opin Drug Saf, 2007. 6(4): p. 341-55.
9. Plaa, G.L. and W.R. Hewitt, *Toxicology of the liver*. 1998, Washington, DC: Taylor & Francis.
10. Smith, G., M.J. Stubbins, L.W. Harries, and C.R. Wolf, *Molecular genetics of the human cytochrome P450 monooxygenase superfamily*. Xenobiotica, 1998. 28(12): p. 1129-65.
11. Danielson, P.B., *The Cytochrome P450 Superfamily: Biochemistry, Evolution and Drug Metabolism in Humans*. Current Drug Metabolism, 2002. 3: p. 561-597.
12. Gonzalez, F.J., *Role of cytochromes P450 in chemical toxicity and oxidative stress: studies with CYP2E1*. Mutat Res, 2005. 569(1-2): p. 101-10.
13. James, L.P., P.R. Mayeux, and J.A. Hinson, *Acetaminophen-induced hepatotoxicity*. Drug Metab Dispos, 2003. 31(12): p. 1499-506.
14. Cederbaum, A.I., *CYP2E1--biochemical and toxicological aspects and role in alcohol-induced liver injury*. Mt Sinai J Med, 2006. 73(4): p. 657-72.
15. Lieber, C.S., *Cytochrome P-4502E1: its physiological and pathological role*. Physiol Rev, 1997. 77(2): p. 517-44.
16. Lu, Y. and A.I. Cederbaum, *CYP2E1 and oxidative liver injury by alcohol*. Free Radic Biol Med, 2008. 44(5): p. 723-38.
17. Fontana, R.J., K.S. Lown, M.F. Paine, L. Fortlage, R.M. Santella, J.S. Felton, M.G. Knize, A. Greenberg, and P.B. Watkins, *Effects of a chargrilled meat diet on expression of CYP3A, CYP1A, and P-glycoprotein levels in healthy volunteers*. Gastroenterology, 1999. 117(1): p. 89-98.
18. Draganov, P., H. Durrence, C. Cox, and A. Reuben, *Alcohol-acetaminophen syndrome. Even moderate social drinkers are at risk*. Postgrad Med, 2000. 107(1): p. 189-95.

19. Farrell, G.C., *Drug-induced liver disease*. 1994, Edinburgh, New York: Churchill Livingstone.
20. Lee, W.M. and R. Williams, *Acute liver failure*. 1997, Cambridge: Cambridge University Press.
21. Thummel, K.E., J.T. Slattery, H. Ro, J.Y. Chien, S.D. Nelson, K.E. Lown, and P.B. Watkins, *Ethanol and production of the hepatotoxic metabolite of acetaminophen in healthy adults*. *Clin Pharmacol Ther*, 2000. 67(6): p. 591-9.
22. Seagle, C.M., *Development of an Electrostatic Device for the Encapsulation of Cells in Gel Matrix and a Novel NMR Method for Comparative Analysis of Media Streams from Bioreactors*, in *Biomedical Engineering*. 2005, University of North Carolina: Chapel Hill.
23. Lebedzinska, M., G. Szabadkai, A.W. Jones, J. Duszynski, and M.R. Wieckowski, *Interactions between the endoplasmic reticulum, mitochondria, plasma membrane and other subcellular organelles*. *Int J Biochem Cell Biol*, 2009. 41(10): p. 1805-16.
24. Pumford, N.R. and N.C. Halmes, *Protein targets of xenobiotic reactive intermediates*. *Annu Rev Pharmacol Toxicol*, 1997. 37: p. 91-117.
25. Cohen, S.D., N.R. Pumford, E.A. Khairallah, K. Boekelheide, L.R. Pohl, H.R. Amouzadeh, and J.A. Hinson, *Selective protein covalent binding and target organ toxicity*. *Toxicol Appl Pharmacol*, 1997. 143(1): p. 1-12.
26. Qiu, Y., L.Z. Benet, and A.L. Burlingame, *Identification of the hepatic protein targets of reactive metabolites of acetaminophen in vivo in mice using two-dimensional gel electrophoresis and mass spectrometry*. *J Biol Chem*, 1998. 273(28): p. 17940-53.
27. Tygstrup, N., S.A. Jensen, B. Krog, and K. Dalhoff, *Expression of liver functions following sub-lethal and non-lethal doses of allyl alcohol and acetaminophen in the rat*. *J Hepatol*, 1997. 27(1): p. 156-62.
28. Gupta, S., L.K. Rogers, S.K. Taylor, and C.V. Smith, *Inhibition of carbamyl phosphate synthetase-I and glutamine synthetase by hepatotoxic doses of acetaminophen in mice*. *Toxicol Appl Pharmacol*, 1997. 146(2): p. 317-27.
29. Bender, D.A. and P.A. Mayes, *Glycolysis and the Oxidation of Pyruvate*, in *Harper's Illustrated Biochemistry*, R.K. Murray, D.K. Granner, and V.W. Rodwell, Editors. 2003, McGraw-Hill: New York, NY.
30. Hames, D. and N. Hooper, *Biochemistry*. 2005, New York, NY: Taylor and Francis Group.
31. Kutzbach, C. and E.L.R. Stokstad, *Partial purification of a 10-formyl-tetrahydrofolate: NADP oxidoreductase from mammalian liver*. *Biochemical and Biophysical Research Communications*, 1968. 30(2): p. 111-117.
32. Macdonald, J.M., O. Schmidlin, and T.L. James, *In vivo monitoring of hepatic glutathione in anesthetized rats by ¹³C NMR*. *Magn Reson Med*, 2002. 48(3): p. 430-9.
33. Iynedjian, P., *Molecular Physiology of Mammalian Glucokinase*. *Cellular and Molecular Life Sciences*, 2009. 66(1): p. 27-42.
34. Kamata, K., M. Mitsuya, T. Nishimura, J.-i. Eiki, and Y. Nagata, *Structural Basis for Allosteric Regulation of the Monomeric Allosteric Enzyme Human Glucokinase*. *Structure*, 2004. 12(3): p. 429-438.

35. Arita, M., *In silico atomic tracing by substrate-product relationships in Escherichia coli intermediary metabolism*. Genome Res, 2003. 13(11): p. 2455-66.
36. Arita, M., *The metabolic world of Escherichia coli is not small*. Proc Natl Acad Sci U S A, 2004. 101(6): p. 1543-7.
37. Bender, D.A. and P.A. Mayes, *The Citric Acid Cycle: The Catabolism of Acetyl-CoA*, in *Harper's Illustrated Biochemistry*, R.K. Murray, D.K. Granner, and V.W. Rodwell, Editors. 2003, McGraw-Hill: New York, NY.
38. Evans, P.R., G.W. Farrants, and P.J. Hudson, *Phosphofructokinase: structure and control*. Philos Trans R Soc Lond B Biol Sci, 1981. 293(1063): p. 53-62.
39. Verne, J. and S. Hebert, [*Hepatocytes in Culture in the Presence of Insulin, Cortisone and Adrenaline.*]. C R Seances Soc Biol Fil, 1963. 157: p. 1924-5.
40. Brady, R.O., C. Borek, and R.M. Bradley, *Composition and synthesis of gangliosides in rat hepatocyte and hepatoma cell lines*. J Biol Chem, 1969. 244(23): p. 6552-4.
41. Verne, J., J. Bescol-Liversac, and C. Guillam, [*Modes of Incorporation of C14-Glucose by Fibroblasts and Hepatocytes Cultivated Outside the Organism.*]. C R Seances Soc Biol Fil, 1964. 158: p. 1448-50.
42. Berry, M.N. and D.S. Friend, *High-yield preparation of isolated rat liver parenchymal cells: a biochemical and fine structural study*. J Cell Biol, 1969. 43(3): p. 506-20.
43. Moldeus, P., J. Hogberg, and S. Orrenius, *Isolation and use of liver cells*. Methods Enzymol, 1978. 52: p. 60-71.
44. Reid, L.M. and M. Rojkind, *New techniques for culturing differentiated cells: reconstituted basement membrane rafts*. Methods Enzymol, 1979. 58: p. 263-78.
45. Michalopoulos, G., F. Russell, and C. Biles, *Primary cultures of hepatocytes on human fibroblasts*. In Vitro, 1979. 15(10): p. 796-806.
46. Macdonald, J.M., M. Grillo, O. Schmidlin, D.T. Tajiri, and T.L. James, *NMR spectroscopy and MRI investigation of a potential bioartificial liver*. NMR Biomed, 1998. 11(2): p. 55-66.
47. Macdonald, J.M., J.L. Griffin, H. Kubota, L. Griffith, J. Fair, and L.M. Reid, *Bioartificial Livers*, in *Cell Encapsulation Technology and Therapeutics*, W. Kuhlreiber, R.P. Lanza, and W.L. Chick, Editors. 1999, Birkhauser Boston: Cambridge, MA. p. 252 - 286.
48. Miyazaki, K., R. Takaki, F. Nakayama, S. Yamauchi, A. Koga, and S. Todo, *Isolation and primary culture of adult human hepatocytes. Ultrastructural and functional studies*. Cell Tissue Res, 1981. 218(1): p. 13-21.
49. Schuetz, E.G., D. Li, C.J. Omiecinski, U. Muller-Eberhard, H.K. Kleinman, B. Elswick, and P.S. Guzelian, *Regulation of gene expression in adult rat hepatocytes cultured on a basement membrane matrix*. J Cell Physiol, 1988. 134(3): p. 309-23.
50. Baker, T.K., M.A. Carfagna, H. Gao, E.R. Dow, Q. Li, G.H. Searfoss, and T.P. Ryan, *Temporal gene expression analysis of monolayer cultured rat hepatocytes*. Chem Res Toxicol, 2001. 14(9): p. 1218-31.
51. Kremers, P., L. Roelandt, N. Stouvenakers, G. Goffinet, and J.P. Thome, *Expression and induction of drug-metabolizing enzymes in cultured fetal rat hepatocytes*. Cell Biol Toxicol, 1994. 10(2): p. 117-25.

52. Arterburn, L.M., J. Zurlo, J.D. Yager, R.M. Overton, and A.H. Heifetz, *A morphological study of differentiated hepatocytes in vitro*. *Hepatology*, 1995. 22(1): p. 175-87.
53. Hansen, L.K., J. Wilhelm, and J.T. Fassett, *Regulation of hepatocyte cell cycle progression and differentiation by type I collagen structure*. *Curr Top Dev Biol*, 2006. 72: p. 205-36.
54. Elaut, G., T. Henkens, P. Papeleu, S. Snykers, M. Vinken, T. Vanhaecke, and V. Rogiers, *Molecular mechanisms underlying the dedifferentiation process of isolated hepatocytes and their cultures*. *Curr Drug Metab*, 2006. 7(6): p. 629-60.
55. Padgham, C.R., C.C. Boyle, X.J. Wang, S.M. Raleigh, M.C. Wright, and A.J. Paine, *Alteration of transcription factor mRNAs during the isolation and culture of rat hepatocytes suggests the activation of a proliferative mode underlies their de-differentiation*. *Biochem Biophys Res Commun*, 1993. 197(2): p. 599-605.
56. Sidhu, J.S. and C.J. Omiecinski, *Modulation of xenobiotic-inducible cytochrome P450 gene expression by dexamethasone in primary rat hepatocytes*. *Pharmacogenetics*, 1995. 5(1): p. 24-36.
57. Zeisberg, M., K. Kramer, N. Sindhi, P. Sarkar, M. Upton, and R. Kalluri, *De-differentiation of primary human hepatocytes depends on the composition of specialized liver basement membrane*. *Mol Cell Biochem*, 2006. 283(1-2): p. 181-9.
58. Wang, X.J., C.P. Hodgkinson, M.C. Wright, and A.J. Paine, *Temperature-sensitive mRNA degradation is an early event in hepatocyte de-differentiation*. *Biochem J*, 1997. 328 (Pt 3)(Pt 3): p. 937-44.
59. Hammond, A.H. and J.R. Fry, *Effect of serum-free medium on cytochrome P450-dependent metabolism and toxicity in rat cultured hepatocytes*. *Biochem Pharmacol*, 1992. 44(7): p. 1461-4.
60. Tuschl, G. and S.O. Mueller, *Effects of cell culture conditions on primary rat hepatocytes-cell morphology and differential gene expression*. *Toxicology*, 2006. 218(2-3): p. 205-15.
61. Macdonald, J.M., A.S. Xu, H. Kubota, E.L. Lecluyse, G. Hamilton, H. Liu, Y.W. Rong, N. Moss, C. Lodestro, T. Luntz, S.P. Wolfe, and L.M. Reid, *Epithelial Cell Culture: Liver*, in *Methods in Tissue Engineering*, W.L. Lanza, R. Langer, and J. Vacanti, Editors. 2001, Academic Press: San Diego, CA. p. 151 - 201.
62. Washizu, J., F. Berthiaume, Y. Mokuno, R.G. Tompkins, M. Toner, and M.L. Yarmush, *Long-term maintenance of cytochrome P450 activities by rat hepatocyte/3T3 cell co-cultures in heparinized human plasma*. *Tissue Eng*, 2001. 7(6): p. 691-703.
63. Washizu, J., C. Chan, F. Berthiaume, R.G. Tompkins, M. Toner, and M.L. Yarmush, *Amino acid supplementation improves cell-specific functions of the rat hepatocytes exposed to human plasma*. *Tissue Eng*, 2000. 6(5): p. 497-504.
64. Li, A.P., M.K. Reith, A. Rasmussen, J.C. Gorski, S.D. Hall, L. Xu, D.L. Kaminski, and L.K. Cheng, *Primary human hepatocytes as a tool for the evaluation of structure-activity relationship in cytochrome P450 induction potential of xenobiotics: evaluation of rifampin, rifapentine and rifabutin*. *Chem Biol Interact*, 1997. 107(1-2): p. 17-30.

65. Garcia, M., J. Rager, Q. Wang, R. Strab, I.J. Hidalgo, A. Owen, and J. Li, *Cryopreserved human hepatocytes as alternative in vitro model for cytochrome p450 induction studies*. *In Vitro Cell Dev Biol Anim*, 2003. 39(7): p. 283-7.
66. Olefsky, J.M., J. Johnson, F. Liu, P. Jen, and G.M. Reaven, *The effects of acute and chronic dexamethasone administration on insulin binding to isolated rat hepatocytes and adipocytes*. *Metabolism*, 1975. 24(4): p. 517-27.
67. Kletzien, R.F., M.W. Pariza, J.E. Becker, and V.R. Potter, *A "permissive" effect of dexamethasone on the glucagon induction of amino acid transport in cultured hepatocytes*. *Nature*, 1975. 256(5512): p. 46-7.
68. Jauregui, H.O., P.N. McMillan, J. Driscoll, and S. Naik, *Attachment and long term survival of adult rat hepatocytes in primary monolayer cultures: comparison of different substrata and tissue culture media formulations*. *In Vitro Cell Dev Biol*, 1986. 22(1): p. 13-22.
69. Driscoll, J.L., N.T. Hayner, R. Williams-Holland, G. Spies-Karotkin, P.M. Galletti, and H.O. Jauregui, *Phenolsulfonphthalein (phenol red) metabolism in primary monolayer cultures of adult rat hepatocytes*. *In Vitro*, 1982. 18(10): p. 835-42.
70. Hewitt, N.J., E.L. Lecluyse, and S.S. Ferguson, *Induction of hepatic cytochrome P450 enzymes: methods, mechanisms, recommendations, and in vitro-in vivo correlations*. *Xenobiotica*, 2007. 37(10-11): p. 1196-224.
71. Coundouris, J.A., M.H. Grant, J.G. Simpson, and G.M. Hawksworth, *Drug metabolism and viability studies in cryopreserved rat hepatocytes*. *Cryobiology*, 1990. 27(3): p. 288-300.
72. Coundouris, J.A., M.H. Grant, J. Engeset, J.C. Petrie, and G.M. Hawksworth, *Cryopreservation of human adult hepatocytes for use in drug metabolism and toxicity studies*. *Xenobiotica*, 1993. 23(12): p. 1399-409.
73. Ostrowska, A., K. Gu, D.C. Bode, and R.G. Van Buskirk, *Hypothermic storage of isolated human hepatocytes: a comparison between University of Wisconsin solution and a hypothermosol platform*. *Arch Toxicol*, 2009. 83(5): p. 493-502.
74. Sosef, M.N., J.M. Baust, K. Sugimachi, A. Fowler, R.G. Tompkins, and M. Toner, *Cryopreservation of isolated primary rat hepatocytes: enhanced survival and long-term hepatospecific function*. *Ann Surg*, 2005. 241(1): p. 125-33.
75. Jones, J.G., M.A. Solomon, S.M. Cole, A.D. Sherry, and C.R. Malloy, *An integrated (2)H and (13)C NMR study of gluconeogenesis and TCA cycle flux in humans*. *Am J Physiol Endocrinol Metab*, 2001. 281(4): p. E848-56.
76. Jones, J.G., M.A. Solomon, A.D. Sherry, F.M. Jeffrey, and C.R. Malloy, *13C NMR measurements of human gluconeogenic fluxes after ingestion of [U-13C]propionate, phenylacetate, and acetaminophen*. *Am J Physiol*, 1998. 275(5 Pt 1): p. E843-52.
77. Jones, J.G., R.A. Carvalho, B. Franco, A.D. Sherry, and C.R. Malloy, *Measurement of hepatic glucose output, krebs cycle, and gluconeogenic fluxes by NMR analysis of a single plasma glucose sample*. *Anal Biochem*, 1998. 263(1): p. 39-45.
78. Jin, E.S., J.G. Jones, M. Merritt, S.C. Burgess, C.R. Malloy, and A.D. Sherry, *Glucose production, gluconeogenesis, and hepatic tricarboxylic acid cycle fluxes measured by nuclear magnetic resonance analysis of a single glucose derivative*. *Anal Biochem*, 2004. 327(2): p. 149-55.
79. Burgess, S.C., T. He, Z. Yan, J. Lindner, A.D. Sherry, C.R. Malloy, J.D. Browning, and M.A. Magnuson, *Cytosolic phosphoenolpyruvate carboxykinase does not solely*

- control the rate of hepatic gluconeogenesis in the intact mouse liver.* Cell Metab, 2007. 5(4): p. 313-20.
80. Brand, M.D., M.E. Harper, and H.C. Taylor, *Control of the effective P/O ratio of oxidative phosphorylation in liver mitochondria and hepatocytes.* Biochem J, 1993. 291 (Pt 3): p. 739-48.
 81. Ainscow, E.K. and M.D. Brand, *Internal regulation of ATP turnover, glycolysis and oxidative phosphorylation in rat hepatocytes.* Eur J Biochem, 1999. 266(3): p. 737-49.
 82. Ainscow, E.K. and M.D. Brand, *The responses of rat hepatocytes to glucagon and adrenaline. Application of quantified elasticity analysis.* Eur J Biochem, 1999. 265(3): p. 1043-55.
 83. Ainscow, E.K. and M.D. Brand, *Top-down control analysis of ATP turnover, glycolysis and oxidative phosphorylation in rat hepatocytes.* Eur J Biochem, 1999. 263(3): p. 671-85.
 84. Ainscow, E.K. and M.D. Brand, *Quantifying elasticity analysis: how external effectors cause changes to metabolic systems.* Biosystems, 1999. 49(2): p. 151-9.
 85. Berthiaume, F., A.D. MacDonald, Y.H. Kang, and M.L. Yarmush, *Control analysis of mitochondrial metabolism in intact hepatocytes: effect of interleukin-1beta and interleukin-6.* Metab Eng, 2003. 5(2): p. 108-23.
 86. Gille, C., S. Hoffmann, and H.G. Holzhutter, *Combining bioinformatics resources for the structural modelling of eukaryotic metabolic networks.* Genome Inform, 2005. 16(1): p. 223-32.
 87. Yoon, J. and K. Lee, *Metabolic flux profiling of reaction modules in liver drug transformation.* Pac Symp Biocomput, 2007: p. 193-204.
 88. Srivastava, S. and C. Chan, *Application of metabolic flux analysis to identify the mechanisms of free fatty acid toxicity to human hepatoma cell line.* Biotechnol Bioeng, 2008. 99(2): p. 399-410.
 89. Yang, H., C.M. Roth, and M.G. Ierapetritou, *A rational design approach for amino acid supplementation in hepatocyte culture.* Biotechnol Bioeng, 2009. 103(6): p. 1176-91.
 90. Chan, C., F. Berthiaume, K. Lee, and M.L. Yarmush, *Metabolic flux analysis of hepatocyte function in hormone- and amino acid-supplemented plasma.* Metab Eng, 2003. 5(1): p. 1-15.
 91. Marin, S., W.N. Lee, S. Bassilian, S. Lim, L.G. Boros, J.J. Centelles, J.M. Fernandez-Novell, J.J. Guinovart, and M. Cascante, *Dynamic profiling of the glucose metabolic network in fasted rat hepatocytes using [1,2-13C2]glucose.* Biochem J, 2004. 381(Pt 1): p. 287-94.
 92. Bessman, S.P., W. Wang, and C. Mohan, *Ammonia inhibits insulin stimulation of the Krebs cycle: further insight into mechanism of hepatic coma.* Neurochem Res, 1991. 16(7): p. 805-11.
 93. Chan, C., F. Berthiaume, K. Lee, and M.L. Yarmush, *Metabolic flux analysis of cultured hepatocytes exposed to plasma.* Biotechnol Bioeng, 2003. 81(1): p. 33-49.
 94. Crozier, G.L., *Medium-chain triglyceride feeding over the long term: the metabolic fate of [14C]octanoate and [14C]oleate in isolated rat hepatocytes.* J Nutr, 1988. 118(3): p. 297-304.

95. Li, Z., M.L. Yarmush, and C. Chan, *Insulin concentration during preconditioning mediates the regulation of urea synthesis during exposure to amino acid-supplemented plasma*. Tissue Eng, 2004. 10(11-12): p. 1737-46.
96. Martin, G., N. Vincent, J. Combet, and G. Baverel, *A simple model for alanine metabolism in isolated rat hepatocytes*. Biochim Biophys Acta, 1993. 1175(2): p. 161-73.
97. Nagrath, D., M. Avila-Elchiver, F. Berthiaume, A.W. Tilles, A. Messac, and M.L. Yarmush, *Integrated energy and flux balance based multiobjective framework for large-scale metabolic networks*. Ann Biomed Eng, 2007. 35(6): p. 863-85.
98. Schwendel, A., T. Grune, H.G. Holzhutter, and W.G. Siems, *Models for the regulation of purine metabolism in rat hepatocytes: evaluation of tracer kinetic experiments*. Am J Physiol, 1997. 273(1 Pt 1): p. G239-46.
99. Lligona-Trulla, L., A. Arduini, T.A. Aldaghlis, M. Calvani, and J.K. Kelleher, *Acetyl-L-carnitine flux to lipids in cells estimated using isotopomer spectral analysis*. J Lipid Res, 1997. 38(7): p. 1454-62.
100. Maier, K., U. Hofmann, A. Bauer, A. Niebel, G. Vacun, M. Reuss, and K. Mauch, *Quantification of statin effects on hepatic cholesterol synthesis by transient (¹³C)-flux analysis*. Metab Eng, 2009. 11(4-5): p. 292-309.
101. Maier, K., U. Hofmann, M. Reuss, and K. Mauch, *Identification of metabolic fluxes in hepatic cells from transient ¹³C-labeling experiments: Part II. Flux estimation*. Biotechnol Bioeng, 2008. 100(2): p. 355-70.
102. Cohen, S.M., P. Glynn, and R.G. Shulman, *¹³C NMR study of gluconeogenesis from labeled alanine in hepatocytes from euthyroid and hyperthyroid rats*. Proc Natl Acad Sci U S A, 1981. 78(1): p. 60-4.
103. Cohen, S.M., R.G. Shulman, and A.C. McLaughlin, *Effects of ethanol on alanine metabolism in perfused mouse liver studied by ¹³C NMR*. Proc Natl Acad Sci U S A, 1979. 76(10): p. 4808-12.
104. Hausler, N., J. Browning, M. Merritt, C. Storey, A. Milde, F.M. Jeffrey, A.D. Sherry, C.R. Malloy, and S.C. Burgess, *Effects of insulin and cytosolic redox state on glucose production pathways in the isolated perfused mouse liver measured by integrated ²H and ¹³C NMR*. Biochem J, 2006. 394(Pt 2): p. 465-73.
105. Ladriere, L., F. Malaisse-Lagae, I. Verbruggen, R. Willem, and W.J. Malaisse, *Effects of starvation and diabetes on the metabolism of [2,3-¹³C]succinic acid dimethyl ester in rat hepatocytes*. Metabolism, 1999. 48(1): p. 102-6.
106. Malaisse, W.J., L. Ladriere, H. Jijakli, R. Laatikainen, M. Niemitz, I. Verbruggen, M. Biesernans, and R. Willem, *Metabolism of the dimethyl ester of [2,3-(¹³C)]succinic acid in rat hepatocytes*. Mol Cell Biochem, 1998. 189(1-2): p. 137-44.
107. Malaisse, W.J., T.M. Zhang, I. Verbruggen, and R. Willem, *D-glucose generation from [2-¹³C]pyruvate in rat hepatocytes: implications in terms of enzyme-to-enzyme channelling*. Arch Biochem Biophys, 1996. 332(2): p. 341-51.
108. Alexander, D.P., A.S. Huggett, and W.F. Widdas, *Rate of formation foetal fructose investigated with ¹⁴C glucose*. J Physiol, 1951. 115(1): p. 36 P.
109. Balmain, J.H., S.J. Folley, and R.F. Glascock, *Relative utilization of glucose and acetate carbon for lipogenesis by mammary gland slices, studied with tritium, ¹³C and ¹⁴C*. Biochem J, 1953. 53(4): p. xxvi.

110. Beloff-Chain, A., R. Catanzaro, E.B. Chain, I. Masi, and F. Pocchiara, *Fate of uniformly labelled 14C glucose in brain slices*. Proc R Soc Lond B Biol Sci, 1955. 144(914): p. 22-8.
111. Claus, T.H., S.J. Pilkis, and C.R. Park, *Stimulation by glucagon of the incorporation of U-14C-labeled substrates into glucose by isolated hepatocytes from fed rats*. Biochim Biophys Acta, 1975. 404(1): p. 110-23.
112. Katz, J., P.A. Wals, S. Golden, and R. Rognstad, *Recycling of glucose by rat hepatocytes*. Eur J Biochem, 1975. 60(1): p. 91-101.
113. Plas, C. and J. Nunez, *Role of cortisol on the glycogenolytic effect of glucagon and on the glycogenic response to insulin in fetal hepatocyte culture*. J Biol Chem, 1976. 251(5): p. 1431-7.
114. Rognstad, R., P. Wals, and J. Katz, *Metabolism of [5-T]fructose by isolated liver cells*. J Biol Chem, 1975. 250(22): p. 8642-6.
115. Seglen, P.O., *Incorporation of radioactive amino acids into protein in isolated rat hepatocytes*. Biochim Biophys Acta, 1976. 442(3): p. 391-404.
116. Seglen, P.O. and A.E. Solheim, *Effects of aminooxyacetate, alanine and other amino acids on protein synthesis in isolated rat hepatocytes*. Biochim Biophys Acta, 1978. 520(3): p. 630-41.
117. Smith, C.M., L.M. Rovamo, M.P. Kekomaki, and K.O. Raivio, *Purine metabolism in isolated rat hepatocytes*. Can J Biochem, 1977. 55(11): p. 1134-9.
118. Nilsson, A., *Increased cholesterol-ester formation during forced cholesterol synthesis in rat hepatocytes*. Eur J Biochem, 1975. 51(2): p. 337-42.
119. Levine, G.A., M.J. Bissell, and D.M. Bissell, *Conversion of glucose to sorbitol and fructose by liver-derived cells in culture*. J Biol Chem, 1978. 253(17): p. 5985-9.
120. Pilkis, S.J., J.P. Riou, and T.H. Claus, *Hormonal control of [14C]glucose synthesis from [U-14C]dihydroxyacetone and glycerol in isolated rat hepatocytes*. J Biol Chem, 1976. 251(24): p. 7841-52.
121. Freychet, P. and A. Le Cam, *Amino acid transport in isolated hepatocytes: effect of glucagon*. Ciba Found Symp, 1977(55): p. 247-62.
122. Yang, Y.T. and M.A. Williams, *Comparison of C18-, C20- and C22-unsaturated fatty acids in reducing fatty acid synthesis in isolated rat hepatocytes*. Biochim Biophys Acta, 1978. 531(2): p. 133-40.
123. Orlandi, F., F. Bamonti, M. Dini, M. Koch, and A.M. Jezequel, *Hepatic cholesterol synthesis in man: effect of diazepam and other drugs*. Eur J Clin Invest, 1975. 5(2): p. 139-46.
124. Pang, K.S. and J.R. Gillette, *Kinetics of metabolite formation and elimination in the perfused rat liver preparation: differences between the elimination of preformed acetaminophen and acetaminophen formed from phenacetin*. J Pharmacol Exp Ther, 1978. 207(1): p. 178-94.
125. Cohen, S.M., S. Ogawa, and R.G. Shulman, *13C NMR studies of gluconeogenesis in rat liver cells: utilization of labeled glycerol by cells from euthyroid and hyperthyroid rats*. Proc Natl Acad Sci U S A, 1979. 76(4): p. 1603-9.
126. Cline, G.W. and G.I. Shulman, *Quantitative analysis of the pathways of glycogen repletion in periportal and perivenous hepatocytes in vivo*. J Biol Chem, 1991. 266(7): p. 4094-8.

127. Cline, G.W. and G.I. Shulman, *Mass and positional isotopomer analysis of glucose metabolism in periportal and pericentral hepatocytes*. J Biol Chem, 1995. 270(47): p. 28062-7.
128. Desage, M., R. Guilluy, J.L. Brazier, J.P. Riou, M. Beylot, S. Normand, and H. Vidal, *Positional isotopic analysis of ¹³C-labelled glucose by mass spectrometry: applications to the study of gluconeogenesis in liver cells*. Biomed Environ Mass Spectrom, 1989. 18(11): p. 1010-5.
129. Previs, S.F., P.T. Hallowell, K.D. Neimanis, F. David, and H. Brunengraber, *Limitations of the mass isotopomer distribution analysis of glucose to study gluconeogenesis. Heterogeneity of glucose labeling in incubated hepatocytes*. J Biol Chem, 1998. 273(27): p. 16853-9.
130. Malaisse, W.J., L. Ladriere, I. Verbruggen, G. Grue-Sorenson, F. Bjorkling, and R. Willem, *Metabolism of [1,3-¹³C]glycerol-1,2,3-tris(methylsuccinate) and glycerol-1,2,3-tris(methyl[2,3-¹³C]succinate) in rat hepatocytes*. Metabolism, 2000. 49(2): p. 178-85.
131. Malaisse, W.J., L. Ladriere, I. Verbruggen, and R. Willem, *Effects of D-glucose upon D-fructose metabolism in rat hepatocytes: A ¹³C NMR study*. Mol Cell Biochem, 2002. 241(1-2): p. 103-6.
132. Malaisse, W.J., L. Ladriere, I. Verbruggen, and R. Willem, *Metabolism of ¹³C-enriched D-fructose in hepatocytes from Goto-Kakizaki rats*. Int J Mol Med, 2004. 13(5): p. 697-703.
133. Malaisse, W.J. and R. Willem, *Anomeric specificity of D-glucose production by rat hepatocytes*. Mol Cell Biochem, 2004. 266(1-2): p. 145-50.
134. Verbruggen, I., L. Ladriere, R. Willem, and W.J. Malaisse, *Asymmetrical labeling of D-glucose generated from [3(-¹³C)]pyruvate in rat hepatocytes*. Biochem Mol Med, 1997. 61(2): p. 229-35.
135. Lobley, G.E., A. Connell, M.A. Lomax, D.S. Brown, E. Milne, A.G. Calder, and D.A. Farningham, *Hepatic detoxification of ammonia in the ovine liver: possible consequences for amino acid catabolism*. Br J Nutr, 1995. 73(5): p. 667-85.
136. Otto, M., J. Breinholt, and N. Westergaard, *Metformin inhibits glycogen synthesis and gluconeogenesis in cultured rat hepatocytes*. Diabetes Obes Metab, 2003. 5(3): p. 189-94.
137. Petersen, K.F. and N. Grunnet, *Gluconeogenesis in hepatocytes determined with [2-¹³C]acetate and quantitative ¹³C NMR spectroscopy*. Int J Biochem, 1993. 25(1): p. 1-5.
138. Harnack, K., G. Andersen, and V. Somoza, *Quantitation of alpha-linolenic acid elongation to eicosapentaenoic and docosahexaenoic acid as affected by the ratio of n6/n3 fatty acids*. Nutr Metab (Lond), 2009. 6: p. 8.
139. Hofmann, U., K. Maier, A. Niebel, G. Vacun, M. Reuss, and K. Mauch, *Identification of metabolic fluxes in hepatic cells from transient ¹³C-labeling experiments: Part I. Experimental observations*. Biotechnol Bioeng, 2008. 100(2): p. 344-54.
140. Malloy, C.R., A.D. Sherry, and F.M. Jeffrey, *Carbon flux through citric acid cycle pathways in perfused heart by ¹³C NMR spectroscopy*. FEBS Lett, 1987. 212(1): p. 58-62.

141. Malloy, C.R., A.D. Sherry, and F.M. Jeffrey, *Evaluation of carbon flux and substrate selection through alternate pathways involving the citric acid cycle of the heart by ¹³C NMR spectroscopy*. J Biol Chem, 1988. 263(15): p. 6964-71.
142. Sherry, A.D., C.R. Malloy, R.E. Roby, A. Rajagopal, and F.M. Jeffrey, *Propionate metabolism in the rat heart by ¹³C n.m.r. spectroscopy*. Biochem J, 1988. 254(2): p. 593-8.
143. Jones, J.G., G.L. Cottam, B.C. Miller, A.D. Sherry, and C.R. Malloy, *A method for obtaining ¹³C isotopomer populations in ¹³C-enriched glucose*. Anal Biochem, 1994. 217(1): p. 148-52.
144. Holleran, A.L., B. Lindenthal, T.A. Aldaghas, and J.K. Kelleher, *Effect of tamoxifen on cholesterol synthesis in HepG2 cells and cultured rat hepatocytes*. Metabolism, 1998. 47(12): p. 1504-13.
145. Mailloux, R.J., R. Hamel, and V.D. Appanna, *Aluminum toxicity elicits a dysfunctional TCA cycle and succinate accumulation in hepatocytes*. J Biochem Mol Toxicol, 2006. 20(4): p. 198-208.
146. Fabre, G., J. Combalbert, Y. Berger, and J.P. Cano, *Human hepatocytes as a key in vitro model to improve preclinical drug development*. Eur J Drug Metab Pharmacokinet, 1990. 15(2): p. 165-71.
147. Guillouzo, A., *Acquisition and use of human in vitro liver preparations*. Cell Biol Toxicol, 1995. 11(3-4): p. 141-5.
148. Hawksworth, G.M., *Advantages and disadvantages of using human cells for pharmacological and toxicological studies*. Hum Exp Toxicol, 1994. 13(8): p. 568-73.
149. Donato, M.T., A. Lahoz, J.V. Castell, and M.J. Gomez-Lechon, *Cell lines: a tool for in vitro drug metabolism studies*. Curr Drug Metab, 2008. 9(1): p. 1-11.
150. Guillouzo, A., *Liver cell models in in vitro toxicology*. Environ Health Perspect, 1998. 106 Suppl 2: p. 511-32.
151. LeCluyse, E.L., *Human hepatocyte culture systems for the in vitro evaluation of cytochrome P450 expression and regulation*. Eur J Pharm Sci, 2001. 13(4): p. 343-68.
152. Li, A.P., *Human hepatocytes: isolation, cryopreservation and applications in drug development*. Chem Biol Interact, 2007. 168(1): p. 16-29.
153. Gerlach, J.C., K. Zeilinger, and J.F. Patzer II, *Bioartificial liver systems: why, what, whither?* Regen Med, 2008. 3(4): p. 575-95.
154. Nicholson, J.K., J. Connelly, J.C. Lindon, and E. Holmes, *Metabonomics: a platform for studying drug toxicity and gene function*. Nat Rev Drug Discov, 2002. 1(2): p. 153-61.
155. Nicholson, J.K. and I.D. Wilson, *Opinion: understanding 'global' systems biology: metabonomics and the continuum of metabolism*. Nat Rev Drug Discov, 2003. 2(8): p. 668-76.
156. Fiehn, O., *Combining genomics, metabolome analysis, and biochemical modelling to understand metabolic networks*. Comp Funct Genomics, 2001. 2(3): p. 155-68.
157. Griffin, J.L., *Metabonomics: NMR spectroscopy and pattern recognition analysis of body fluids and tissues for characterisation of xenobiotic toxicity and disease diagnosis*. Curr Opin Chem Biol, 2003. 7(5): p. 648-54.
158. Nicholson, J.K., J.C. Lindon, and E. Holmes, *'Metabonomics': understanding the metabolic responses of living systems to pathophysiological stimuli via multivariate*

- statistical analysis of biological NMR spectroscopic data*. *Xenobiotica*, 1999. 29(11): p. 1181-9.
159. Robertson, D.G., *Metabonomics in toxicology: a review*. *Toxicol Sci*, 2005. 85(2): p. 809-22.
 160. Gibney, M.J., M. Walsh, L. Brennan, H.M. Roche, B. German, and B. van Ommen, *Metabolomics in human nutrition: opportunities and challenges*. *Am J Clin Nutr*, 2005. 82(3): p. 497-503.
 161. Rezzi, S., Z. Ramadan, L.B. Fay, and S. Kochhar, *Nutritional metabonomics: applications and perspectives*. *J Proteome Res*, 2007. 6(2): p. 513-25.
 162. Kochhar, S., D.M. Jacobs, Z. Ramadan, F. Berruex, A. Fuerholz, and L.B. Fay, *Probing gender-specific metabolism differences in humans by nuclear magnetic resonance-based metabonomics*. *Anal Biochem*, 2006. 352(2): p. 274-81.
 163. Slupsky, C.M., K.N. Rankin, J. Wagner, H. Fu, D. Chang, A.M. Weljie, E.J. Saude, B. Lix, D.J. Adamko, S. Shah, R. Greiner, B.D. Sykes, and T.J. Marrie, *Investigations of the effects of gender, diurnal variation, and age in human urinary metabolomic profiles*. *Anal Chem*, 2007. 79(18): p. 6995-7004.
 164. Gavaghan, C.L., E. Holmes, E. Lenz, I.D. Wilson, and J.K. Nicholson, *An NMR-based metabonomic approach to investigate the biochemical consequences of genetic strain differences: application to the C57BL10J and Alpk:ApfCD mouse*. *FEBS Lett*, 2000. 484(3): p. 169-74.
 165. Zuppi, C., I. Messana, F. Forni, F. Ferrari, C. Rossi, and B. Giardina, *Influence of feeding on metabolite excretion evidenced by urine 1H NMR spectral profiles: a comparison between subjects living in Rome and subjects living at arctic latitudes (Svalbard)*. *Clin Chim Acta*, 1998. 278(1): p. 75-9.
 166. Lenz, E.M., J. Bright, I.D. Wilson, A. Hughes, J. Morrisson, H. Lindberg, and A. Lockton, *Metabonomics, dietary influences and cultural differences: a 1H NMR-based study of urine samples obtained from healthy British and Swedish subjects*. *J Pharm Biomed Anal*, 2004. 36(4): p. 841-9.
 167. Lenz, E.M., J. Bright, I.D. Wilson, S.R. Morgan, and A.F. Nash, *A 1H NMR-based metabonomic study of urine and plasma samples obtained from healthy human subjects*. *J Pharm Biomed Anal*, 2003. 33(5): p. 1103-15.
 168. Stella, C., B. Beckwith-Hall, O. Cloarec, E. Holmes, J.C. Lindon, J. Powell, F. van der Ouderaa, S. Bingham, A.J. Cross, and J.K. Nicholson, *Susceptibility of human metabolic phenotypes to dietary modulation*. *J Proteome Res*, 2006. 5(10): p. 2780-8.
 169. Walsh, M.C., L. Brennan, J.P. Malthouse, H.M. Roche, and M.J. Gibney, *Effect of acute dietary standardization on the urinary, plasma, and salivary metabolomic profiles of healthy humans*. *Am J Clin Nutr*, 2006. 84(3): p. 531-9.
 170. Assfalg, M., I. Bertini, D. Colangiuli, C. Luchinat, H. Schafer, B. Schutz, and M. Spraul, *Evidence of different metabolic phenotypes in humans*. *Proc Natl Acad Sci U S A*, 2008. 105(5): p. 1420-4.
 171. Watkins, P.B., P.J. Seligman, J.S. Pears, M.I. Avigan, and J.R. Senior, *Using controlled clinical trials to learn more about acute drug-induced liver injury*. *Hepatology*, 2008. 48(5): p. 1680-9.
 172. Senior, J.R., *Monitoring for hepatotoxicity: what is the predictive value of liver "function" tests?* *Clin Pharmacol Ther*, 2009. 85(3): p. 331-4.

173. Russo, M.W. and P.B. Watkins, *Genetic basis for susceptibility to drug induced liver injury*, in *Drug Induced Liver Disease*, N. Kaplowitz and L. Deleve, Editors. 2007, Informa Healthcare: New York, NY, USA. p. 207-222.
174. Clayton, T.A., J.C. Lindon, O. Cloarec, H. Antti, C. Charuel, G. Hanton, J.P. Provost, J.L. Le Net, D. Baker, R.J. Walley, J.R. Everett, and J.K. Nicholson, *Pharmacometabonomic phenotyping and personalized drug treatment*. *Nature*, 2006. 440(7087): p. 1073-7.
175. Li, H., Y. Ni, M. Su, Y. Qiu, M. Zhou, M. Qiu, A. Zhao, L. Zhao, and W. Jia, *Pharmacometabonomic phenotyping reveals different responses to xenobiotic intervention in rats*. *J Proteome Res*, 2007. 6(4): p. 1364-70.
176. Andersson, U., J. Lindberg, S. Wang, R. Balasubramanian, M. Marcusson-Stahl, M. Hannula, C. Zeng, P.J. Juhasz, J. Kolmert, J. Backstrom, L. Nord, K. Nilsson, S. Martin, B. Glinghammar, K. Cederbrant, and I. Schuppe-Koistinen, *A systems biology approach to understanding elevated serum alanine transaminase levels in a clinical trial with ximelagatran*. *Biomarkers*, 2009. 14(8): p. 572-86.
177. Watkins, P.B., N. Kaplowitz, J.T. Slattery, C.R. Colonese, S.V. Colucci, P.W. Stewart, and S.C. Harris, *Aminotransferase elevations in healthy adults receiving 4 grams of acetaminophen daily: a randomized controlled trial*. *JAMA*, 2006. 296(1): p. 87-93.
178. Harrill, A.H., P.B. Watkins, S. Su, P.K. Ross, D.E. Harbourt, I.M. Stylianou, G.A. Boorman, M.W. Russo, R.S. Sackler, S.C. Harris, P.C. Smith, R. Tennant, M. Bogue, K. Paigen, C. Harris, T. Contractor, T. Wiltshire, I. Rusyn, and D.W. Threadgill, *Mouse population-guided resequencing reveals that variants in CD44 contribute to acetaminophen induced liver injury*. *Genome Research* (in press), 2009.
179. Trygg, J. and S. Wold, *Orthogonal projections to latent structures (O-PLS)*. *Journal of Chemometrics*, 2002. 16: p. 119-128.
180. Wiklund, S., E. Johansson, L. Sjostrom, E.J. Mellerowicz, U. Edlund, J.P. Shockcor, J. Gottfries, T. Moritz, and J. Trygg, *Visualization of GC/TOF-MS-based metabolomics data for identification of biochemically interesting compounds using OPLS class models*. *Anal Chem*, 2008. 80(1): p. 115-22.
181. Pessayre, D., A. Dolder, J.Y. Artigou, J.C. Wandscheer, V. Descatoire, C. Degott, and J.P. Benhamou, *Effect of fasting on metabolite-mediated hepatotoxicity in the rat*. *Gastroenterology*, 1979. 77(2): p. 264-71.
182. Sato, C., Y. Matsuda, and C.S. Lieber, *Increased hepatotoxicity of acetaminophen after chronic ethanol consumption in the rat*. *Gastroenterology*, 1981. 80(1): p. 140-8.
183. Lauterburg, B.H., G.B. Corcoran, and J.R. Mitchell, *Mechanism of action of N-acetylcysteine in the protection against the hepatotoxicity of acetaminophen in rats in vivo*. *J Clin Invest*, 1983. 71(4): p. 980-91.
184. Price, V.F. and D.J. Jollow, *Role of UDPGA flux in acetaminophen clearance and hepatotoxicity*. *Xenobiotica*, 1984. 14(7): p. 553-9.
185. Tee, L.B., D.S. Davies, C.E. Seddon, and A.R. Boobis, *Species differences in the hepatotoxicity of paracetamol are due to differences in the rate of conversion to its cytotoxic metabolite*. *Biochem Pharmacol*, 1987. 36(7): p. 1041-52.
186. Jepson, M.A., M.J. Davis, A.A. Horton, and D.G. Walker, *Histochemical and biochemical observations on the cytotoxicity of paracetamol and its effects on glycogen metabolism in rat liver*. *Toxicology*, 1987. 47(3): p. 325-37.

187. Katyare, S.S. and J.G. Satav, *Impaired mitochondrial oxidative energy metabolism following paracetamol-induced hepatotoxicity in the rat*. Br J Pharmacol, 1989. 96(1): p. 51-8.
188. Strubelt, O. and M. Younes, *The toxicological relevance of paracetamol-induced inhibition of hepatic respiration and ATP depletion*. Biochem Pharmacol, 1992. 44(1): p. 163-70.
189. Parmar, D.V., G. Ahmed, M.A. Khandkar, and S.S. Katyare, *Mitochondrial ATPase: a target for paracetamol-induced hepatotoxicity*. Eur J Pharmacol, 1995. 293(3): p. 225-9.
190. Hinson, J.A., A.B. Reid, S.S. McCullough, and L.P. James, *Acetaminophen-induced hepatotoxicity: role of metabolic activation, reactive oxygen/nitrogen species, and mitochondrial permeability transition*. Drug Metab Rev, 2004. 36(3-4): p. 805-22.
191. Dauterman, W.C., *Metabolism of Toxicants: Phase II Reactions*. Introduction to Biochemical Toxicology, ed. E. Hodgson and F.E. Guthrie. 1984, New York: Elsevier Science Publishing Company.
192. Stevens, J.L. and D.P. Jones, *The Mercapturic Acid pathway: Biosynthesis, Intermediary Metabolism, and Physiological Disposition*, in *Glutathione: Chemical, Biochemical, and Medical Aspects Part B*, D. Dolphin, R. Poulson, and O. Avramovic, Editors. 1989, Wiley-Interscience Publishers: New York.
193. Vance, M.A., P.D. Gray, and K.G. Tolman, *Effect of glycine on valproate toxicity in rat hepatocytes*. Epilepsia, 1994. 35(5): p. 1016-22.
194. Ireland, Z., A.P. Russell, T. Wallimann, D.W. Walker, and R. Snow, *Developmental changes in the expression of creatine synthesizing enzymes and creatine transporter in a precocial rodent, the spiny mouse*. BMC Dev Biol, 2009. 9: p. 39.
195. Clayton, T.A., J.C. Lindon, J.R. Everett, C. Charuel, G. Hanton, J.L. Le Net, J.P. Provost, and J.K. Nicholson, *Hepatotoxin-induced hypercreatinemia and hypercreatinuria: their relationship to one another, to liver damage and to weakened nutritional status*. Arch Toxicol, 2004. 78(2): p. 86-96.
196. Clayton, T.A., J.C. Lindon, J.R. Everett, C. Charuel, G. Hanton, J.L. Le Net, J.P. Provost, and J.K. Nicholson, *An hypothesis for a mechanism underlying hepatotoxin-induced hypercreatinuria*. Arch Toxicol, 2003. 77(4): p. 208-17.
197. Fan, T.W., A.N. Lane, R.M. Higashi, M.A. Farag, H. Gao, M. Bousamra, and D.M. Miller, *Altered regulation of metabolic pathways in human lung cancer discerned by (13)C stable isotope-resolved metabolomics (SIRM)*. Mol Cancer, 2009. 8: p. 41.
198. Jemnitz, K., Z. Veres, K. Monostory, L. Kobori, and L. Vereczkey, *Interspecies differences in acetaminophen sensitivity of human, rat, and mouse primary hepatocytes*. Toxicol In Vitro, 2008. 22(4): p. 961-7.
199. Fannin, R.D., M. Russo, T.M. O'Connell, K. Gerrish, J.H. Winnike, J. Macdonald, J. Newton, S. Malik, S.O. Sieber, J. Parker, R. Shah, T. Zhou, P.B. Watkins, and R.S. Paules, *Acetaminophen dosing of humans results in blood transcriptome and metabolome changes consistent with impaired oxidative phosphorylation*. Hepatology, 2010. 51(1): p. 227-36.
200. Anand, K.J.S., W.G. Sippell, and A. Aynsley-Green, *Randomized trial of fentanyl anaesthesia in preterm babies undergoing surgery: effects on the stress response*. The Lancet, 1987. 329(8524): p. 62-66.

201. Weissman, C., *The metabolic response to stress: an overview and update*. Anesthesiology, 1990. 73(2): p. 308-27.
202. Winder, C.L., W.B. Dunn, S. Schuler, D. Broadhurst, R. Jarvis, G.M. Stephens, and R. Goodacre, *Global metabolic profiling of Escherichia coli cultures: an evaluation of methods for quenching and extraction of intracellular metabolites*. Anal Chem, 2008. 80(8): p. 2939-48.
203. Maharjan, R.P. and T. Ferenci, *Global metabolite analysis: the influence of extraction methodology on metabolome profiles of Escherichia coli*. Anal Biochem, 2003. 313(1): p. 145-54.
204. Sellick, C.A., R. Hansen, A.R. Maqsood, W.B. Dunn, G.M. Stephens, R. Goodacre, and A.J. Dickson, *Effective quenching processes for physiologically valid metabolite profiling of suspension cultured Mammalian cells*. Anal Chem, 2009. 81(1): p. 174-83.
205. Sze, D.Y. and O. Jardetzky, *Determination of metabolite and nucleotide concentrations in proliferating lymphocytes by 1H-NMR of acid extracts*. Biochim Biophys Acta, 1990. 1054(2): p. 181-97.
206. Fajjes, M., A.E. Mars, and E.J. Smid, *Comparison of quenching and extraction methodologies for metabolome analysis of Lactobacillus plantarum*. Microb Cell Fact, 2007. 6: p. 27.
207. Kimball, E. and J.D. Rabinowitz, *Identifying decomposition products in extracts of cellular metabolites*. Anal Biochem, 2006. 358(2): p. 273-80.
208. Folch, J., M. Lees, and G.H. Sloane Stanley, *A simple method for the isolation and purification of total lipides from animal tissues*. J Biol Chem, 1957. 226(1): p. 497-509.
209. Botham, K.M. and P.A. Mayes, *Oxidation of Fatty Acids: Ketogenesis*, in *Harper's Illustrated Biochemistry*, R.K. Murray, D.K. Granner, and V.W. Rodwell, Editors. 2003, McGraw-Hill: New York, NY.
210. Fan, T.W., M. Kucia, K. Jankowski, R.M. Higashi, J. Ratajczak, M.Z. Ratajczak, and A.N. Lane, *Rhabdomyosarcoma cells show an energy producing anabolic metabolic phenotype compared with primary myocytes*. Mol Cancer, 2008. 7: p. 79.
211. Nobes, C.D., W.W. Hay, Jr., and M.D. Brand, *The mechanism of stimulation of respiration by fatty acids in isolated hepatocytes*. J Biol Chem, 1990. 265(22): p. 12910-5.
212. Leverve, X., B. Sibille, A. Devin, M.A. Piquet, P. Espie, and M. Rigoulet, *Oxidative phosphorylation in intact hepatocytes: quantitative characterization of the mechanisms of change in efficiency and cellular consequences*. Mol Cell Biochem, 1998. 184(1-2): p. 53-65.
213. Desborough, J.P., *The stress response to trauma and surgery*. Br J Anaesth, 2000. 85(1): p. 109-17.
214. Miyazaki, K., C. Takemoto, T. Satoh, K. Ueno, T. Igarashi, and H. Kitagawa, *Toxicity and biotransformation of acetaminophen in rat hepatocytes (I). Uptake and release*. Res Commun Chem Pathol Pharmacol, 1983. 39(1): p. 77-86.
215. McLean, S., *Metabolism of phenacetin and N-hydroxyphenacetin in isolated rat hepatocytes*. Naunyn Schmiedebergs Arch Pharmacol, 1978. 305(2): p. 173-80.
216. Moldeus, P., *Paracetamol metabolism and toxicity in isolated hepatocytes from rat and mouse*. Biochem Pharmacol, 1978. 27(24): p. 2859-63.

217. Mizuma, T., M. Hayashi, and S. Awaza, *Factors influencing drug sulfate and glucuronic acid conjugation rates in isolated rat hepatocytes: significance of preincubation time*. *Biochem Pharmacol*, 1985. 34(14): p. 2573-5.
218. Milam, K.M. and J.L. Byard, *Acetaminophen metabolism, cytotoxicity, and genotoxicity in rat primary hepatocyte cultures*. *Toxicol Appl Pharmacol*, 1985. 79(2): p. 342-7.
219. Emery, S., H.G. Oldham, S.J. Norman, and R.J. Chenery, *The effect of cimetidine and ranitidine on paracetamol glucuronidation and sulphation in cultured rat hepatocytes*. *Biochem Pharmacol*, 1985. 34(9): p. 1415-21.
220. Pang, K.S., P. Kong, J.A. Terrell, and R.E. Billings, *Metabolism of acetaminophen and phenacetin by isolated rat hepatocytes. A system in which the spatial organization inherent in the liver is disrupted*. *Drug Metab Dispos*, 1985. 13(1): p. 42-50.
221. Sweeny, D.J. and L.A. Reinke, *Sulfation of acetaminophen in isolated rat hepatocytes. Relationship to sulfate ion concentrations and intracellular levels of 3'-phosphoadenosine-5'-phosphosulfate*. *Drug Metab Dispos*, 1988. 16(5): p. 712-5.
222. Boobis, A.R., L.B. Tee, C.E. Hampden, and D.S. Davies, *Freshly isolated hepatocytes as a model for studying the toxicity of paracetamol*. *Food Chem Toxicol*, 1986. 24(6-7): p. 731-6.
223. Kane, R.E., A.P. Li, and D.R. Kaminski, *Sulfation and glucuronidation of acetaminophen by human hepatocytes cultured on Matrigel and type I collagen reproduces conjugation in vivo*. *Drug Metab Dispos*, 1995. 23(3): p. 303-7.
224. George, J., B. Goodwin, C. Liddle, M. Tapner, and G.C. Farrell, *Time-dependent expression of cytochrome P450 genes in primary cultures of well-differentiated human hepatocytes*. *J Lab Clin Med*, 1997. 129(6): p. 638-48.
225. McCarver, D.G. and R.N. Hines, *The ontogeny of human drug-metabolizing enzymes: phase II conjugation enzymes and regulatory mechanisms*. *J Pharmacol Exp Ther*, 2002. 300(2): p. 361-6.
226. Rother, K.I. and W.F. Schwenk, *Hepatic glycogen accurately reflected by acetaminophen glucuronide in dogs refed after fasting*. *Am J Physiol*, 1995. 269(4 Pt 1): p. E766-73.
227. Burcham, P.C. and A.W. Harman, *Paracetamol-induced stimulation of glycogenolysis in isolated mouse hepatocytes is not directly associated with cell death*. *Biochem Pharmacol*, 1989. 38(14): p. 2357-62.
228. Iynedjian, P.B., S. Marie, A. Gjinovci, B. Genin, S.P. Deng, L. Buhler, P. Morel, and G. Mentha, *Glucokinase and cytosolic phosphoenolpyruvate carboxykinase (GTP) in the human liver. Regulation of gene expression in cultured hepatocytes*. *J Clin Invest*, 1995. 95(5): p. 1966-73.
229. Burcham, P.C. and A.W. Harman, *Acetaminophen toxicity results in site-specific mitochondrial damage in isolated mouse hepatocytes*. *J Biol Chem*, 1991. 266(8): p. 5049-54.
230. Burcham, P.C. and A.W. Harman, *Mitochondrial dysfunction in paracetamol hepatotoxicity: in vitro studies in isolated mouse hepatocytes*. *Toxicol Lett*, 1990. 50(1): p. 37-48.

231. Kyle, M.E., I. Sakaida, A. Serroni, and J.L. Farber, *Metabolism of acetaminophen by cultured rat hepatocytes. Depletion of protein thiol groups without any loss of viability*. *Biochem Pharmacol*, 1990. 40(6): p. 1211-8.
232. Rombach, E.M. and R.P. Hanzlik, *Detection of benzoquinone adducts to rat liver protein sulfhydryl groups using specific antibodies*. *Chem Res Toxicol*, 1997. 10(12): p. 1407-11.
233. Birge, R.B., J.B. Bartolone, S.G. Hart, E.V. Nishanian, C.A. Tyson, E.A. Khairallah, and S.D. Cohen, *Acetaminophen hepatotoxicity: correspondence of selective protein arylation in human and mouse liver in vitro, in culture, and in vivo*. *Toxicol Appl Pharmacol*, 1990. 105(3): p. 472-82.
234. Tong, C., M.F. Laspia, S. Telang, and G.M. Williams, *The use of adult rat liver cultures in the detection of the genotoxicity of various polycyclic aromatic hydrocarbons*. *Environ Mutagen*, 1981. 3(4): p. 477-87.
235. McQueen, C.A. and G.M. Williams, *Cytotoxicity of xenobiotics in adult rat hepatocytes in primary culture*. *Fundam Appl Toxicol*, 1982. 2(3): p. 139-44.
236. Metcalfe, S.A. and G.E. Neal, *The metabolism of aflatoxin B1 by hepatocytes isolated from rats following the in vivo administration of some xenobiotics*. *Carcinogenesis*, 1983. 4(8): p. 1007-12.
237. DeBerardinis, R.J., A. Mancuso, E. Daikhin, I. Nissim, M. Yudkoff, S. Wehrli, and C.B. Thompson, *Beyond aerobic glycolysis: transformed cells can engage in glutamine metabolism that exceeds the requirement for protein and nucleotide synthesis*. *Proc Natl Acad Sci U S A*, 2007. 104(49): p. 19345-50.
238. London, R.E., C.E. Hildebrand, E.S. Olson, and N.A. Matwiyoff, *Carbon-13 nuclear magnetic resonance spectroscopy of suspensions of chinese hamster ovary cells specifically enriched with (methyl-13C)choline*. *Biochemistry*, 1976. 15(25): p. 5480-6.
239. Unkefer, C.J. and R.E. London, *In vivo studies of pyridine nucleotide metabolism in Escherichia coli and Saccharomyces cerevisiae by carbon-13 NMR spectroscopy*. *J Biol Chem*, 1984. 259(4): p. 2311-20.
240. Gebhardt, R., H. Fitzke, M. Fausel, I. Eisenmann-Tappe, and D. Mecke, *Influence of hormones and drugs on glutathione-S-transferase levels in primary culture of adult rat hepatocytes*. *Cell Biol Toxicol*, 1990. 6(4): p. 365-78.
241. Lindsay, C.K., R.J. Chenery, and G.M. Hawksworth, *Primary culture of rat hepatocytes in the presence of dimethyl sulphoxide. A system to investigate the regulation of cytochrome P450 IA*. *Biochem Pharmacol*, 1991. 42 Suppl: p. S17-25.
242. Morand, C., C. Besson, C. Demigne, and C. Remesy, *Importance of the modulation of glycolysis in the control of lactate metabolism by fatty acids in isolated hepatocytes from fed rats*. *Arch Biochem Biophys*, 1994. 309(2): p. 254-60.
243. Lin, X., S.H. Adams, and J. Odle, *Acetate represents a major product of heptanoate and octanoate beta-oxidation in hepatocytes isolated from neonatal piglets*. *Biochem J*, 1996. 318 (Pt 1): p. 235-40.
244. Rossi, R., M. Geronimi, P. Gloor, M.C. Seebacher, and E. Scharrer, *Hyperpolarization of the cell membrane of mouse hepatocytes by fatty acid oxidation*. *Physiol Behav*, 1995. 57(3): p. 509-14.
245. Kasumov, T., J.E. Adams, F. Bian, F. David, K.R. Thomas, K.A. Jobbins, P.E. Minkler, C.L. Hoppel, and H. Brunengraber, *Probing peroxisomal beta-oxidation and*

- the labelling of acetyl-CoA proxies with [1-(13C)]octanoate and [3-(13C)]octanoate in the perfused rat liver. Biochem J, 2005. 389(Pt 2): p. 397-401.*
246. Otto, D.A., *Relationship of the ATP/ADP ratio to the site of octanoate activation. J Biol Chem, 1984. 259(9): p. 5490-4.*
 247. Sibille, B., C. Keriél, E. Fontaine, F. Catelloni, M. Rigoulet, and X.M. Leverve, *Octanoate affects 2,4-dinitrophenol uncoupling in intact isolated rat hepatocytes. Eur J Biochem, 1995. 231(2): p. 498-502.*
 248. Sherry, A.D. and C.R. Malloy, *13C Isotopomer Analysis of Glutamate, A NMR Method to Probe Metabolic Pathways Intersecting in the Citric Acid Cycle*, in *Biological Magnetic Resonance: In Vivo Carbon-13 NMR*, L.J. Berliner and P.M. Robitaille, Editors. 2002, Kluwer Academic Publishers: New York.
 249. Fan, T.W.M. and A.N. Lane, *Structure-based profiling of metabolites and isotopomers by NMR. Progress in Nuclear Magnetic Resonance Spectroscopy, 2008. 52(2-3): p. 69-117.*
 250. Lane, A.N., T.W. Fan, and R.M. Higashi, *Stable isotope-assisted metabolomics in cancer research. IUBMB Life, 2008. 60(2): p. 124-9.*
 251. Lane, A.N., T.W. Fan, and R.M. Higashi, *Isotopomer-based metabolomic analysis by NMR and mass spectrometry. Methods Cell Biol, 2008. 84: p. 541-88.*
 252. Laughlin, M.R. and J.K. Kelleher, *Tracer Theory and 13C NMR*, in *Biological Magnetic Resonance: In Vivo Carbon-13 NMR*, L.J. Berliner and P.M. Robitaille, Editors. 2002, Kluwer Academic Publishers: New York.
 253. Fan, T.W., A.J. Clifford, and R.M. Higashi, *In vivo 13C NMR analysis of acyl chain composition and organization of perirenal triacylglycerides in rats fed vegetable and fish oils. J Lipid Res, 1994. 35(4): p. 678-89.*